Order Number 9218218

Quantum optical properties of polariton waves

Artoni, Maurizio, Ph.D.

City University of New York, 1992

U·M·I
300 N. Zeeb Rd.
Ann Arbor, MI 48106

QUANTUM OPTICAL PROPERTIES OF POLARITON WAVES

by

Maurizio ARTONI

A dissertation submitted to the Graduate Faculty in Physics in partial fulfillment of
the requirements for the degree of Doctor of Philosophy,
The City University of New York

1992

This manuscript has been accepted for the Graduate Faculty in Physics in satisfaction of the Dissertation requirement for the degree of Doctor of Philosophy

10/17/91
Date

Prof. J.L. Birman
Chair of Examining Committee

11/11/91
Date

Prof. Joseph B. Krieger
Executive Officer

Prof. H. Z. Cummins

Prof. M. Lax

Prof. M. Hillery

Dr. R. Slusher

The City University of New York

ABSTRACT

QUANTUM OPTICAL PROPERTIES OF POLARITON WAVES

by

Maurizio ARTONI

Adviser: Prof. Joseph L. Birman

Polariton, the normal mode of the coupled matter-radiation system, has been well known for at least 40 years. Certain properties of the polaritons have been extensively studied by a variety of spectroscopic methods. In particular, resonant Brillouin scattering techniques and delicate steady-state optical reflection and transmission studies using polarized light have permitted careful and quantitative mapping of the frequency-wavenumber dispersion $\omega(k) \equiv \omega_k$ for exciton-polaritons. Phonon polaritons have been studied by related methods, which in many cases antedate the work on exciton-polaritons. Despite this extensive literature the investigations of the quantum-optical properties of these crystal mixed modes has lagged. By contrast the study of the quantum optical properties of the single and multimode cavity electromagnetic radiation, either in isolation or in interaction with one or more atoms has been extensively developed. Part of this impetus has been the expectation that low noise radiation ("squeezed light") can be used e.g. for gravity wave detectors or in communication.

Of course the study of the basic statistical properties of light is itself a major stimulus for such investigations. These effects found in optics have a certain generality and they may have analogs in the condensed media.

We develop a quantum mechanical hamiltonian formulation to treat the polariton in the framework of quantum optics. We exploit two specific hamiltonians: the conventional Hopfield model, and a more general hamiltonian. For both of these, exciton-polariton quantum states are found to be squeezed (*intrinsic* polariton squeezing) with respect to states of an intrinsic, non-polariton, mixed photon-exciton boson. The amount and duration of intrinsic squeezing during the polariton period are studied for exciton-polaritons in typical I-VII and III-V semiconductors. Among the new features is the possibility of tuning the amount of intrinsic squeezing by varying the frequency-wavevector of the polariton mode. We further analyse the photon statistics of the electromagnetic component of the polariton. Squeezing and tunable non-poissonian photon statistics are found in the electromagnetic component (*optical* polariton squeezing) of the exciton polariton. This entails the reduction of the fluctuations of the polariton electromagnetic field component below the limit set by the vacuum fluctuations. The Mandel Q-factor for the number distribution of photon in a polariton coherent state has been evaluated. Although small for I-VII and III-V materials in the range of modes analysed, the Q-factor could be enhanced for phonon-polaritons and for other materials. Interpretations of the origin of squeezing in polariton states are presented.

ACKNOWLEDGEMENTS

This work is dedicated to my family. My appreciation for them is much to deep for words.

I am deeply indebted to Prof. Joseph L. Birman, for introducing me to the fields of polariton physics and non-classical properties of the electromagnetic field. I must express my deep gratitude to him for his very patient guidance, and encouragement during the course of my research. I certainly wish to show gratitude for respecting my ideas and for giving me the time and the freedom to develop them.

I am especially grateful to Prof. J. Birman, Prof. T. Boyer, Prof. H. Cummins, Prof. M. Lax, and Prof. N. P. Chang for the invaluable education they provided me. A special recognition to Prof. B.S. Wang, Prof. S. Tikhodeev, Dr. C. Ortiz, Dr. A. Bulatov and Dr. H. Choi for valid discussions and suggestions during my thesis work.

Many thanks to all the members of Prof. Birman's group, Mrs. De, Prof. J. Jaric, Prof. D. Schmeltzer, Dr. S. Branis., Prof. O. Martin, Mr. J. Zhang, Dr. R. Berenson and Dr. S. Deonarine for their interest in my research and the pleasant working atmosphere. I then thank all the members of my thesis committee for their guidance and help.

Last but not the least, I would like to thank Lucy Francesco, as well as all my friends for their patience, love and the wonderful time we have spent together.

TABLE OF CONTENTS

Appendices

LIST OF FIGURES

LIST OF TABLES

CHAPTER I

Introduction

1.1 Electromagnetic field fluctuations

Can a beam of light ever be truly "quiet", and free from the random fluctuations called noise? All light fields fluctuate: their amplitudes and phases are subject to a stochastic indeterminacy. Much of this indeterminacy in practical light sources derives from environmental influences. For example, radiating atoms can collide with other atoms so that the phase of the emitted light is disrupted, optical components in a light source can vibrate in an uncontrolled fashion and lead to random changes in frequency and amplitude, and the rate of atomic excitation in any light source can vary in a random way. These factors can in principle be eliminated by a careful design of the light source. Even if all of these influences are removed, however, we are left with a more fundamental kind of optical noise. Optical fields obey the laws of quantum mechanics and have an inherent quantum indeterminacy which cannot be removed no matter how carefully the light source is controlled.

A beam of light consists of an oscillating electromagnetic field. In the world view of classical physics, the oscillations of the field can be pictured as a smooth wave, whose shape can be described with absolute certainty. According to the quantum mechanical uncertainty principle, however, the best one can say is that the wave's shape fits within a particular envelope of uncertainty [1]. That uncertainty is manifested as noise: small random fluctuations in the

electromagnetic field. A measure of the minimum size of this quantum optical noise for a single-mode field of frequency ω is given by the quantity $\Im_o = (\hbar\omega / 2\varepsilon_o V)^{1/2}$, where V is the volume over which the field is excited [1,2,3]. The noise has the same magnitude for any strength of excitation of the field mode. We represent in Fig.s 1.1 a *classical* electromagnetic field, with a precisely defined amplitude as well as the variation of the mean amplitude of a *quantum* electromagnetic field with the size of the fluctuations around the mean indicated by the shaded band.

1.2 Electromagnetic field vacuum fluctuations

Thus quantum theory states that any light field must be accompanied by a certain minimum amount of fluctuation. Furthermore, according to quantum mechanics there must be some amount of noise even when no other light is present [1,2,4,5]. In classical physics the wave representing darkness would be flat, with no undulations (in some sense it would not really be a wave at all). In quantum mechanics, on the other hand, one can say only that this wave is flat to within some small degree of uncertainty; within the envelope of uncertainty the wave fluctuates randomly. This is represented in Fig. 1.2. One has in this case that the envelope of field fluctuations is $\Im_o$. In practical terms this means that even in a vacuum with no external light sources there must still be small fluctuations in the e.m. field.

In a sense it is really these vacuum fluctuations that underlie the fluctuations within ordinary beams of light. The wave representing a light beam can be seen as

consisting of the fuzzy, irregular vacuum fluctuations superimposed on the smooth wave described by classical physics. One could say that it is the interference with the vacuum fluctuations that causes ordinary light waves to be noisy.

This noise fundamentally limits the degree of precision possible in measurements involving light. It limits e.g. the precision of interferometers that gauge the interference patterns arising between beams of light that have been reflected by massive objects and then combined; such interferometers, which detect very small changes in the relative positions of the massive reflectors are components of devices designed to detect gravitational waves [6,7,8,9]. Noise also limits the precision of spectroscopy, in which the frequency and intensity of the radiation emitted by atoms or molecules yield information about their properties [7,8,9]. Eventually quantum noise will also limit the power of such technologies as optical computing and optical communications [7,8,9].

1.3 Electromagnetic field squeezed vacuum fluctuations

In spite of the fundamental noise limit set by the vacuum fluctuations of the electromagnetic field recent work on squeezed states of light has demonstrated ways in which the electric field uncertainty may be reduced below $\mathcal{E}_o$. It is indeed possible to "squeeze" the noise in a light beam by redistributing it so that parts of the light wave become less noisy than before, although other parts of the wave becomes noisier [7,8,9,10].

In Fig.s 1.3 we represent an electromagnetic field in a squeezed state with the same mean amplitude as that of Fig.s 1.1. The size of the fluctuations around the mean are indicated by the shaded band.

Squeezing is an important addition to the class of effects requiring field quantization for their explanation [11]. Squeezed states of light were first studied by theorists interested in their properties as generalized minimum-uncertainty states [6,12-19]. These properties were discovered independently by several workers using different terminologies and have been described variously as "pulsating wave packets" [12], "new coherent states" [18], and "ideal squeezed states" [6]. The first experimental realization of squeezed light was reported by Slusher and coworkers [20] using four-wave mixing in sodium atoms. They were able to reduce the optical noise below the vacuum fluctuations level by 7 to 10 % using a combination of phase-stable laser excitation and cavity field enhancement. Four-wave mixing in an optical fiber was used by Shelby and coworkers [21] to generate squeezed light with a 12 % reduction below the vacuum noise value. Furthermore use of a parametric down-conversion process to produce highly correlated pairs of photons at the subharmonic frequency of the pump laser could also lead to a considerable noise reduction (63 %) [22]. Clearly after these successes vacuum fluctuations can now be manipulated by non-linear-optical scientists.

1.4 Quantization of the electromagnetic field.

In order to illustrate these results and set the stage for the next chapters we will present in this section an outline of the description of quantized radiation fields. Full discussion of the topic may be found in the textbooks by Power [23] , Loudon [1], and Sargent, Scully and Lamb [3]. The aim is here to show that each field mode has the characteristics of a simple harmonic oscillator and that each can be quantized using results for the quantum harmonic oscillator.

Classical Fields

In classical electrodynamics the e.m. field in vacuum can be described by the lagrangian density [1,24]

$$l(\vec{r},t)=\frac{E^2(\vec{r},t)}{8\pi}-\frac{B^2(\vec{r},t)}{8\pi} \tag{1.4.1}$$

which is most conveniently written as

$$l(\vec{r},t)=\frac{1}{8\pi}[\,\vec{\nabla}\varphi(\vec{r},t)+\frac{1}{c}\frac{\partial\vec{a}(\vec{r},t)}{\partial t}]^2-\frac{[\vec{\nabla}\wedge\vec{a}(\vec{r},t)]^2}{8\pi} \tag{1.4.2}$$

if the electric and magnetic fields are expressed in terms of the scalar and vector potentials φ and $\vec{a}$ respectively,

$$\vec{E}(\vec{r},t)\equiv-\vec{\nabla}\varphi(\vec{r},t)-\frac{1}{c}\frac{\partial\vec{a}(\vec{r},t)}{\partial t}\qquad\vec{B}(\vec{r},t)\equiv\vec{\nabla}\wedge\vec{a}(\vec{r},t) \tag{1.4.3}$$

Variations of the components of φ and $\vec{a}$ gives a set of Eqs. of motion that can be written together as

$$\frac{1}{c}\frac{\partial\,\vec{\nabla}\varphi(\vec{r},t)}{\partial t}+\frac{1}{c^2}\frac{\partial\vec{a}(\vec{r},t)}{\partial t}+\vec{\nabla}\wedge\vec{\nabla}\wedge\vec{a}(\vec{r},t)=0 \tag{1.4.4}$$

$$\vec{\nabla}\cdot\vec{\nabla}\varphi(\vec{r},t)+\frac{1}{c}\vec{\nabla}\cdot\frac{\partial\vec{a}(\vec{r},t)}{\partial t}=0 \tag{1.4.5}$$

In conjunction with the definitions (1.4.3) these can be rewritten as

$$\frac{1}{c}\frac{\partial \vec{E}(\vec{r},t)}{\partial t} = \vec{\nabla} \wedge \vec{B}(\vec{r},t) \tag{1.4.6}$$

$$\vec{\nabla} \cdot \vec{E}(\vec{r},t) = 0 \tag{1.4.7}$$

Also, from (1.4.3) it follows directly

$$\frac{1}{c}\frac{\partial \vec{B}(\vec{r},t)}{\partial t} = -\vec{\nabla} \wedge \vec{E}(\vec{r},t) \tag{1.4.8}$$

$$\vec{\nabla} \cdot \vec{B}(\vec{r},t) = 0 \tag{1.4.9}$$

Eqs. (1.4.6-1.4.9) are the Maxwell Eqs. in vacuum: therefore (1.4.2) is a suitable lagrangian for our problem. If the potentials are known, Eqs. (1.4.3) enable $\vec{B}$ and $\vec{E}$ to be found. $\vec{B}$ and $\vec{E}$, which are physically measurable fields, do not depend on the choice of gauge. Here we find it convenient to work in the gauge in which

$$\vec{\nabla} \cdot \vec{a} = 0 \qquad \text{and} \qquad \varphi = 0$$

We now derive now the hamiltonian. The momentum conjugate to the field variable $\vec{a}$ is

$$\vec{p}_a(\vec{r},t) = \frac{1}{4\pi c^2}\frac{\partial \vec{a}(\vec{r},t)}{\partial t} = -\frac{1}{4\pi c}\vec{E}(\vec{r},t) \tag{1.4.10}$$

hence the hamiltonian density is

$$h = \vec{p}_a \cdot \frac{\partial \vec{a}}{\partial t} - L = 2\pi c^2 p_a^2 + \frac{1}{8\pi}(\vec{\nabla} \wedge \vec{a})^2 \tag{1.4.11}$$

The corresponding Hamilton Eqs. of motion are

$$\frac{\partial \vec{a}}{\partial t} = 4\pi c^2 \vec{p}_a \qquad \frac{\partial \vec{p}_a}{\partial t} = -\frac{1}{4\pi} \vec{\nabla} \wedge \vec{\nabla} \wedge \vec{a} \tag{1.4.12}$$

and h finally becomes

$$h = \int_V d\vec{r}\, 2\pi c^2 p_a^2 + \frac{1}{8\pi}(\vec{\nabla} \wedge \vec{a})^2 = \frac{1}{8\pi}\int_V d\vec{r}\ (E^2 + B^2) \tag{1.4.13}$$

which is the hamiltonian in terms of the field potential $\vec{a}$ and its conjugate momentum $\vec{p}_a$, or equivalently the electric and magnetic fields. Eq. (1.4.13) represents the total e.m. energy for the e.m. field in vacuum.

Normal modes and normal coordinates

The vector potential $\vec{a}$ is given by the Maxwell Eq. (1.4.6),

$$\nabla^2 \vec{a}(\vec{r},t) - \frac{1}{c^2}\frac{\partial^2 \vec{a}(\vec{r},t)}{\partial t^2} = 0 \tag{1.4.14}$$

Solutions are obtained by expanding and assuming separation of variables

$$\vec{a}(\vec{r},t) = \sum_{\lambda} \{a_\lambda(t)\vec{u}_\lambda(\vec{r}) + a_\lambda^*(t)\vec{u}_\lambda^*(\vec{r})\} \tag{1.4.15}$$

The (vector) mode $\vec{u}_\lambda(\vec{r})$ and the amplitudes $A_\lambda(t)$ obey the equations

$$\vec{\nabla} \wedge \vec{\nabla} \wedge \vec{u}_\lambda(\vec{r}) - \frac{\omega_\lambda^2}{c^2}\vec{u}_\lambda(\vec{r}) = 0 \tag{1.4.16}$$

$$\frac{\partial^2 a_\lambda(t)}{\partial t^2} + \omega_\lambda^2 a_\lambda(t) = 0 \tag{1.4.17}$$

with ω_λ a separation constant for each λ. Solutions of (1.4.17) are oscillating amplitudes with the frequency ω_λ

$$a_\lambda(t) = a_\lambda(t_o)e^{\pm i\omega_\lambda(t-t_o)} \tag{1.4.18}$$

with $a_\lambda(t_o)$ the amplitude of the potential $\vec{a}$ at some time t_o. The solutions of Eq. (1.4.16) are periodic. Depending on the nature of the problem the space properties of an e.m. wave can be described in terms of e.g. traveling waves or standing waves. Analogous treatments apply to both cases and for definiteness we will consider in the following *plane waves*. We then take

$$\vec{u}_\lambda(\vec{r}) \rightarrow \vec{u}_{\vec{k}}(\vec{r}) \equiv \hat{e}_{\vec{k}} e^{\pm i\vec{k}\cdot\vec{r}} \tag{1.4.19}$$

subject to periodic boundary conditions, i.e. the components of $\vec{k}$ take on the infinite series of discrete values

$$k_j = \frac{2\pi}{V^{1/3}} n_j \qquad j = x,y,z \qquad n_j = 0,\pm 1,\pm 2,\pm 3,.. \tag{1.4.20}$$

The $\vec{u}_{\vec{k}}(\vec{r})$'s are solutions of the Eq. (1.4.16) provided

$$k^2 = \frac{\omega_\lambda^2}{c^2} \equiv \frac{\omega_k^2}{c^2} \tag{1.4.21}$$

and provided

$$\hat{e}_{\vec{k}} \cdot \vec{k} = 0 \tag{1.4.22}$$

The latter derives from the Coulomb gauge condition and yields two independent directions of $\vec{u}_{\vec{k}}(\vec{r})$ for each $\vec{k}$, i.e. $\hat{e}_k^{(1)}$ and $\hat{e}_k^{(2)}$ (unit polarization vectors). Without loss of generality we consider only one of them (single polarization). The complete vector potential and conjugate momentum inside an *arbitrary* volume V are

$$\vec{a}(\vec{r},t) = \sum_{\vec{k}} \hat{e}_k \{a_{\vec{k}}(t_o) e^{-i|\vec{k}|c(t-t_o)+i\vec{k}\cdot\vec{r}} + a_{\vec{k}}^*(t_o) e^{+i|\vec{k}|c(t-t_o)-i\vec{k}\cdot\vec{r}}\} \tag{1.4.23}$$

$$\vec{p}_a(\vec{r},t) = \sum_{\vec{k}} \hat{e}_k \frac{|\vec{k}|}{4\pi c i} \{a_{\vec{k}}(t_o) e^{-i|\vec{k}|c(t-t_o)+i\vec{k}\cdot\vec{r}} - a_{\vec{k}}^*(t_o) e^{+i|\vec{k}|c(t-t_o)-i\vec{k}\cdot\vec{r}}\} \tag{1.4.24}$$

while the electric and magnetic fields are

$$\vec{E}(\vec{r},t) \equiv \sum_{\vec{k}} \vec{E}_{\vec{k}}(\vec{r},t) = i\sum_{\vec{k}} \hat{e}_k |\vec{k}| \{a_{\vec{k}}(t_o) e^{-i|\vec{k}|c(t-t_o)+i\vec{k}\cdot\vec{r}} - a_{\vec{k}}^*(t_o) e^{+i|\vec{k}|c(t-t_o)-i\vec{k}\cdot\vec{r}}\} \tag{1.4.25}$$

$$\vec{B}(\vec{r},t) \equiv \sum_{\vec{k}} \vec{B}_{\vec{k}}(\vec{r},t) = i\sum_{\vec{k}} \vec{k} \wedge \hat{e}_k \{a_{\vec{k}}(t_o) e^{-i|\vec{k}|c(t-t_o)+i\vec{k}\cdot\vec{r}} - a_{\vec{k}}^*(t_o) e^{+i|\vec{k}|c(t-t_o)-i\vec{k}\cdot\vec{r}}\} \tag{1.4.26}$$

Furthermore, using Eqs. (1.4.25-1.4.26), one can write the hamiltonian as

$$h \equiv \sum_{\vec{k}} h_{\vec{k}} \tag{1.4.27}$$

The decomposition in terms of the $a_{\vec{k}}(t)$'s enables us to describe the radiation by means of a *discrete* ensemble of variables $a_{\vec{k}}(t)$ instead of a *continuous* one. The $a_{\vec{k}}(t)$'s give the time variation of the amplitude of the electric and magnetic field associated with the normal mode of wavevector $\vec{k}$. As Eq. (1.4.17) suggests $a_{\vec{k}}(t)$ is also the oscillating coordinate of a harmonic oscillator (h.o.): the analogy with the h.o. is best seen by introducing an effective *"position"* and *"momentum"* associated with the mode

$$q_{\vec{k}}(t) = \sqrt{\frac{V}{4\pi c^2}}[z_{\vec{k}}(t) + z_{\vec{k}}^*(t)] \tag{1.4.28}$$

$$p_{\vec{k}}(t) = -ick\sqrt{\frac{V}{4\pi c^2}}[a_{\vec{k}}(t) - a_{\vec{k}}^*(t)] \tag{1.4.29}$$

in terms of which the hamiltonian reduces to

$$h = \frac{1}{2}\sum_{\vec{k}} \{p_{\vec{k}}^2 + c^2k^2q_{\vec{k}}^2\} \tag{1.4.30}$$

Each mode of the radiation field is then formally equivalent to a single h.o. of frequency ck.

The fields can be expressed in terms of the q_k's and P_k's, by inverting Eqs. (1.4.28-1.4.29)

$$A_{\vec{k}}(t) = \frac{i}{k}\sqrt{\frac{\pi}{V}}[p_{\vec{k}}(t) - ickq_{\vec{k}}(t)] \tag{1.4.31}$$

$$A_{\vec{k}}^*(t) = -\frac{i}{k}\sqrt{\frac{\pi}{V}}[p_{\vec{k}}(t) + ickq_{\vec{k}}(t)] \tag{1.4.32}$$

and substituting into Eqs. (1.4.23-1.4.24)

$$\vec{a}(\vec{r},t) = \sum_{\vec{k}} \frac{\hat{e}_k}{k}\sqrt{\frac{4\pi}{V}}\{ckq_{\vec{k}}(t)\cos\vec{k}\cdot\vec{r} - p_{\vec{k}}(t)\sin\vec{k}\cdot\vec{r}\} \tag{1.4.33}$$

$$\vec{p}_A(\vec{r},t) = -\sum_{\vec{k}} \frac{\hat{e}_k}{c}\sqrt{\frac{1}{4\pi V}}\{ckq_{\vec{k}}(t)\sin\vec{k}\cdot\vec{r} + p_{\vec{k}}(t)\cos\vec{k}\cdot\vec{r}\} \tag{1.4.34}$$

and

$$\vec{E}(\vec{r},t) = -\sum_{\vec{k}} \hat{e}_k\sqrt{\frac{4\pi}{V}}\{ckq_{\vec{k}}(t)\sin\vec{k}\cdot\vec{r} + p_{\vec{k}}(t\cos\vec{k}\cdot\vec{r}\} \tag{1.4.35}$$

$$\vec{B}(\vec{r},t) = -\sum_{\vec{k}}(\vec{k}\wedge\hat{e}_k)\{ck\,q_{\vec{k}}(t)\sin\vec{k}\cdot\vec{r} + p_{\vec{k}}(t)\cos\vec{k}\cdot\vec{r}\} \tag{1.4.36}$$

The q_k's and p_k's are 90° out of phase components of the fields.

Quantum fields

The *classical* e.m. field is converted into a *quantum* field in the following way. The starting point is the hamiltonian (1.4.13) and the field variables $\vec{a}$, $\vec{p}_a$. The Eq of motion for a generic classical field variable F is [4,5]

$$\frac{d\,F}{d\,t} = \frac{\partial\,F}{\partial\,t} + \{F\,,\,H\,\} \tag{1.4.37}$$

while the Eq. of motion for the corresponding quantum variable is obtained replacing the Poisson bracket {,} in (1.4.37) by the commutator bracket [,] divided by $i\hbar$ and replacing the classical field variable by an operator. Therefore for the field operators $\hat{\vec{a}}$ and $\hat{\vec{p}}_a$ one has

$$\frac{d}{dt}\begin{Bmatrix}\hat{\vec{a}}(\vec{r},t)\\ \hat{\vec{p}}_a(\vec{r},t)\end{Bmatrix}=\frac{\partial}{\partial t}\begin{Bmatrix}\hat{\vec{a}}(\vec{r},t)\\ \hat{\vec{p}}_a(\vec{r},t)\end{Bmatrix}-i\hbar\begin{bmatrix}\hat{\vec{a}}(\vec{r},t)\ ,\hat{h}\\ \hat{\vec{p}}_a(\vec{r},t),\hat{h}\end{bmatrix} \tag{1.4.38}$$

where $\hat{h}$ is the relevant hamiltonian operator. These field operators satisfy the commutation rules

$$\begin{aligned}&[\hat{\vec{a}}(\vec{r},t)\ ,\hat{\vec{a}}(\vec{r}',t)]=[\hat{\vec{p}}_a(\vec{r},t)\ ,\hat{\vec{p}}_a(\vec{r}',t)]=0\\ &[\hat{\vec{a}}(\vec{r},t)\ ,\hat{\vec{p}}_a(\vec{r}',t)]=i\hbar\delta(\vec{r}-\vec{r}')\end{aligned} \tag{1.4.39}$$

That these are the correct commutation rules can be proved by showing that the Eq. of motion (1.4.38) with (1.4.39) give the corresponding classical Hamilton Eqs. (1.12) [25]. Using the result (1.4.39) along with Eqs. (1.4.33-34), the commutation rules for the position and momentum operators can also be derived,

$$[\hat{q}_k(t)\ ,\hat{p}_{k'}(t)]=[\hat{q}_k(t_o)\ ,\hat{p}_{k'}(t_o)]=ih\delta_{k,k'} \tag{1.4.40}$$

In turn from this and the definitions in Eqs. (1.4.31-32) one can derive the commutation rules for the operators corresponding to the classical Fourier amplitudes $a_{\underline{k}}(t)$ and $a^*_{\underline{k}}(t)$, i.e.

$$[\hat{a}_k(t)\ ,\hat{a}^\dagger_{k'}(t)]=[\hat{a}_k(t_o)\ ,\hat{a}^\dagger_{k'}(t_o)]=\frac{2\pi\hbar c}{kV}\delta_{k,k'} \tag{1.4.41}$$

while all other pairs commute. The results (1.4.40-41) directly stem from the commutation relation (1.4.39). Equivalently the commutation rule (1.4.40) can be

obtained from Eq. (1.38) by using Eqs. (1.4.23-24), from which one can in turn obtain eq (1.4.40) by using Eqs. (1.4.28-29).

We finally turn to the quantum mechanical expression for the hamiltonian. Substitution of Eqs. (1.4.33-34) (or 1.4.35-36) into the hamiltonian (1.4.13) yields

$$\hat{h} \equiv \sum_k h_k = \sum_k \frac{1}{2}(\hat{p}_k^2 + c^2 k^2 \hat{q}_k^2) \tag{1.4.42}$$

This is equivalent to converting directly (q,p) into quantum-mechanical position and momentum operators $(\hat{q},\hat{p})$ obeying the commutation rules of Eq. (1.4.40). The most useful form of $\hat{h}$ however is the one in terms of the discrete number of quanta. Substituting the expressions of $(\hat{q},\hat{p})$ in terms of $\hat{a}_k$ and $\hat{a}_k^\dagger$ into Eq. (1.4.42) one obtains

$$\hat{h} = \sum_k \frac{Vk^2}{2\pi}(\hat{a}_k \hat{a}_k^\dagger + \hat{a}_k^\dagger \hat{a}_k) \tag{1.4.43}$$

Adopting the definition

$$\hat{n}_k \equiv \frac{Vk}{2\pi\hbar c}\hat{a}_k^\dagger \hat{a}_k \tag{1.4.43}$$

the hamiltonian becomes

$$\hat{h} = \sum_k \hbar ck(\hat{n}_k + \frac{1}{2}) = \sum_k \hbar ck(\hat{\hat{a}}_k^\dagger \hat{\hat{a}}_k + \frac{1}{2}) \tag{1.4.45}$$

$\hat{\tilde{a}}_k \equiv \sqrt{Vk/2\pi\hbar c}\,\hat{a}_k$, and here $\hat{n}_k$ each have integer eigenvalues. Eq. (1.4.45) is equivalent to Planck's quantum hypothesis: the energy associated with each (plane) electromagnetic wave is an integer multiple of the fundamental quantum $h\nu = \hbar ck$. In addition to the Planck energy there is the harmonic oscillator zero-point energy of one-half quantum per mode of the field, which is infinite since there are an infinite number of modes [1,24].

The transition from classical to quantum mechanics is thus achieved by replacing the classical Fourier coefficients a_k and a_k^* respectively with the destruction and creation operators $\hat{\tilde{a}}_k$ and $\hat{\tilde{a}}_k^\dagger$. It should be noted that the latter rather than the $\hat{a}_k$'s and $\hat{a}_k^\dagger$'s provide the correct full analogy with the harmonic oscillator. The quantization procedure indeed is such as to guarantee the energy expressions to be of the form shown in Eq. (1.4.45); in other words the choice of numerical factors in the transition to quantum mechanical operators is governed by the requirement that the mode energy should have the harmonic-oscillator form, both in the classical and the quantum mechanical case.

1.5 Quantum states of a single mode electromagnetic field

In this section we will discuss those properties of the quantum states of the radiation field of relevance to us. We will consider for definiteness a *cavity single mode*: it is defined by a given wavevector, polarisation and frequency of the electropmagnetic field inside the cavity. This behaves like a single harmonic oscillator of unit mass and is described by the "position" and "momentum" operators $\hat{q}$ and $\hat{p}$ related to the conjugate electric field and magnetic operators $\hat{E}$ and $\hat{B}$ (see § 1.4). If we assume for simplicity that the field is confined within a one

dimensional cavity whose axis is parallel to the z-axis, and is linearly polarized, we can write (cf. Eq.)

$$\hat{E}(z,t) = (2\omega^2 / \varepsilon_o V)^{1/2} \hat{q}(t) \sin kz \qquad \hat{B}(z,t) = (2\varepsilon_o c^2 / V)^{1/2} \hat{p}(t) \cos kz \tag{1.5.1}$$

In terms of the destruction and creation operators $\hat{a}$ and $\hat{a}^\dagger$ the electric field operator for the cavity mode of frequency ω can be written as

$$\hat{E}(z,t) = (\mathcal{E}_c / 2)[\hat{a}(t) + \hat{a}^\dagger(t)] \qquad \hat{a}(t) = \hat{a}(0) e^{i\omega t} \qquad \mathcal{E}_c \equiv 2^{3/2} \mathcal{E}_o \sin kz \tag{1.5.2}$$

where $\mathcal{E}_c$ is the natural unit of electric field strength in the cavity and $\mathcal{E}_o$ the electric field per photon (see § 1.1)

Vacuum state.

Any discussion of quantum states begins with the vacuum state $|0\rangle$. A discussion of the physics relevant to this state has been given in § 1.2. This is the state of the electromagnetic field in which no photons are excited in any of the field modes. This state has the interesting property that although no excitation is present, the energy does not vanish, it equals $\hbar\omega / 2$. This quantity is called the *zero-point energy* of the field: it is the energy of the ground state of the harmonic oscillator associated with the field mode. Mathematically it is defined as the state which is annihilated by the annihilation operator $\hat{a}$

$$\hat{a}|0\rangle = 0 \tag{1.5.3}$$

Number states.

The single mode number states $|n\rangle$ are the states where *exactly* n photons of the given mode are excited. They are energy eigenstates of the harmonic oscillator associated with the electromagnetic field in the mode. These are a convenient basis when experiments with a fixed number of particles are involved and they have simple properties. Although these states are not of direct significance in a typical optical experiment where the exciting probe is usually a light source such as a laser with *no definite* numbers of photons, recent developments in the production of number states should be mentioned. It has been in fact possible to generate extremely sub-poissonian light fields by using feed-back stabilized laser and even one-photon wavepackets using an optical shutter technique based on coincidence counting of the of the output of a paramplifier [see e.g. ref. 87].

From a mathematical point of view an n-photon state can be introduced by defining the repeated action of the photon creation operator on the vacuum, i.e.

$$|n\rangle = (n!)^{-1/2}\,\hat{a}^{\dagger n}|0\rangle \tag{1.5.4}$$

This in turn gives the important lowering and raising characteristics of the photon destruction and creation operators on number states,

$$\hat{a}|n\rangle = n^{1/2}|n-1\rangle \qquad \hat{a}^{\dagger}|n\rangle = (n+1)^{1/2}|n+1\rangle \tag{1.5.5}$$

Coherent states.

The single mode states of physical importance correspond not to the individual number states but to linear superpositions of the states $|n\rangle$. A wide variety of superposition states is possible but one kind, the coherent state, is of particular importance in the practical applications of quantum theory of light. These states have an electric field variation that in the limit of high excitation approaches that of the classical electromagnetic wave with stable amplitude and fixed phase. They are important not only because they are the closest quantum-mechanical approach to a classical electromagnetic wave, but also because a single mode laser operated well above its threshold of oscillation generates such a state.

From a mathematical point of view the coherent state can be introduced as the eigenstate of the annihilation operator $\hat{a}$

$$\hat{a}|\alpha\rangle = \alpha|\alpha\rangle \tag{1.5.6}$$

where α is a complex amplitude $\alpha \equiv |\alpha| \exp[i\phi]$. A useful and unique expansion in terms of number states $|n\rangle$ can be given as

$$|\alpha\rangle = \exp(-\frac{|\alpha|^2}{2}) \sum_{n=0}^{\infty} \frac{\alpha^n}{\sqrt{n!}} |n\rangle \tag{1.5.7}$$

It can be shown that the probability number distribution P_n in this state is Poissonian

$$P_n \equiv |\langle n|\alpha\rangle|^2 = \exp(-|\alpha|^2) \frac{\alpha^{2n}}{n!} \tag{1.5.8}$$

The number of photons that may be found in a coherent state is unbounded: it may range from 0 to ∞. From Eq. (1.5.8) follows that the magnitude of the eigenvalue α has a simple physical interpretation: its square gives either the spread of the distribution or the mean number of photons in the coherent state

$$\langle\alpha|(\Delta\hat{n})^2|\alpha\rangle = |\alpha|^2 = \langle\alpha|\hat{n}|\alpha\rangle \qquad \hat{n} \equiv \hat{a}^\dagger\hat{a} \tag{1.5.9}$$

In the harmonic oscillator picture $|\alpha|$ is the analogue of the amplitude of the oscillator and ϕ the analogue of the oscillator phase. The coherent state (1.5.9) is normalised and the set of coherent states is overcomplete [1,3].

Squeezed states.

From a mathematical point of view these states are unitarily related to the vacuum, number, and coherent states above, in the sense that

$$|0\rangle_{sq.} = S(r,\phi)\,|0\rangle \qquad \textit{Squeezed vacuum state} \tag{1.5.10}$$

$$|n\rangle_{sq.} = S(r,\phi)\,|n\rangle \qquad \textit{Squeezed number state} \tag{1.5.11}$$

$$|\alpha\rangle_{sq.} = S(r,\phi)\,|\alpha\rangle \qquad \textit{Squeezed coherent state} \tag{1.5.12}$$

The unitary transformation S can be written as

$$S(r,\phi) = \exp[\tfrac{1}{2}z^*\hat{a}^2 - \tfrac{1}{2}z\hat{a}^{\dagger 2}] \qquad z \equiv re^{i\phi} \tag{1.5.13}$$

where r is a real number and ϕ is a (real) phase angle. Equivalently, $|0\rangle_{sq.}$, $|n\rangle_{sq.}$, and $|\alpha\rangle_{sq.}$ can be defined through the eigenvector equations

$$\hat{\mu}\,|0\rangle_{sq.} = 0 \qquad \textit{Squeezed vacuum state} \qquad (1.5.14)$$

$$\hat{\mu}^{\dagger}\hat{\mu}|n\rangle_{sq.} = n|n\rangle_{sq.} \qquad \textit{Squeezed number state} \qquad (1.5.15)$$

$$\hat{\mu}|\alpha\rangle_{sq.} = \mu\,|\alpha\rangle_{sq.} \qquad \textit{Squeezed coherent state} \qquad (1.5.16)$$

where $\hat{\mu} \equiv S\hat{a}S = \hat{a}\cosh r + \hat{a}^{\dagger}e^{i\phi}\sinh r$ is the squeeze annihilation operator.

Minimum uncertainty states.

Now consider the fluctuations in an observable $\hat{O}$. These can be described by the variance $\langle(\Delta\hat{O})^2\rangle \equiv \langle\hat{O}^2\rangle - \langle\hat{O}\rangle^2$ where for brevity $\langle\hat{O}\rangle$ stands for $\langle\psi|\hat{O}|\psi\rangle$. The variance is a state dependent quantity. We note that the variances of two observable quantities for the same state $|\psi\rangle$ satisfy the uncertainty relation

$$\langle(\Delta\hat{A})^2\rangle\langle(\Delta\hat{B})^2\rangle \geq \frac{1}{4}|\langle[\hat{A},\hat{B}]\rangle|^2 \qquad (1.5.17)$$

and if the equality sign holds, the state $|\psi\rangle$ is called a *minimum uncertainty state* [MUS].

The "position" and "momentum" operators $\hat{q}$ and $\hat{p}$ introduced in the previous section are useful quantities to describe the conjugate electric field and magnetic operators $\hat{E}$ and $\hat{B}$. However $\hat{q}$ and $\hat{p}$ have different dimensions and we find it convenient to introduce dimensionless operators

$$\hat{X} \equiv \frac{1}{2}(\hat{a} + \hat{a}^{\dagger}) = \sqrt{\frac{\omega}{2\hbar}}\,\hat{q} \tag{1.5.18}$$

and

$$\hat{Y} \equiv \frac{1}{2i}(\hat{a} - \hat{a}^{\dagger}) = \sqrt{\frac{1}{2\hbar\omega}}\,\hat{p} \tag{1.5.19}$$

The electric field operator e.g. in terms of these new quadratures is (cf. Eq. 1.5.1-2)

$$\hat{E}(z,t) = \Im_e(\hat{X}\cos\omega t + \hat{Y}\sin\omega t) \tag{1.5.20}$$

The quadratures satisfy the commutation rules

$$[\hat{X},\hat{Y}] = i/2 \tag{1.5.21}$$

and their variances satisfy the uncertainty relation

$$\langle(\Delta\hat{X})^2\rangle\langle(\Delta\hat{Y})^2\rangle \geq \frac{1}{16} \tag{1.5.22}$$

in agreement with Eq. (1.5.17).

It is straightforward to show that for a coherent state or for the special case of the vacuum state the variances of the two quadratures are equal $\langle(\Delta\hat{X})^2\rangle = \langle(\Delta\hat{Y})^2\rangle = 1/4$ and, since the equal sign holds in the inequality (1.5.22), the coherent and vacuum states of the radiation field are MUS for the quadrature operators $\hat{X}$ and $\hat{Y}$. Conversely, for a number state the quadrature variances are equal

$$\langle(\Delta\hat{X})^2\rangle=\langle(\Delta\hat{Y})^2\rangle=\frac{1}{4}(2n+1) \tag{1.5.23}$$

but these states are not MUS, except again for the special case of the vacuum, to which Eq. (5.1.23) reduces when $n=0$. A different and interesting scenario emerges in the case of squeezed states in that

$$\langle(\Delta\hat{X})^2\rangle=\frac{1}{4}[e^{-2r}\cos^2\frac{\phi}{2}+e^{+2r}\sin^2\frac{\phi}{2}] \tag{1.5.24}$$

$$\langle(\Delta\hat{Y})^2\rangle=\frac{1}{4}[e^{-2r}\sin^2\frac{\phi}{2}+e^{+2r}\cos^2\frac{\phi}{2}] \tag{1.5.25}$$

are the variances for the squeezed vacuum and squeezed coherent states, whereas

$$\langle(\Delta\hat{X})^2\rangle=\frac{(2n+1)}{4}[\cosh 2r-\cos\phi\sinh 2r] \tag{1.5.26}$$

$$\langle(\Delta\hat{Y})^2\rangle=\frac{(2n+1)}{4}[\cosh 2r+\cos\phi\sinh 2r] \tag{1.5.27}$$

are those for squeezed number states. Note that when $r=0$ these give the results for the vacuum, number and coherent states with equal variances. In particular, unlike *coherent* and *vacuum states* which are MUS with two equal quadrature uncertainties, *coherent* and *vacuum squeezed states* have unequal quadrature uncertainties. The uncertainty product obtained from Eqs. (1.5.24-25) is

$$\langle(\Delta\hat{X})^2\rangle\langle(\Delta\hat{Y})^2\rangle=\frac{1}{16}[\cos^2\phi+\cosh^2 2r\sin^2\phi] \tag{1.5.28}$$

This takes the minimum (uncertainty state) value

$$\langle(\Delta\hat{X})^2\rangle\langle(\Delta\hat{Y})^2\rangle=\frac{1}{16} \qquad \text{for} \qquad \phi=0 \ \text{or} \ \pi \qquad (1.5.29)$$

but is larger for other angles, with a maximum value

$$\langle(\Delta\hat{X})^2\rangle\langle(\Delta\hat{Y})^2\rangle=\frac{1}{16}\cosh^2 2r \qquad \text{for} \qquad \phi=\frac{1}{2}\pi \ \text{or} \ \frac{3}{2}\pi \qquad (1.5.30)$$

The squeezed vacuum and squeezed coherent states may, but need not, be MUS. Only for the two values of ϕ above they indeed remain MUS. Eqs. (1.5.24-25) display the main feature of squeezed states of light, i.e. quantum states in which the zero-point energy fluctuations of the electromagnetic field can be reduced below the vacuum noise limit in one of the field quadratures and that is by compressing one variance at the expense of an expansion of the conjugate variance. The particular case for $\phi=0 \ \text{or} \ \pi$ explains it rather clearly. Strictly speaking the squeezed vacuum and squeezed coherent states are called quadrature-squeezed states as opposed to other states of the radiation field in which effects of squeezing occur in observables other than quadratures [26]. Incidentally note that squeezed number states ($n \neq 0$) are not quadrature-squeezed states; in fact the variances in Eqs. (1.5.26-27) are never smaller than 1/4. The quadratures of a light wave and the relevant fluctuations (noise) can be measured via phase-sensitive detection schemes. Homodyning, for instance, is currently used to extract the quadrature of the field carrying reduced fluctuations

Representation

In the last part of this section we provide representations for the quantum states of light that we have discussed above. It is useful to depict these states in an X vs. Y phase space, the two coordinates being respectively $X \equiv \langle \hat{X} \rangle$ and $Y \equiv \langle \hat{Y} \rangle$. The square roots of the corresponding variances, that is $\Delta X \equiv \langle (\Delta \hat{X})^2 \rangle^{1/2}$ and $\Delta Y \equiv \langle (\Delta \hat{Y})^2 \rangle^{1/2}$, are equal to the projections of the circle on the X and Y axes.

In Fig. 1.4 coherent light is depicted as having a mean field $|\alpha|$ and a phase ϕ. The quantum uncertainty about this mean field value is represented by an error circle of area $\pi/16$: this involves the measurement process as the circle is only a schematic representation of a Gaussian distribution. The special case when $|\alpha|=0$, complete darkness, is represented as an error circle about the origin (see Fig. 1.5).

In Fig. 1.6 a representative squeezed state is depicted. As with the coherent state, a squeezed state will generally have a mean field specified by an amplitude $|\alpha|$ and a phase ϕ. One now has an error ellipse which requires at least two more numbers to specify it: the degree to which the radius has been reduced below the diameter of uncertainty for a coherent or vacuum value, and the angular orientation of the ellipse. A simple application of elliptical theory [27] shows that the projections of the ellipse on to the X and Y axes are equal to the square roots of the corresponding variances (cf. Fig. 1.6). When $\Delta X \Delta Y = 1/4$ then the squeeze state is said to be a MUS and the area of the ellipse is the same as that of the coherent or vacuum state i.e. $\pi/16$. As predicted in Eq. (1.5.29) this can be achieved only for $\phi = 0$ *or* π, namely when the long diameter of the ellipse is normal or parallel to the X axis.

In Fig. 1.7 we report the quadrature-phase space representation of the mean value and uncertainty contour for a number state and a squeezed number state.

1.6 Quantum states of a two-mode (multimode) electromagnetic field.

The light produced by any optical system is an excitation of several modes of the electromagnetic field. In one-photon devices, like lasers, photons are emitted into the output modes one at a time whereas in two-photon devices the output light is generated by simultaneous emission of two photons into two of the output modes. Two-photon devices are, for instance, parametric amplifiers, where the simultaneously excited output modes are referred to as the signal and the idler, and four wave mixers, where the output modes are the transmitted and reflected waves. In a paramplifier for instance an intense laser beam (pump) at frequency 2Ω illuminates a suitable medium whose nonlinearity couples the pump beam to other modes of the e.m. field in such a way that a pump photon at frequency 2Ω can be annihilated to create signal and idler photons at different frequencies ω_1 and ω_2, with $2\Omega = \omega_1 + \omega_2$. Conversely, signal and idler photons can be annihilated to create a pump photon. Thus the light produced in this device consists in a pair of simultaneously emitted photons which excite pairs of modes at the frequencies $\omega_{1,2}$.

One can introduce vacuum, number and coherent states for a two-mode radiation field as much in the same way as done in § 1.5. The mathematical foundation for the two-mode formalism was given by Shumaker and Caves [28,29] who showed that two-mode properties can be written as compactly as the comparable properties for a single mode. Although we will refer to their work, without repeating definitions and properties of two-mode states of the

electromagnetic field, we will however emphasize here the two-mode squeezed states. Two-photon devices can, in principle, produce two-mode squeezed states. A parametric amplifier e.g. can ideally produce squeezed light with characteristics similar to the single or the two-mode varieties described here [7-10]. Real squeezing experiments are indeed carried out generally over a range of frequencies, not a single frequency [7-10].

Two mode squeezed states

In the theory of squeezing one has then to distinguish between squeezed states in one mode of radiation and those which are related to two modes of radiation [29]. Introduced independently by C. Caves [30] in analysis of quantum limits of performance of linear amplifiers, by W.G. Unruh in a quantum mechanical analysis of an interferometer [31] and also studied formally by A.O. Barut [32], A.M. Perelomov [33] and G.J. Milburn [34], two-mode squeezed states are defined in analogy with Eqs. (1.5.10-12) and (Eqs. (1.5.14-16). Here the generator of the squeeze transformation is

$$S(r,\phi) = \exp[\hat{a}_1\hat{a}_2 re^{-2i\phi} - \hat{a}_1^\dagger \hat{a}_2^\dagger re^{+2i\phi}] \tag{1.6.1}$$

while the annihilation operator is $\hat{\mu}_{1,2} \equiv S\,\hat{a}_{1,2}\,S = \hat{a}_1 \cosh r + \hat{a}_2^\dagger e^{2i\phi} \sinh r$. Quadrature phase amplitudes can be defined with respect to the frequency $\omega_c \equiv (\omega_1 + \omega_2)/2$

$$\hat{\alpha}_X = \sqrt{\frac{\omega_1}{2\omega_c}}\,\hat{a}_1 + \sqrt{\frac{\omega_2}{2\omega_c}}\,\hat{a}_2^\dagger \qquad \hat{\alpha}_Y = -i\sqrt{\frac{\omega_1}{2\omega_c}}\,\hat{a}_1 + i\sqrt{\frac{\omega_2}{2\omega_c}}\,\hat{a}_2^\dagger \tag{1.6.2}$$

so that the electric field again takes the form

$$\hat{E}(z,t) = \hat{X}(z,t)\cos\omega_c(t-\tfrac{z}{c}) + \hat{Y}(z,t)\sin\omega_c(t-\tfrac{z}{c}) \quad (1.6.3)$$

Here

$$\hat{X}(z,t) = \sqrt{\omega_c}\,\{\exp[-i(t-\tfrac{z}{c})\omega_m\,\hat{\alpha}_X + h.c.\} \quad (1.6.4)$$

$$\omega_m \equiv \frac{\omega_1 - \omega_2}{2}$$

$$\hat{Y}(z,t) = \sqrt{\omega_c}\,\{\exp[-i(t-\tfrac{z}{c})\omega_m\,\hat{\alpha}_Y + h.c.\} \quad (1.6.5)$$

are the relevant quadrature operators. In the parametric generation of two-mode squeezed states ω_c and ω_m are respectively referred to as the carrier and modulation frequencies whereas ω_1 and ω_2 are the idler and signal frequencies. As for the single mode counterpart, in a two-mode squeezed state the variance of one of the conjugate quadratures in Eqs. (1.6.4-5) can be made smaller than it would be in a coherent or vacuum state of the field [2,8,9].

Incidentally, from Eqs. (1.6.4-5) we see that if we were to squeeze $\hat{X}$ to zero we would require $\hat{a}_1 \cong -\hat{a}_2^\dagger$ and similarly if we wanted to squeeze $\hat{Y}$ to zero we would require $\hat{a}_1 \cong \hat{a}_2^\dagger$. Hence squeezing amounts to establishing correlations in the quantum noise between pairs of frequencies symmetric about ω_c. Correlations produced by two-photon processes cannot be expressed in terms of independently excited single modes. The difference between one-photon and two-photon processes resides in the fact that, unlike the former one-photon process, the latter have indeed correlated complex amplitudes. Mode correlations can be viewed in

general as the origin of quadrature noise reduction in two-mode squeezed states [8,9,35].

1.7 The polariton mode

Concept

In the usual classical electrodynamics light propagating in a dispersive dielectric or magnetic medium is characterized by phase, group and energy transport velocities, Poynting vectors and energy densities. The optical properties of the medium are expressed in terms of the frequency and wavevector dependent complex dielectric constant and magnetic permeability tensors of the medium. The dielectric constant and magnetic permeability tensors are in turn expressed in terms of the electric dipole and magnetic excitations of the medium. The e.m. wave equation, obtained from Maxwell's equation and the constitutive relations $\vec{D} = \varepsilon \vec{E}$ and $\vec{B} = \mu \vec{H}$, is used as a mean of expressing the phase velocities of the wave in terms of the dielectric constant and magnetic permeability tensors.

Exactly as the photon describes an excitation of the e.m. field, phonon, magnon, plasmon, polaron and exciton describe an excitation of several fields in the crystal. Phonons are associated with elastic excitations, magnons are elementary magnetic excitations, plasmons are collective coulomb interactions of electrons, polarons are electrons or holes dressed by the elastic polarization field and excitons are neutral electronic quasi-particles associated with the dielectric polarization field [36].

Under certain conditions these excitations of the crystal may interact with an external radiation field [36-37]. Transverse optical phonons and transverse photons

couple and at resonance the phonon-photon coupling entirely changes the character of the propagation. By resonance we mean a condition in which the frequencies and wavevectors of both participating particles are approximately equal. Similarly for the exciton. The resulting normal mode of the coupled polarization-radiation system is called a *polariton* mode [37], specifically the phonon-photon coupled mode is referred to as phonon-polariton, while that of the coupled exciton-photon as exciton-polariton.

Theory

Polaritons have been well known for at least 40 years since the independently pioneering work of Tolpygo [38] and Huang [39]. Tolpygo in 1950 and Huang in 1951 derived the dispersion relation $\omega = \omega(k) \equiv \omega_k$ for the infrared active optical lattice vibrations of a cubic ionic crystal by combining the classical equations of motion for the lattice vibrations with Maxwell's equations. In doing so they showed that the transverse eigenmodes of the crystal correspond to coupled *e.m. radiation-lattice vibration modes* whose relative radiative and lattice vibrational components were functions of the frequency and wavevector. They also showed that the longitudinal modes of the crystal were decoupled, and remain identical to the longitudinal optical lattice vibrations. This showed that the coupled transverse modes were in fact the propagating modes of this medium.

The theoretical framework for predicting and analyzing the optical properties of these mixed modes was early developed among others by Pekar [40], Ginzburg and Agranovich [41] and Hopfield [42]. Striking success was achieved by using rather simple theoretical models which encompass the major relevant physics.

Pekar [40] formulated a macroscopic theory of the coupled *e.m. radiation-exciton modes* analogous to the theory which Huang had developed for the coupled e.m. radiation optical lattice vibration modes. Note that when effects of spatial dispersion (finite wavevector effects) are disregarded a forbidden band is established in the polariton spectrum. Pekar emphasized the importance of spatial dispersion and proved the existence of an additional light wave at frequency higher than the longitudinal exciton frequency. Since the boundary conditions imposed by Maxwell equations are not sufficient to specify the relative intensity of the two modes, an additional boundary condition (ABC) is required. A persistent theoretical effort has been made on this direction especially by Pekar [40], Agranovich and Ginzburg [43], and Birman [44], leading to different ABC conditions.

In 1956, Fano [45] independently formulated a *quantum theory* of the modes arising from the interaction of an assembly of electronic oscillations, representing the long-wave excitations of matter, with the e.m. field oscillators.

Subsequently, Hopfield [42] developed the detailed quantum treatment of the interaction of excitons with e.m. radiation in isotropic crystals and showed that the eigenstates of the coupled crystal-radiation field are composite particles of photons and excitons, i.e. polariton modes. Also Hopfield started the microscopic theory of exciton-polaritons using the Frenkel model of the exciton [44] to treat its interaction with the electromagnetic field. Agranovich [41,43] then developed a microscopic theory of Frenkel excitons in interaction with the electromagnetic field, including spatial dispersion.

With respect to the usual classical electrodynamics formulation, the polariton approach provides an alternate method for describing the optical properties of a medium. But more significantly, as pointed out by Pekar, Agranovich, Ginzburg,

Hopfield, and Loudon it provides a proper physical basis for observing and interpreting new optical phenomena [40-43,46].

Experiment

On the experimental side certain properties of the polaritons have been extensively investigated by a variety of spectroscopic methods. In particular, the resonant Brillouin scattering (RBS) technique first predicted and theoretically analyzed by Brenig, Zeyher and Birman [47] has permitted careful and quantitative mapping of the frequency-wavenumber dispersion $\omega = \omega_k$ for exciton-polaritons. In addition delicate steady-state optical reflection and transmission studies using polarized light, and optical pulse (transient) studies have complemented the RBS scattering experiments to determine ω_k with very high precision. Many details are given in several review volumes [48]. Phonon polaritons have been studied by related methods, which in many cases antedate the work on exciton-polaritons [49].

We report in Fig. 1.8 dispersion curves for exciton-polaritons in CuCl (spatial dispersion not included) [48].

1.8 Precis

Quantum electrodynamics has made possible to explain and predict a very large number of phenomena associated with the behaviour of photons, such as the effect of squeezing. The study of this new phenomenum is of undoubted interest as one further possibility of verifying directly the predictions of quantum electrodynamics. Some of the early work, particularly that of Stoler [14,15] and Walls [10] was

definitely motivated by fundamental issues involving the quantum nature of light. However, this does not exhaust its value. It was realized in the early stages of squeezed light research that the ability to influence the randomness and granularity of light might be useful in improving the performance of communication systems. In fact most of the work on squeezed light, work carried out by Takahashi [12] as well as Yuen [18,50] and Shapiro [50], primarily addressed quantum communication issues. It is essential to emphasize that issues involving the ultimate sensitivity of measurement instruments, in particular gravitational wave detectors, also provided a strong drive for squeezed states research, e.g. in the work of Hollenhorst [19] and Caves [6, 30]. Very striking was the demonstration by Caves that interferometry sensitivity can be greatly enhanced injecting squeezed light into the unused port of the interferometer [6]. With the successful generation of squeezed light by a number of laboratories [7-10], it has now been learned how to exercise some modest degree of control over photon statistics.

However, this new effect found in optics has a certain generality and it may therefore have analogs in the physics of condensed media. The mathematical resemblance in the formulation of physical problems allows one to investigate the role of collective quantum states not only in quantum optics, but also in condensed matter physics.

Theoretically, collective states in the quantum optical problems are generated by various types of boson interactions. The simplest of these processes is described by the hamiltonian [29]

$$\hat{H} = \hbar\omega(\hat{b}^{\dagger}\hat{b} + 1/2) + (g\hat{b}\hat{b} + g^{*}\hat{b}^{\dagger}\hat{b}^{\dagger}) \qquad (1.8.1)$$

The first term is simply the free evolution of the field mode that is being squeezed. $\hat{b},\hat{b}^{\dagger}$ are respectively the annihilation and creation operators for the photon field. The interaction term, that contains terms quadratic in the creation or annihilation operators of the field, cause pairs of quanta to be created or annihilated in the mode. Amplitude squeezing is produced by an interaction which depends quadratically on the field amplitude such as $\hat{H}$ above. Other quadratic hamiltonians that generate squeezing have been systematically analysed by Schumaker [29]. It is crucial to stress that in this simple case and more complicated ones the system hamiltonian is bilinear in Bose operators, which allows one to get exact solutions with the help of a canonical Bogoliubov transformation so that different physical phenomena can be studied in much the same manner.

Goal of the Thesis.

In this thesis the polariton hamiltonian will be examined within the framework of squeezing. We will exploit a variety of novel physical consequences of the simple mathematical result that the linear canonical Bogoliubov transformation which diagonalizes the matter-radiation hamiltonian to produce polaritons is a squeeze transformation. This turns out to have a two-fold purpose, namely,

I) *to extend the effects of squeezing to Bose fields other than photon, especially to mixed, composite, Bose fields*

II) *to investigate the quantum optical properties of the radiation field associated with polaritons.*

In part (I) squeezing is shown with respect to certain boson quasiparticles (c) which are admixtures of photon and exciton, yet not polaritons. They are intrinsic to the polariton structure and this squeezing will be therefore referred to as *intrinsic squeezing*. Appropriate interpretations of the intrinsic squeezing in polaritons are presented. We analyse the dependence of the intrinsic squeezing on which particular polariton mode which is excited, and the periodic reduction of the envelope of fluctuations of the boson field c below the vacuum value.

In part (II) we show that the the quantum-statistics of the photonic part of the polariton is non-classical. The deviations from classical are tunable in that they depend on the mode that is populated. The Mandel Q-factor for the number distribution of photons in polariton states is determined. In particular *optical squeezing*, that is the reduction of the fluctuations of the electromagnetic field of polariton states below the vacuum state value as due to squeezing, is established. It is helpful to point out here that non-poissonian statistics does not necessarily imply squeezing [2,51].

Magnitudes for the non-classical effects associated with polaritons are illustrated by numerical calculations for exciton-polaritons in typical I-VII and III-V types of semiconductors.

Polaritons certainly have been studied for a long time and many of their properties have been extensively given experimental evidence by a variety of spectroscopic methods. Several review volumes [48] were presented in § 1.7. Various theoretical approaches for predicting and analyzing optical properties of

polaritons are also fairly well established. Despite the extensive literature on polaritons, the investigations of the quantum-optical properties of these crystal mixed modes has lagged. The prospect of part (I) and (II) is intended to fill in this gap of the polariton literature. Note by contrast that the study of the quantum optical properties of the single and multimode cavity electromagnetic radiation, either in isolation or in interaction with one or few atoms has ben extensively developed [7,10].

Following our theoretical predictions of non-classical properties of polariton radiation, we will ultimately analyse experiments which can demonstrate the existence of polariton optical squeezing and/or departures from the classical photocount statistics.

CHAPTER II

The Polariton

When light propagates in a material, the electric and magnetic fields associated with it excite internal degrees of freedom of the material to which it couples. In a dielectric material for example the electric field may couple with optical excitations due to lattice vibrations such as *phonons*, or with electronic excitations such as *excitons*. The phase velocity of an e.m. wave in a dielectric differs from the velocity of light in vacuum since $\varepsilon \neq 1$. Since the external radiation excites internal degrees of freedom of the system as it progresses through the material, the energy resides partly in the e.m. field associated with it and partly in the specific polar excitation of the medium. The wave propagating in the medium is thus a complex entity when its composition is examined in detail, and we shall refer to this coupled mode as a *polariton*.

2.1 The model.

A very extended literature exists on polaritons [37,43,48]. For the purposes addressed in this thesis we will limit ourselves to considering a Frenkel-type [44,52] of exciton-polariton, excited at a *fixed frequency* (ω), in a *homogeneous, isotropic, frequency and spatially dispersive* and *non-magnetic* material. This can indeed be achieved by shining light of frequency ω onto such a material. In a number of instances, the study e.g. of Brillouin scattering of laser radiation from e.m. in solids has allowed both the frequency and the wavevector of the polariton

wave to be measured [48]. The frequency can be swept through a region of anomalous dispersion, which allows one to construct a plot of the frequency of the polariton wave as a function of its wavevector (*dispersion relation*). For each frequency the relation between the dielectric function ε_d and the wavenumber $\vec{k}$ of the polariton is, if the local optics assumption holds with $\varepsilon(\omega)$ independent of q

$$\varepsilon_d \equiv \varepsilon_d(\omega) = c^2 k^2 / \omega^2 \qquad (2.1.1)$$

or in the case of spatial dispersion $\varepsilon_d \equiv \varepsilon_d(\omega,k)$.

In the model which we adopt the propagating polariton excitation consists of the oscillating e.m. field *dressed* by the polarization, and the oscillating polarization field *dressed* by the external radiation field. The dressed e.m. field and the dressed polarization field of the exciton both oscillate with frequency ω.

From the point of view of quantum field theory the quanta of the dressed e.m. field component (dressed photons) are represented by certain frequency dependent combinations of bare photon operators and similarly for the dressed excitons. Dressed particle components, with respect to the vacuum ones, define the "physical" photons and "physical" excitons associated with the polariton wave. Dressing of the vacuum particle components is intrinsic to the mixed nature of the polariton.

2.2 Polariton hamiltonian

Following a macroscopic approach we here derive the hamiltonian for our exciton-polariton problem. Our approach relies on the description of the polariton field as a sum of its dressed e.m. field and its dressed exciton-polarization field components. It should be emphasized that this is a non-traditional approach; usually *bare* fields are introduced and coupled, leading to dressed fields and their renormalized dispersion equations. The hamiltonian reduces to the sum (integral) of independent harmonic oscillator hamiltonians. The quantization procedure is therefore straightforward [1,4,5]. The hamiltonian depends on phenomenological parameters that are fixed by fitting the experimentally measured polariton energies [37,48].

Classically the dressed radiation field associated with the single frequency exciton-polariton considered here can be described in terms of single-frequency electric ($\vec{E}$) and magnetic ($\vec{H}$) fields (not vacuum) through the phenomenological lagrangian

$$L_r = \frac{1}{8\pi}\int_v d\vec{r}\,[\vec{E}\cdot\vec{D} - H^2] \qquad \vec{D} \equiv \varepsilon_d \vec{E} \tag{2.2.1}$$

ε_d is the value of the exciton-polariton dielectric function at ω. Vector and scalar potentials $\vec{A}_{e.m.}$ and Φ can be introduced via

$$\vec{E} = -\frac{1}{c}\frac{\partial \vec{A}_{e.m.}}{\partial t} - \vec{\nabla}\Phi \qquad \vec{H} = \vec{\nabla} \wedge \vec{A}_{e.m.} \tag{2.2.2}$$

In the absence of free charges and currents we adopt the Coulomb gauge $\vec{\nabla}\cdot\vec{A}_{em.}=0$ (Coulomb) and $\Phi=0$. From Eqs. (2.2.1-2) the macroscopic Maxwell equations in absence of free sources

$$\vec{\nabla}\cdot\vec{D}=0 \qquad \vec{\nabla}\wedge\vec{E}=-\frac{1}{c}\frac{\partial\vec{H}}{\partial t}$$
$$\vec{\nabla}\cdot\vec{H}=0 \qquad \vec{\nabla}\wedge\vec{H}=\frac{1}{c}\frac{\partial\vec{D}}{\partial t} \tag{2.2.3}$$

can be derived, in particular the Eq. of motion for $\vec{A}_{e.m.}$ i.e.

$$\vec{\nabla}\wedge\vec{\nabla}\wedge\vec{A}_{em.}+\frac{\varepsilon_d}{c^2}\frac{\partial^2\vec{A}_{em.}}{\partial t^2}=0 \tag{2.2.4}$$

The dressed exciton field associated with the polariton can also be described classically in terms of a lagrangian i.e.

$$L_p=2\pi\int_V d\vec{r}\,[(\frac{\partial P}{\partial t})^2-\omega^2P^2] \tag{2.2.5}$$

and the relevant Eq. of motion for the exciton-polarization density $\vec{P}$ is

$$\frac{\partial^2\vec{P}}{\partial t^2}+\omega^2\vec{P}=0 \tag{2.2.6}$$

Note that $\vec{E},\vec{H}$ and $\vec{P}$ are generic fields, however taken to oscillate with the same frequency of the polariton. By solving Eqs. (2.2.3) and (2.2.6), expressions for $\vec{E},\vec{H}$

and $\vec{P}$ appropriate to our problem will be obtained. We shall express $\vec{P}$ in terms of a vector potential $\vec{A}_{exc.}$

$$\vec{P} = \frac{\sqrt{\varepsilon_d}}{4\pi\sqrt{2}\,c}\vec{A}_{exc.} + \frac{1}{4\pi\sqrt{2}\,\omega}\vec{\nabla}\wedge\vec{A}_{exc.} \tag{2.2.7}$$

Since for consideration of optical properties longitudinal exciton modes do not couple with the radiation and since we restrict ourselves to isotropic media, in what follows $\vec{P}$ is transverse to the direction $\vec{k}$ of propagation of the polariton wave, and is parallel to the electric field $\vec{E}$. $\vec{A}_{exc.}$ is chosen so that these conditions are fulfilled. The polariton lagrangian in terms of the potentials

$$\begin{aligned} L \equiv L_r + L_p = &\frac{1}{8\pi}\int_v d\vec{r}\,[(\frac{\partial_t \vec{A}_{em.}}{c/\sqrt{\varepsilon_d}})^2 - \frac{1}{8\pi}(\vec{\nabla}\wedge\vec{A}_{em.})^2] \\ &+\frac{1}{8\pi}\int_v d\vec{r}\,[(\frac{\partial_t \vec{A}_{exc.}}{c/\sqrt{\varepsilon_d}})^2 - \frac{1}{8\pi}(\vec{\nabla}\wedge\vec{A}_{exc.})^2] \end{aligned} \tag{2.2.8}$$

takes the form [53]

$$L = \frac{1}{8\pi}\int_v d\vec{r}\,[(\frac{\sqrt{\varepsilon_d}}{c}\frac{\partial \vec{A}}{\partial t})^2 - (\vec{\nabla}\wedge\vec{A})^2] \qquad \vec{A} \equiv \vec{A}_{em.} + \vec{A}_{exc.} \tag{2.2.9}$$

If $\vec{M} \equiv \partial L / \partial(\partial_t \vec{A})$ is the momentum conjugate to $\vec{A}$, the polariton hamiltonian is

$$H = \int_v d\vec{r}\,[\frac{2\pi c^2}{\varepsilon_d}M^2 + \frac{1}{8\pi}(\vec{\nabla}\wedge\vec{A})^2] \tag{2.2.10}$$

The e.m. field associated with an exciton-polariton of fixed frequency ω is given by Eq. (2.2.2) for single frequency solutions of Maxwell Eqs.. If periodic boundary conditions are assumed in V, a general solution for $\vec{A}_{e.m.}$ is [54]

$$\vec{A}_{e.m.}(z,t) = \sum_k \alpha_k [v_k \vec{A}^{\circ}_{e.m.}(t,z,\omega)_k + v_{-k} \vec{A}^{\circ}_{e.m.}(t,z,-\omega)_{-k}] \tag{2.2.11}$$

where

$$\vec{A}^{\circ}_{e.m.}(t,z,\omega)_k \equiv \sqrt{\frac{2\pi\hbar c^2}{V\omega}} [\vec{u}_k(z) a_k e^{-i\omega t} + \vec{u}_k^*(z) a_k^* e^{+i\omega t}] \tag{2.2.12}$$

The orthogonal set of functions $\vec{u}_k(z) \equiv u_k(z)\hat{e}_k$ gives the space dependence where the unit vector $\hat{e}_k$, transverse to $\vec{k}$, accounts for the polarization of the radiation field. a_k is a complex amplitude for a vacuum photon of wavevector $\vec{k}$, while the v_k's are (real) coefficients. Similarly for the transverse exciton field of the polariton one has (cf. Eqs. (2.2.6-7))

$$\vec{A}_{exc.}(z,t) = \sum_k \beta_k [\upsilon_k \vec{A}^{\circ}_{exc.}(t,z,\omega)_k + \upsilon_{-k} \vec{A}^{\circ}_{exc.}(t,z,-\omega)_{-k}] \tag{2.2.13}$$

where

$$\vec{A}^{\circ}_{exc.}(t,z,\omega)_k \equiv \sqrt{\frac{2\pi\hbar c^2}{V\omega|}} [\vec{v}_k(z) b_k e^{-i\omega t} + \vec{v}_k^*(z) b_k^* e^{+i\omega t}] \tag{2.2.14}$$

b_k is the bare exciton complex amplitude, the υ_k's (real) coefficients, and $\vec{v}_k(z) \equiv u_k(z)\hat{h}_k$ with $\hat{h}_k$ unit vector that accounts for the polarization of the exciton. The expansions in Eqs. (2.2.11) and (2.2.13) are over those modes that satisfy the dispersion Eq. (2.1.1) for the given frequency ω. In $\vec{A}_{e.m.}$ and $\vec{A}_{exc.}$, α_k and β_k are weights with which e.m. and excitonic components take part in the polariton mixture. The $\vec{A}^{\circ}$'s are classical vacuum amplitudes. Changing from a classical to a *quantum* description consists in replacing $\vec{A}$ and $\vec{M}$ in the harmonic oscillator hamiltonian Eq. (2.2.10) by conjugate operators, or equivalently by replacing the amplitudes a_k's and b_k's with operators satisfying the commutation relations $[\hat{a}_k, \hat{a}_{k'}^{\dagger}] = [\hat{b}_k, \hat{b}_{k'}^{\dagger}] = \delta_{k,k'}$. The vector potential can be written as an expansion of mode operators

$$\hat{\vec{A}}(t,z,) = \sum_k \sqrt{\frac{2\pi\hbar c^2}{V\omega}} [u_k(z)\hat{\vec{\varsigma}}_k e^{-i\omega t} + u_k^*(z)\hat{\vec{\varsigma}}_k^{\dagger} e^{+i\omega t}] \tag{2.2.15}$$

where for the generic mode

$$\hat{\vec{\varsigma}}_k \equiv \alpha_k[\vec{v}_k\hat{a}_k + \vec{v}_{-k}^*\hat{a}_{-k}^{\dagger}] + i\beta_k[\vec{\upsilon}_k\hat{b}_k - \vec{\upsilon}_{-k}^*\hat{b}_{-k}^{\dagger}] \tag{2.2.16}$$

Here $\varepsilon_k \equiv \hbar\omega_k = \hbar\omega$, $\vec{v}_{\pm k} \equiv v_{\pm k}\hat{e}_{\pm k}$, $\vec{\upsilon}_{\pm k} \equiv -i\upsilon_{\pm k}\hat{h}_{\pm k}$, whereas $\hat{a}_{\pm k}, \hat{a}_{\pm k}^{+}$ and $\hat{b}_{\pm k}, \hat{b}_{\pm k}^{+}$ are annihilation and creation operators for the corresponding normal modes of the bare exciton and bare e.m. field. Further requiring the $\hat{\varsigma}$'s to be boson operators with $[\hat{\varsigma}_k, \hat{\varsigma}_{k'}^{\dagger}] = \delta_{k,k'}$ constrains the coupling coefficients such that

$$|\alpha_{\pm k}|^2(|\vec{v}_{\pm k}|^2 - |\vec{v}_{\mp k}|^2) + |\beta_{\pm k}|^2(|\vec{\upsilon}_{\pm k}|^2 - |\vec{\upsilon}_{\mp k}|^2) = 1 \tag{2.2.17}$$

We may choose

$$\begin{pmatrix} v_k \equiv v_k^+ \\ v_k \equiv v_k^+ \end{pmatrix} \equiv \begin{pmatrix} \cosh s_k^{ph.} \\ \cosh s_k^{exc.} \end{pmatrix}, \quad \begin{pmatrix} v_{-k} \equiv v_k^- \\ v_{-k} \equiv v_k^- \end{pmatrix} \equiv \begin{pmatrix} \sinh s_k^{ph.} \\ \sinh s_k^{exc.} \end{pmatrix}, \quad \begin{aligned} \alpha_{\pm k} &\equiv \alpha_k^{\pm} \equiv \cos\theta_{\pm k} \\ \beta_{\pm k} &\equiv \beta_k^{\pm} \equiv \sin\theta_{\pm k} \end{aligned} \tag{2.2.18}$$

Substituting $\vec{A}$ and $\vec{M}$ into Eq. (2.2.10), carrying out the integration using

$$\begin{aligned} &\int_V d\vec{r}\, u_k(z) \cdot u_{k'}^*(z) = V \delta_{k,-k'} \\ &[\vec{k} \wedge \hat{e}_k] \cdot [\vec{k} \wedge \hat{e}_k^*] = [\vec{k} \wedge \hat{h}_k] \cdot [\vec{k} \wedge \hat{h}_k^*] = k^2, \end{aligned} \tag{2.2.19}$$

the quantized form of H in terms of bare photon and exciton operators follows (cf. Eq. A1.2)

$$\hat{H} = \sum_{k \geq 0} \{\hat{H}_k + \hat{H}_{-k}\} + h.c. \tag{2.2.20}$$

$$\begin{aligned} \hat{H}_k - h_k^o = {} & E_k^{ph} \hat{a}_k^+ \hat{a}_k + E_k^{exc} \hat{b}_k^+ \hat{b}_k \\ & + B'_k \hat{a}_k \hat{a}_{-k} - C'_k \hat{b}_k \hat{b}_{-k} + i A_{1k} \hat{a}_{-k} \hat{b}_k + i A_{2k} \hat{a}_k^+ \hat{b}_k \end{aligned}$$

with

$$E_k^{ph} \equiv \frac{\hbar ck}{2} + B_k ; E_k^{exc} \equiv \frac{\hbar \omega_T}{2} - C_k ; h_k^o \equiv \frac{1}{4}[\hbar ck + \hbar \omega_T + 2(B_k - C_k)]$$

The bare photon and transverse exciton frequencies (ck, ω_T) have been introduced along with the new parameters $\{A_{1k}, A_{2k}, B_k, B'_k, C_k, C'_k\}$ in terms of the old ones $\{\varepsilon_k, v_k^{\pm}, \upsilon_k^{\pm}, \alpha_k^{\pm}, \beta_k^{\pm}\}$ [55]. The photon-exciton couplings A_{1k} and A_{2k}, the

photon-photon couplings B_k and B_k', and the exciton-exciton couplings C_k and C_k' are to be determined from experimentally measured dispersion curves [48].

2.3 Polariton vector potential

We now turn our attention to the generalized potential $\hat{\vec{A}}$.

$$\begin{aligned}\hat{\vec{A}}(t,z) &= \hat{\vec{A}}_{e.m.}(t,z) + \hat{\vec{A}}_{exc.}(t,z) \\ &= \sum_k \alpha_k \sqrt{\frac{2\pi\hbar c^2}{V\omega}} [u_k(z)\hat{\vec{A}}_k e^{-i\omega t} + u_k^*(z)\hat{\vec{A}}_k^\dagger e^{+i\omega t}] \\ &+ \sum_k \beta_k \sqrt{\frac{2\pi\hbar c^2}{V\omega}} [u_k(z)\hat{\vec{B}}_k e^{-i\omega t} + u_k^*(z)\hat{\vec{B}}_k^\dagger e^{+i\omega t}]\end{aligned} \tag{2.3.1}$$

where

$$\hat{\vec{A}}_{\pm k} \equiv \vec{v}_k^{\pm}\hat{a}_{\pm k} + \vec{v}_k^{\mp *}\hat{a}_{\mp k}^\dagger \qquad \vec{B}_{\pm k} \equiv i(\vec{v}_k^{\pm}\hat{b}_{\pm k} - \vec{v}_k^{\mp *}b_{\mp k}^\dagger) \tag{2.3.2}$$

The positive and negative frequency parts of the e.m. component of $\hat{\vec{A}}$ are given by expansions in terms of "dressed" photon annihilation ($\hat{\vec{A}}_k$) and creation ($\hat{\vec{A}}_k^\dagger$) operators, respectively. The difference between these operators and the "vacuum" ones $\hat{a}_k$ and $\hat{a}_k^\dagger$ is substantial. The $\hat{\vec{A}}_k$'s are expressed in terms of vacuum annihilation operators $\hat{a}_k$ and vacuum creation operators $\hat{a}_{-k}^\dagger$ which occur as well: a superposition mediated by the $v_k^{\pm}$'s. This physically arises from the fact that the bare exciton-polarization of the dielectric introduces a coupling between the bare radiation field $\pm\vec{k}$ waves [56,57]. The $v_k^{\pm}$'s give the admixture of bare photons with opposite wavevectors inside V. A similar discussion holds for $\hat{\vec{A}}_{exc}$. On the other hand in presence of radiation $\hat{b}_k$ is no longer the appropriate exciton

annihilation operator, but rather $\hat{\tilde{B}}_k$ is, and relevant expansions of the exciton-polarization field into positive and negative frequency parts occur in terms of $\hat{b}_k$ and $\hat{b}_k^\dagger$. The admixture of bare excitons in the "dressed" exciton $\hat{\tilde{B}}_k$ inside V is mediated by the coefficients $\upsilon_k^\pm$, and it originates from the presence of radiation inside the dielectric material to which the exciton-polarization couples.

The underlying physics is that light and exciton components of the polariton *coexist* inside V, so the vacuum fields are no longer the physical ones: $\hat{\tilde{A}}_k$ and $\hat{\tilde{B}}_k$ are instead the operators that represent the "physical" photons and excitons in polaritons [58]. Note that, on the basis of our formulation, the substantial difference between bare photons or excitons and polariton dressed photons or excitons essentially relies on the parameters $s^{ph.}$ and $s^{exc.}$, respectively: when $(s^{ph.}, s^{exc.}) \to 0$, the dressed particles (2.3.2) tend to the bare ones with a consequent change in the physical significance of the potential $\hat{\tilde{A}}$. The idea that the s's may be related to the dielectric properties of the medium will be implemented later.

2.4 Physical polariton hamiltonians

Eq. (2.2.20) has the typical structure of a polariton hamiltonian and the relevant physics of each of its terms is discussed in Appendix A1, yet it requires a certain number of parameters. We will be mostly concerned with *two* specific parametrizations of $\hat{H}$. However in both cases the requirements that

$$\alpha_k^\pm \neq \beta_k^\pm, \qquad v_k^+ \neq v_k^-, \qquad \upsilon_k^+ \neq \upsilon_k^-$$

must hold. The first derives from the fact that photon and exciton weights in a polariton depend on k and branch, and so they are in general different from one mode to the other [37,42,43], while the other two conditions are needed to preserve the polariton boson nature.

In chapter III we will be interested in the realization of $\hat{H}$ for which $\alpha_k^+ = \alpha_k^-$, $\beta_k^+ = \beta_k^-, v_k^\pm = v_k^\pm \neq 1$. Such a parametrization leads to the hamiltonian (cf. Appendix A1) the structure of which is

$$\hat{H} \rightarrow \hat{H}^{pol} = \{\hat{H}_k^{pol} + \hat{H}_{-k}^{pol}\} + h.c.$$
$$\hat{H}_k^{pol} = \overline{h}_k^{\circ} + \overline{E}_k^{ph}\hat{a}_k^\dagger\hat{a}_k + \overline{E}_k^{exc}\hat{b}_k^\dagger\hat{b}_k + \overline{B}_k\hat{a}_k\hat{a}_{-k} - \overline{C}_k\hat{b}_k\hat{b}_{-k}$$
$$+ i\overline{A}_{1k}\hat{a}_{-k}\hat{b}_k + i\overline{A}_{2k}\hat{a}_k^\dagger\hat{b}_k \qquad (2.4.1)$$

This can be shown to represent a "physical" polariton hamiltonian in that a set of parameters $\{\overline{A}_{1k}, \overline{A}_{2k}, \overline{B}_k, \overline{B}'_k, \overline{C}_k, \overline{C}'_k\}$ can and will be found so that $\hat{H}^{pol}$ correctly reproduces the experimentally measured energies for exciton-polaritons, for both upper and lower polariton branches [48]. More interesting for our purposes, in addition, is that $\hat{H}^{pol}$ turns out to be a *squeeze* hamiltonian [28,29,10].

In chapter IV we will be interested in the realization of $\hat{H}$ for which $v_{-k} = 0$, $v_{-k} = v_k - 1/2$. Such a parametrization leads to the hamiltonian (cf. Appendix A1)

$$\hat{H} \rightarrow \hat{H}^{\circ} = \{\hat{H}_k^{\circ} + \hat{H}_{-k}^{\circ}\} + h.c.$$
$$\hat{H}_k^{\circ} = h_k^{\circ} + (\frac{\hbar ck}{2} + B_k)\hat{a}_k^\dagger\hat{a}_k + \frac{\hbar\omega_T}{2}\hat{b}_k^\dagger\hat{b}_k + B_k\hat{a}_k\hat{a}_{-k} + iA_k(\hat{a}_{-k}\hat{b}_k + \hat{a}_k\hat{b}_k^\dagger) \qquad (2.4.2)$$

This has just the same structure of the Hopfield hamiltonian in ref. [42]. Therefore the latter is a special instance of Eq. (2.4.1). The coefficients in front of the operator entities either in Eq. (2.4.1) or (2.4.2) are complicated functions of $\{\varepsilon_k, v_k^{\pm}, \upsilon_k^{\pm}, \alpha_k^{\pm}, \beta_k^{\pm}\}$ that are only given in Appendix A1 where these two particular parametrizations of $\hat{H}$ are extensively studied.

Before using the two model hamiltonians above to investigate the quantum statistical properties of polariton waves, it is worthwhile stressing what follows: $\hat{H}_k^{pol.}$ constitutes an *enlargement* with respect to $\hat{H}^o$ because,

1) the exciton-exciton coupling is included;
2) the couplings of an exciton $\hat{b}_k$ (photon $\hat{a}_k$) with an exciton $\hat{b}_{-k}$ or $\hat{b}_k^{\dagger}$ (photon $\hat{a}_{-k}$ or $\hat{a}_k^{\dagger}$) are considered a priori as distinct;
3) the coupling of an exciton $\hat{b}_k$ with a photon $\hat{a}_{-k}$ or $\hat{a}_k^{\dagger}$ are also considered a priori as distinct.

Apart from the diversification in the coupling coefficients, the polariton hamiltonian $\hat{H}^{pol}$ clearly involves an additional physical process, the $\hat{b}_k\hat{b}_{-k}$ (and conjugate) interaction, that the Hopfield one omits. From a group theoretical point of view the presence of these terms in the polariton problem stems from the fact that the hamiltonian with the structure of $\hat{H}^{pol}$ realizes the complete Lie algebra Sp (8,C), while the Hopfield hamiltonian does not [59].

2.5 Dispersion law

We now calculate the eigenenergies of the hamiltonian (2.2.20). There exists a Bogoliubov transformation which reduces this hamiltonian from a system of coupled harmonic oscillators, to a system of uncoupled harmonic oscillator normal modes $\hat{\eta}_k$. $\hat{H}$ is diagonalized by taking $\hat{\eta}_k \equiv x\hat{a}_k + y\hat{b}_k + z\hat{a}^{\dagger}_{-k} + w\hat{b}^{\dagger}_{-k}$: The Eq. of motion

$$[\hat{\eta}_k, \hat{H}] = \varepsilon_k \hat{\eta}_k \tag{2.5.1}$$

leads to an eigenvalue problem that may be reduced to the following matrix form

$$\begin{pmatrix} 2E_k^{ph} & -iA_{2k} & -2B_k' & -iA_{1k} \\ iA_{2k} & 2E_k^{exc} & -iA_{1k} & 2C_k' \\ 2B_k' & -iA_{1k} & -2E_k^{ph} & -iA_{2k} \\ -iA_{1k} & -2C_k' & iA_{2k} & -2E_k^{exc} \end{pmatrix} \begin{pmatrix} x \\ y \\ z \\ w \end{pmatrix} = \varepsilon_k \begin{pmatrix} x \\ y \\ z \\ w \end{pmatrix} \tag{2.5.2}$$

The resultant dispersion relation is a biquadratic polynomial in eigenvalue ε_k and depends on the parameters $E_k^{ph.}, E_k^{exc.}, B_k', C_k', A_{1k}$ and A_{2k}. ε_k yields the energies of the complete system (material polarization+radiation) and will be hereafter interpreted as such: the physical significance of the contributions to ε_k is evident from the energies $E_k^{ph.}, E_k^{exc.}$ and the couplings B_k', C_k', A_{1k} and A_{2k} as discussed in Appendix A1.

The particular case studied by Hopfield readily follows when we take

$$\begin{aligned} C_k &= C_k' = 0 \\ B_k &= B_k' = \pi\beta_o \hbar\omega_T^2 / ck \end{aligned} \tag{2.5.3}$$

$$A_{1k} = A_{2k} = \sqrt{4\pi\beta_o}\,(\hbar\omega_T)^2 / 2\sqrt{\hbar ck\,\hbar\omega_T} \equiv G_k$$

so that the secular Eq. (2.5.2) reduces to

$$\begin{pmatrix} \hbar ck + 2B_k & -iG_k & -2G_k & -iG_k \\ iG_k & \hbar\omega_T & -iG_k & 0 \\ 2B_k & -iG_k & -\hbar ck - 2B_k & -iG_k \\ -iG_k & 0 & iG_k & -\hbar\omega_T \end{pmatrix} \begin{pmatrix} x \\ y \\ z \\ w \end{pmatrix} = \varepsilon_k \begin{pmatrix} x \\ y \\ z \\ w \end{pmatrix} \qquad (2.5.5)$$

that is in fact Eq. (11) in ref. [42]. The secular Eq. relevant to the other hamiltonian ($\hat{H}^{pol}$) is more complicated and will be given in chapter III.

CHAPTER III

Generalized model polariton squeezing

In the next two chapters we will discuss the non-classical effects of squeezing in polaritons from a theoretical point of view. Specifically, exciton-polariton quantum states are shown to be squeezed. There are several senses in which a polariton manifests squeezing. One can show that the polariton hamiltonian is isomorphic to a standard two-mode *squeeze hamiltonian* [28,29,10]. As well, one can show that the Bogoliubov transformation from the states of bare photons plus bare excitons to polariton states is a *squeeze transformation* [28,29]. Both procedures to demonstrate squeezing in a polariton are illustrated in chapter III and IV respectively.

Certain intermediate bose quasi-particles are being squeezed, which are themselves mixtures of exciton and photon. These have been independently studied in the past [60] and are in fact the quanta of the *propagating* component of the exciton-polariton field: they are not the physical polaritons, their mixing coefficients are not those of the polariton, and their dispersion equations also differ. Attention is devoted below to the interpretation of these quasi-particles. Here, we refer to squeezing as the reduction of the quantum fluctuations of the propagating field of the polariton below the value associated with its vacuum fluctuations. Since these bose quasi-particles are intrinsic to the polariton structure this type of squeezing will be referred to as *intrinsic squeezing*. Interpretations of this kind of squeezing in polariton states are presented below. Both sudden frequency change, within Graham's framework [61,62,63], and wavevector

quantum-correlations are envisaged as mechanisms for producing squeezed fluctuations in the propagating field of the polariton. The former relates to a sudden transition from states of the propagating field of the polariton to states of the actual polariton field. In this context, the quanta of the propagating component of the polariton field may be interpreted qualitatively as *intermediate* quasi-particles in the transient (of time) it takes to turn on the interaction. The latter relates to quantum correlations in polariton states between intrinsic quasiparticles of opposite wavevectors $\pm\vec{k}$. Conversely, the presence of intrinsic squeezing in polaritons may be sought as a signature of correlations between counterpropagating modes. The dependence of the amount of squeezing on the frequency-wavevector of the mode excited (*tuning*) as well as the time-periodic reduction -over a polariton cycle- of the envelope of fluctuations of the polariton propagating field below the vacuum value are major subjects of investigation.

Here, there is a quantitative difference depending on which polariton hamiltonian is used, $\hat{H}^{pol}$ or $\hat{H}^{o}$. Because of this we find it useful to discuss separately (in fact sequentially) the two cases, and to emphasize different properties of the two model hamiltonians. The more general model hamiltonian ($\hat{H}^{pol}$) is studied in chapter III, while the less general model ($\hat{H}^{o}$) is studied in chapter IV. The former includes some additional coupling and belongs more completely to the dynamical algebra Sp (8,C) when compared to the latter local (non-spatially dispersive) Hopfield model. Quantitative calculations are illustrated for non-spatially dispersive exciton-polaritons in typical I-VIII and III-V types of semiconductors. We stress that for these materials using a suitable parametrization either the Hopfield model ($\hat{H}^{o}$) or the enlarged one ($\hat{H}^{pol}$) have been shown to reproduce the correct experimental energy dispersion curves [48].

3.1 Generalized hamiltonian: squeeze picture and magnitudes.

In this section we demonstrate squeezing within the generalized polariton model hamiltonian $\hat{H}^{pol}$ (see § 2.4). This is achieved by showing that $\hat{H}^{pol}$ is isomorphic to a standard two-mode squeeze hamiltonian. Squeezing occurs with respect to certain intermediate bosons which are themselves mixtures of exciton and photon, yet not polaritons. The amount of squeezing that can be attained in the framework of this model is here discussed. In the second quantized form one has

$$\hat{H} \rightarrow \hat{H}^{pol} = \{\hat{H}_k^{pol} + \hat{H}_{-k}^{pol}\} + h.c.$$
$$\hat{H}_k^{pol} = \overline{h}_k^{o} + \overline{E}_k^{ph}\hat{a}_k^{\dagger}\hat{a}_k + \overline{E}_k^{exc}\hat{b}_k^{\dagger}\hat{b}_k + \overline{B}_k\hat{a}_k\hat{a}_{-k} - \overline{C}_k\hat{b}_k\hat{b}_{-k}$$
$$+ i\overline{A}_{1k}\hat{a}_{-k}\hat{b}_k + i\overline{A}_{2k}\hat{a}_k^{\dagger}\hat{b}_k \qquad (3.1.1)$$

with

$$E_k^{ph} \equiv \frac{\hbar ck}{2} + \overline{B}_k ; E_k^{exc} \equiv \frac{\hbar\omega_o}{2} - \overline{C}_k ; h_k^{o} \equiv \frac{\hbar ck}{4} + \frac{\hbar\omega_o}{4} + \frac{1}{2}(\overline{B}_k - \overline{C}_k)$$

($\hbar ck$, $\hbar\omega_o$) are the bare photon and transverse exciton energies, whereas $\{\overline{A}_{1k}, \overline{A}_{2k}, \overline{B}_k, \overline{B}'_k, \overline{C}_k, \overline{C}'_k\}$ are the coefficients that parametrize the hamiltonian treated as phenomenological parameters that we can and do determine by having recourse to the experimentally measured polariton dispersion curves.

We proceed by diagonalizing $\hat{H}^{pol}$, but in two steps. This will permit us to demonstrate the isomorphism between the g[illegible]ralized hamiltonian (3.1.1) and a

standard two-mode squeeze hamiltonian. First perform a partial diagonalization so as to introduce new mixed intermediate quasiparticles and their residual interactions: we represent them by bose operators

$$\hat{c}_{\pm k} \equiv e^{i\psi_k^a}\alpha_k \hat{a}_{\pm k} + e^{i\psi_k^b}\beta_k \hat{b}_{\pm k} \qquad \hat{c}_{\pm k}^{\dagger} \equiv e^{-i\psi_k^a}\alpha_k \hat{a}_{\pm k}^{\dagger} + e^{-i\psi_k^b}\beta_k \hat{b}_{\pm k}^{\dagger} \tag{3.1.2}$$

$$[\hat{c}_k, \hat{c}_{k'}] = [\hat{c}_k^{\dagger}, \hat{c}_{k'}^{\dagger}] = 0 \qquad [\hat{c}_k, \hat{c}_{k'}^{\dagger}] = \delta_{k,k'} \tag{3.1.3}$$

The α_k's and β_k's are real. After some algebra (3.1.1) can be transformed to the following form:

$$\hat{H}^{pol.} = \sum_{k>0}\{\hat{H}_k^{pol.} + \hat{H}_{-k}^{pol.}\} + h.c. \equiv \hat{H}_o + \hat{H}_{Int} \tag{3.1.4}$$

$$\hat{H}_o \equiv \sum_{k>0} \frac{\Omega_k}{2}(\hat{c}_{+k}^{\dagger}\hat{c}_{+k} + \hat{c}_{-k}^{\dagger}\hat{c}_{-k} + I) + h.c. \tag{3.1.5}$$

$$\hat{H}_{Int} \equiv 2\sum_{k>0} \zeta_k \hat{c}_{+k}\hat{c}_{-k} + h.c. \tag{3.1.6}$$

$\hat{H}^{pol}$ now depends on the new parameters $\Omega_k, \zeta_k, \alpha_k, \beta_k, \psi_k^a, \psi_k^b$ that are related to the old ones by the transformations

$$\Omega_k \alpha_k^2 = \hbar ck + 2B_k \qquad \Omega_k \beta_k^2 = \hbar\omega_o - 2C_k$$
$$\zeta_k \alpha_k^2 = B_k^{'} \qquad \zeta_k \beta_k^2 e^{2i\psi_k} = -C_k^{'}$$
$$2\zeta_k \alpha_k \beta_k e^{i\psi_k} = iA_{1k} \qquad \Omega_k \alpha_k \beta_k e^{i\psi_k} = iA_{2k} \tag{3.1.7}$$

Here we take $\psi_k^a = 0$ and $\psi_k^b = \pi/2$, $\alpha_k = \cos\theta_k$ and $\beta_k = \sin\theta_k$. The later identification is consistent with the commutation rules (3.1.3). The number of parameters in (3.1.4) then reduces to $\Omega_k, \zeta_k, \theta_k$. The next step of our (diagonalization) procedure proceeds by introducing a second bose quasiparticle

$$\hat{\eta}_{\pm k} = M_k \hat{c}_{\pm k} + N_k \hat{c}^{\dagger}_{\mp k} \qquad M_k^2 - N_k^2 = I \tag{3.1.8}$$

in terms of which we can rewrite $\hat{H}^{pol}$ in the fully diagonalized form

$$\hat{H}^{pol.} = \sum_k \varepsilon_k (\hat{\eta}_k^{\dagger} \hat{\eta}_k + \tfrac{1}{2}) \tag{3.1.9}$$

At this stage we observe that finding the coefficients in $\hat{H}_k^{pol}\{A_{1k}, A_{2k}, B_k, B_k', C_k, C_k'\}$ so that for *every* mode,

1-*the eigenenergy* ε_k *reproduces the experimentally measured exciton-polariton energy [48];*

2-*the parameters of* $\hat{H}^{pol}$ *satisfy consistently the isomorphism (3.1.7)*

is equivalent to show that $\hat{H}^{pol}$ represents a physical polariton hamiltonian, and that $\hat{H}^{pol}$ implies squeezing. Eq. (3.1.4) is indeed the usual form of a two-mode squeeze hamiltonian [28,29], and squeezing occurs with respect to the $\hat{c}$'s, mixed bosons whose dispersions is given by Ω_k and whose residual interaction is $\hat{H}_{Int}$ with interaction strength measured by ζ_k. In order not to interrupt the continuity of the presentation we will show in Appendix A2 that it is in fact possible to fulfill the points 1) and 2) above. Thus we can, and do, find all the coefficients, and ,

$$\hat{H}^{pol.}(A_{1k}, A_{2k}, B_k, B_k', C_k, C_k') = \hat{H}^{sq.}(\Omega_k, \zeta_k, \theta_k) \tag{3.1.10}$$

and ε_k is the energy of the physical polariton normal mode $\hat{\eta}_{\pm k}$ which we rewrite in terms of uncoupled particles as (cf. Eq. 3.1.2)

$$\hat{\eta}_{\pm k} \equiv \hat{\eta}_{\pm k}(x,y,z,w) = x\hat{a}_{\pm k} + y\hat{b}_{\pm k} + z\hat{a}^{\dagger}_{\mp k} + w\hat{b}^{\dagger}_{\mp k} \tag{3.1.11}$$

Now we characterize the amount of squeezing relevant to a polariton. We exploit the isomorphism (3.1.10). We first connect the polariton eigenenergy and eigenvectors to the parameters of the squeeze hamiltonian (3.1.4), e.g. by requiring that

$$[\hat{\eta}_k, \hat{H}^{sq}] = \varepsilon_k \hat{\eta}_k \tag{3.1.12}$$

The resulting secular Eq.

$$\begin{vmatrix} [\Omega_k \cos^2\theta_k - \varepsilon_k] & -\frac{i}{2}\Omega_k \sin 2\theta_k & -2\zeta_k \cos^2\theta_k & -i\,\zeta_k \sin 2\theta_k \\ \frac{i}{2}\Omega_k \sin 2\theta & [\Omega_k \sin^2\theta_k - \varepsilon_k] & -i\,\zeta_k \sin 2\theta_k & 2\zeta_k \sin^2\theta_k \\ 2\zeta_k \cos^2\theta_k & -i\,\zeta_k \sin 2\theta_k & -[\Omega_k \cos^2\theta_k + \varepsilon_k] & -\frac{i}{2}\Omega_k \sin 2\theta_k \\ -i\,\zeta_k \sin 2\theta & -2\zeta_k \sin^2\theta_k & \frac{i}{2}\Omega_k \sin 2\theta_k & -[\Omega_k \sin^2\theta_k + \varepsilon_k] \end{vmatrix} = 0$$

yields the eigenvalues

$$\varepsilon_k^2 = \Omega_k^2 - 4\,\zeta_k^2 \tag{3.1.13}$$

and the components of $\hat{\eta}$ (eigenvectors) as functions of $\Omega_k, \zeta_k, \theta_k, \varepsilon_k$. For our purposes it suffices to give [64]

$$|\frac{y}{x}| = \frac{i}{2}\varepsilon_k \sin 2\theta_k [\Omega_k \varepsilon_k + \Omega_k^2 - 4\zeta_k^2] \qquad |\frac{w}{x}| = \sin 2\theta_k \ \zeta_k \varepsilon_k^2 \tag{3.1.14}$$

Next we diagonalize $\hat{H}^{sq}$ by a squeeze canonical transformation, i.e. we transform $\hat{H}^{sq}$ to the form

$$\hat{H}^{sq} = \sum_k \bar{\varepsilon}_k (\hat{\mu}_k^\dagger \hat{\mu}_k + \tfrac{1}{2}) \tag{3.1.15}$$

by transforming the operators $\hat{c}_{\pm k}$ as $\hat{\mu}_{\pm k} = S^\dagger(r_k, \varphi)\hat{c}_{\pm k}S(r_k, \varphi)$ using:

$$S(r_k, \varphi_k) = \exp[r_k (e^{-2i\varphi_k} \hat{c}_{+k}\hat{c}_{-k} - e^{2i\varphi_k} \hat{c}_{+k}^\dagger \hat{c}_{-k}^\dagger)] \tag{3.1.16}$$

is a two-mode squeeze unitary operator [28,29], r_k and φ_k being referred to as the squeeze factor and angle, respectively. Evidently both $\hat{\mu}_{\pm k}$ and $\hat{\eta}_{\pm k}$ diagonalise the same hamiltonian (cf. 3.1.12 to 3.1.15) so they are identical (modulo a phase taken equal to 0) [65], and the eigenenergies are independent of the basis representation, i.e. $\bar{\varepsilon}_k = \varepsilon_k$. Using the properties of S and the explicit definition of $\hat{c}_{\pm k}$ in terms of the original vacuum photon and exciton operators, one can rewrite $\hat{\mu}_{\pm k}$ as

$$\begin{aligned}\hat{\mu}_{\pm k} &= \hat{a}_{\pm k} \cos\theta_k \cosh r_k + \hat{b}_{\pm k} e^{i\psi_k} \sin\theta_k \cosh r_k \\ &+ \hat{a}_{\mp k}^\dagger e^{2i\varphi_k} \cos\theta_k \sinh r_k + \hat{b}_{\mp k}^\dagger e^{-i(\psi_k - 2\varphi_k)} \sin\theta_k \sinh r_k\end{aligned} \tag{3.1.17}$$

whereas term by term comparison of (3.1.17) and (3.1.11) provides the components of $\hat{\eta}_k$ as functions of θ_k, φ_k, r_k : e.g.

$$|y| = \sin\theta_k \cosh r_k \qquad |w| = \sin\theta_k \sinh r_k \tag{3.1.18}$$

Finally by eliminating θ_k from Eqs. (3.1.14) and (3.1.18) the expression for the squeeze factor r_k follows

$$r_k = tgh^{-1}\left[\frac{2\zeta_k}{\varepsilon_k + \Omega_k}\right] \tag{3.1.19}$$

This gives the amount of polariton squeezing. It depends on the wavevector-frequency of the polariton mode that is excited, therefore it can be suitably *tuned* from outside the crystal varying the mode that is to be populated. Squeezing as a function of the polariton wavevector-frequency has been calculated in Fig. 2.1 for different semiconductors.

3.2 Generalized hamiltonian: intrinsic squeezing.

An obvious question may arise about the *interpretation* of $\hat{H}^{pol}$ in the form given by Eq. (3.1.4). Accordingly, the generation of squeezing in polariton states would be by the action of the interaction hamiltonian $\hat{H}_{int}$. The system suggested here to generate squeezing in polaritons is similar to the system of a two-photon laser where two photons of the same frequency with wavevectors $+\vec{k}$ and $-\vec{k}$ can be absorbed in a transition which is of second order in $\vec{A} \cdot \vec{p}$ [18]. In the present case the counterpropagating terms are "spontaneously" present in the hamiltonian using a running wave quantization of the bare photons and excitons. See ref.s [66,67] for the analogous case of phonons. A degenerate parametric amplifier

interpretation may as well be suitable to $\hat{H}^{pol}$ in (3.1.4): this is in fact the hamiltonian for a typical two-photon device [10,29].

These analogies are however only formal [68]. The scenario is here different and the actual validity of the decomposition (3.1.4) for $\hat{H}^{pol}$ directly relies on the physical nature of the mixed boson $\hat{c}$. From the mathematical viewpoint, these arise as a first step when the original hamiltonian is diagonalized in two steps as shown above. In the second step the effective interaction $\hat{H}_{Int.}$ between these mixed quasi-particles is taken into account and the completely diagonalized hamiltonian giving polaritons is achieved by a squeeze transformation. It is instructive to note if the effective interaction is supposed turned off, these intermediate bosons of our system would be the proper normal modes of the exciton-radiation interacting system. Indeed, as discussed in Appendix A3, the $\hat{c}$'s characterize an intrinsic "phase" of the polariton where energy switches back and forth between co-propagating exciton and photon with no coupling due to correlations of opposite wavevectors occurring. In a different context [60] the $\hat{c}$'s have been studied and sought as the actual quanta of the *propagating* component of the polariton field. Thus we can provide H^{pol} as given in Eq. (3.1.4) with a physical interpretation. $\hat{H}_o$ gives the free evolution of the quasiparticle c that is being squeezed. $\hat{H}_{Int}$, giving the squeezing, is the interaction that originates from coupling the $\hat{c}$'s with opposite wavevectors. This type of interaction is intrinsic to the polariton "construction", it originates from the polarization of the exciton that supports a coupling between the $\pm\vec{k}$ modes [56,57] and it produces correlations between counterpropagating $\hat{c}$'s in a polariton state. Specifically this correlation causes pairs $(\hat{c}_{+k}, \hat{c}_{-k})$ to be created or annihilated: that is apparent in the interaction part of the hamiltonian, which contains terms that are purely quadratic in the creation and annihilation operators.

The connection between wavevector mode correlations and squeezing will be discussed later. Since the interaction that produces squeezing in the propagating component of the polariton field is built in (intrinsic) $\hat{H}^{pol}$, polariton squeezing will be referred as to *intrinsic* squeezing.

3.3 Polariton intrinsic squeezing: transition from coherent to squeezed state.

Continuing within the two-mode squeeze framework, in this section we take advantage of the structure of polariton states as squeezed with respect to the states of the boson $\hat{c}$-field to explore an interesting time-development scenario intended to understand polariton intrinsic squeezing. A time-dependent analysis can indeed be implemented if we consider a hypothetical situation in which one can separately control $\hat{H}_{Int}$ (Eq. 3.1.6) and imagine it to be at first absent, so the total hamiltonian is $\hat{H}_o$, and then (at some time $t=0$) turned on. Within this context the boson $\hat{c}$ is the actual quasiparticle describing the photon-exciton system for $t<0$; the $\hat{c}$'s can also be referred to as *intermediate* quasiparticles since they constitute only an intermediate stage during which the process of polariton formation occurs. This intermediate stage represents *physically* the transient of time it takes to the vacuum photon and exciton fields to couple and form a polariton. Now note that turning on the interaction $\hat{H}_{Int}$, with the subsequent energy change $\Omega_k \rightarrow \varepsilon_k$, produces a change (squeezing) in the structure of the photon-exciton system quantum state [69]. This will be discussed here, and we will consider for definiteness the resulting polariton in a coherent state. We now introduce such a state and the properties which we will need by first recalling the separation of the polariton hamiltonian into $\hat{H}_o$ and $\hat{H}_{Int}$. Coherent states of the

diagonal part $\hat{H}_o$ are defined either as the eigenstates of the (mixed) destruction operators $\hat{c}$

$$\hat{c}_{\pm k}|c_{\pm k}\rangle = c_{\pm k}|c_{\pm k}\rangle \tag{3.3.1}$$

or by displacing the vacuum state $|0\rangle$ of the bare photon and bare exciton system

$$|c_{\pm k}\rangle = e^{-\frac{1}{2}(|c_{+k}|^2+|c_{-k}|^2)}\, e^{c_{-k}\hat{c}^{\dagger}_{-k}}\, e^{c_{+k}\hat{c}^{\dagger}_{+k}}|0\rangle \equiv D(c_{+k},\hat{c}_{+k})|0\rangle \tag{3.3.2}$$

The state vector $|c_{\pm k}\rangle$ so constructed is precisely a two-mode coherent state [28] for the free hamiltonian $\hat{H}_o$.

Next we introduce the state that one obtains by applying S to the $|c_{\pm k}\rangle$'s,

$$S(r_k,\varphi)|c_{\pm k}\rangle = |\mu_{\pm k}(r_k,\varphi)\rangle \equiv |\mu_{\pm k}\rangle_z \tag{3.3.3}$$

Using the properties of S and those of the displacement operator D, yields

$$|\mu_{\pm k}\rangle_z = e^{-(|\mu_{+k}|^2+|\mu_{-k}|^2)/2} \sum_{N_{\pm}=0}^{\infty} \frac{\mu_{+k}^{N_{+k}}\,\mu_{-k}^{N_{-k}}}{\sqrt{N_{+k}!\,N_{-k}!}}|N_{\pm k}\rangle_z \tag{3.3.4}$$

where

$$\hat{H}^{pol}|N_{\pm k}\rangle_z = \varepsilon_k(N_{\pm k}+\frac{1}{2})|N_{\pm k}\rangle_z \qquad \hat{H}^{pol} \equiv \sum_k \varepsilon_k(\hat{\mu}_k^{\dagger}\hat{\mu}_k+\tfrac{1}{2}) \tag{3.3.5}$$

The $\bar{\mu}_{\pm}$'s are complex numbers. Since the $|N_{\pm k}\rangle_z$'s are polariton energy eigenstates, from (3.3.4) the squeezed state $|\mu_{\pm k}\rangle_z$ is a polariton coherent state.

Let us now assume it is possible to prepare a polariton cavity where the photon-exciton system inside be described for t<0 by the hamiltonian $\hat{H}_o$. Let the initial state of this system be the coherent state (3.3.1). If at t=0 $\hat{H}_{Int}$ is turned on [70], the system develops for t>0 under the total hamiltonian $\hat{H}_o$ plus $\hat{H}_{Int}$ i.e. $\hat{H}^{pol}$. Conversely, if $\hat{H}_{Int}$ were always absent, the state of the system will remain (3.3.1) for all time. A possible physical mechanism accounting for the switching on of this interaction is a sudden frequency change [61-63] during a Frank-Condon transition (fixed wavevector)

$$|c_{\pm k}\rangle_{(t=0)} \rightarrow |\mu_{\pm k}\rangle_{z\,(t=0)} \tag{3.3.6}$$

Thus for positive times $t > 0$

$$|\mu_{\pm k}\rangle_{z(t>0)} = \exp[-it\hat{H}^{pol}/\hbar]|\mu_{\pm k}\rangle_{z(t=0)} \tag{3.3.7}$$

gives the temporal evolution of a polariton coherent state with energy $\varepsilon_k \neq \Omega_k$. One notes that (two-mode) coherent states of the bare photon/bare exciton field are also coherent states of the boson $\hat{c}$-field, which however are not coherent states for $\hat{H}^{pol}$ (cf. 3.3.3). Therefore the energy change $\Omega_k \rightarrow \varepsilon_k$, that ultimately produces squeezing in the (boson) $\hat{c}$-field component of the polariton is responsible for the change in the statistics.

In the initial state (t<0) the wavefunction of the photon-exciton system is a wavepacket whose width remains constant whereas for t>0 the wavepacket of the

corresponding wavefunction has a complicated time development in that its width changes periodically in time over the polariton period. In order to examine these time-varying features we find it advantageous to decompose the propagating field of the polariton into two amplitude components 90° out of phase. The operators that correspond to these two quadrature components are

$$\hat{X}_k^q = \frac{1}{2\sqrt{\hbar}}[\alpha_k\sqrt{\omega_k}\,\hat{q}_k^{ph.} - \frac{\beta_k\,\hat{p}_k^{exc.}}{\sqrt{\omega_k}}] + (k \to -k) \tag{3.3.8}$$

$$\hat{X}_k^p = \frac{1}{2\sqrt{\hbar}}[\beta_k\sqrt{\omega_k}\,\hat{q}_k^{exc.} + \frac{\alpha_k\,\hat{p}_k^{ph.}}{\sqrt{\omega_k}}] + (k \to -k) \tag{3.3.9}$$

$\hat{q}_k^{ph.} = \sqrt{\hbar/2\omega_k}\,(\hat{a}_k + \hat{a}_k^\dagger)$ and $\hat{p}_k^{ph.} = -i\sqrt{\hbar\omega_k/2}\,(\hat{a}_k - \hat{a}_k^\dagger)$ are the canonical position and momentum operators for photons or excitons if $a_k \to b_k$. Here (3.3.8-9) are canonical variables

$$[\hat{X}_k^q, \hat{X}_k^p] = i/2,$$

hence the product of their variances satisfy the Heisenberg uncertainty principle $\langle|\Delta\hat{X}_k^q|^2\rangle_t\langle|\Delta\hat{X}_k^p|^2\rangle_t \geq 1/16$ which must hold for both states $|\,c_{\pm k}\,\rangle$ and $|\,\mu_{\pm k}\,\rangle_z$. Their variances $\langle|\Delta\hat{X}_k^{q,p}|^2\rangle$ directly relate to the widths ($\Gamma_k^{q,p}$) of the wavefunction that represent the states of the propagating field of the polariton in the coordinate and momentum representation, respectively [71,29].

Polariton quadrature noise: Propagating field coherent states

In the initial state (t<0) the variance of $\hat{X}_k^q$ is

$$ {}_{t}\langle c_{\pm k}|\Delta\hat{X}_k^{q}|^2|c_{\pm k}\rangle_{t} = \frac{1}{4} = \Gamma_k^{(o)q} \equiv \Gamma_k^{o} \tag{3.3.10} $$

and that of the conjugate quadrature is,

$$ {}_{t}\langle c_{\pm k}|\Delta\hat{X}_k^{p}|^2|c_{\pm k}\rangle_{t} = \frac{1}{4} = \Gamma_k^{(o)p} \equiv \Gamma_k^{o} \tag{3.3.11} $$

As expected for a coherent state the two variances are constant in time. Further, coherent states are minimum uncertainty states so that the equality holds for the Heisenberg uncertainty relations, at all times [71,29]. Once again let us emphasize that the states $| c_{\pm k} \rangle$ are coherent states of the *free* part $\hat{H}_o$ of the partially diagonalized hamiltonian and that they refer to the intermediate quasiparticle $\hat{c}$, *not* to physical polaritons.

Polariton quadrature noise: Polariton field coherent states

In the state which evolves in time under $\hat{H}_{int}$, from an initial polariton coherent state, the variances of the two quadratures can be evaluated to give the time-dependent evolution

$$ {}_{t,z}\langle \mu_{\pm k}|\Delta\hat{X}_k^{q}|^2|\mu_{\pm k}\rangle_{t,z} \equiv \Gamma_k^{q}(t) $$
$$ = \frac{e^{-2r_k}}{4} + \frac{\sinh 2r_k}{2}\sin^2(\omega_k t) \tag{3.3.12} $$

and

$$ {}_{t,z}\langle \mu_{\pm k} | \Delta \hat{X}_k^{P} |^2 | \mu_{\pm k} \rangle_{t,z} \equiv \Gamma_k^{P}(t) $$

$$ = \frac{e^{+2r_k}}{4} - \frac{\sinh 2r_k}{2} \sin^2(\omega_k t) \qquad (3.3.13) $$

With respect to the Heisenberg uncertainty relations the *inequality* holds at each time also for these states, yet note that here the *equality* only holds when $\cos 2\omega_k t = 1$. As time evolves these states do *not* constantly remain minimum uncertainty states [71,29]. This has been analyzed in detail over a time interval corresponding to a polariton cycle and for different modes: results are reported in Fig.s 2.2-3. For a certain interval of time (ΔT_{sq}), twice in a cycle, one of the variances becomes smaller than Γ_k^o (coherent or vacuum value), while the conjugate one becomes larger than Γ_k^o in order to enforce the Heisenberg principle. ΔT_{sq} can be evaluated for each energy-wavevector polariton mode, as well as the variable amount of squeezing during ΔT_{sq}. The numerical evaluation of ΔT_{sq} with relative squeezing is discussed in Appendix A4: results are reported in Fig. 3.4 for an illustrative example of CuCl UBP exciton-polaritons, for which typical ΔT_{sq} ~ fraction of femtosecs.

In conclusion, we have shown that the probability density distribution for a polariton coherent state changes remarkably over the polariton cycle. In particular, in this state the propagating field component $\hat{c}$ of the polariton exhibits an uncertainty envelope (fluctuations) that is periodically reduced far below the classical value 1/4 associated with the vacuum state: this reduction, that is squeezing, occurs during a time interval ΔT_{sq} and, within it, takes on different amounts depending on the polariton mode that is populated.

3.4 Polariton intrinsic squeezing: wavevector correlations

In this section we examine quantum correlations as a different mechanism to implement squeezing in polaritons. The definition of correlation to be used is briefly introduced. Let us consider two subsystems associated with opposite directions of propagation i.e. $+\vec{k}$ and $-\vec{k}$. Quantum correlations between this pair of subsystems can give rise to squeezed fluctuations in the quadratures (3.3.8-9). If the state in which the pair of subsystems is prepared can be described by a density matrix ρ, then the reduced density matrices that describe the properties of the subsystems relevant to each direction of propagation are: $\rho_{\pm k} = tr_{\pm k}\rho$. A standard approach can then be used to analyse these correlations, namely if $\rho = \rho_{+k} \otimes \rho_{-k}$ the subsystems under consideration are uncorrelated, while if $\rho \neq \rho_{+k} \otimes \rho_{-k}$ then they are correlated. In order to apply the discussion to the properties of observables and in particular to their squeezing properties, we consider the two sets of operators $\{\hat{c}_{+k}, \hat{c}^{\dagger}_{+k}\}$ and $\{\hat{c}_{-k}, \hat{c}^{\dagger}_{-k}\}$ defined in each of the two subsystems and acting on the space of the $+\vec{k}$ subsystem and $-\vec{k}$ subsystem respectively. A measure of the quantum fluctuations of $\hat{c}_{+k}$ or $\hat{c}_{-k}$ using the mean-square uncertainty gives

$$\langle|\Delta\hat{c}^{2}_{\pm k}|\rangle = tr[\rho_{\pm k}\hat{c}^{2}_{\pm k}] - \{tr[\rho_{\pm k}\hat{c}_{\pm k}]\}^{2} \qquad (3.4.14)$$

Depending only on the reduced densities $\rho_{\pm k}$, $\langle|\Delta\hat{c}^{2}_{\pm k}|\rangle$ are independent of whether or not in the state $|\rangle$ $\hat{c}_{+k}$ and $\hat{c}_{-k}$ are correlated. The variances above do not tell us anything about the correlations between the two subsystems.

The latter can instead be studied by investigating the properties of operators acting on "both" subsystems. In what follows we introduce several of these

operators $(\hat{V},\hat{X}^{qp},\hat{n}_k\hat{n}_{-k})$ for study of specific correlations. Consider for instance the operator $\hat{V}\equiv\hat{c}_{+k}+\hat{c}_{-k}$ whose variance is

$$\langle|\Delta\hat{V}|^2\rangle=\sum_{l=\pm k}\langle|\Delta\hat{c}_l|^2\rangle+\tilde{c} \tag{3.4.15}$$

with $\langle|\Delta\hat{c}_{\pm k}|^2\rangle\equiv 0.5\langle\hat{c}^{\dagger}_{\pm k}\hat{c}_{\pm k}+\hat{c}_{\pm k}\hat{c}^{\dagger}_{\pm k}\rangle-|\langle\hat{c}_{\pm k}\rangle|^2$ and $\tilde{c}=\sum_{l,m=\pm k}{}'[\langle\hat{c}^{\dagger}_l\hat{c}_m\rangle-\langle\hat{c}^{\dagger}_l\rangle\langle\hat{c}_m\rangle]$ (real). In principle, the variance of such an operator indicates whether or not in the state $|\rangle$ the two subsystems are correlated.

For the purpose of the present work let us recall the quadratures $\hat{X}^{qp}_k$ by which we characterized the polariton squeezing in the previous section. $\hat{X}^{q}_k$ is the sum of two operators one acting on each of the two subsystems $+\vec{k}$ and $-\vec{k}$, furthermore it is related to $\hat{V}$. The relevant variance is,

$$\begin{aligned}\langle|\Delta\hat{X}^{q}_k|^2\rangle&=\frac{1}{4}[\langle|\Delta\hat{c}_{+k}|^2\rangle+\langle|\Delta\hat{c}_{-k}|^2\rangle]+\frac{1}{2}\mathrm{Re}\,d_k+\tilde{c}+\mathrm{Re}\,\delta]\\&=\frac{1}{4}[\langle|\Delta\hat{V}|^2\rangle+2\mathrm{Re}\,d_k+\mathrm{Re}\,\delta]\end{aligned} \tag{3.4.16}$$

where $\delta\equiv\sum_k\langle\hat{c}_k{}^2\rangle-\langle\hat{c}_k\rangle^2$. $d_k\equiv\langle\hat{c}_{+k}\hat{c}_{-k}\rangle-\langle\hat{c}_{+k}\rangle\langle\hat{c}_{-k}\rangle$ is a measure of the correlation between the quasiparticles $\hat{c}_{+k}$ and $\hat{c}_{-k}$. Squeezing, that is the reduction of the variance (3.4.16) below 1/4, can now be investigated in terms of correlations. For a polariton coherent state (3.23) it is easy to show that $\tilde{c}$ and δ vanish, and we are left with

$$\langle|\Delta\hat{X}^{q}_k|^2\rangle=\frac{1}{4}[\langle|\Delta\hat{c}_{+k}|^2\rangle+\langle|\Delta\hat{c}_{-k}|^2\rangle]+\frac{1}{2}\mathrm{Re}\,d_k \tag{3.4.17}$$

Further

$$\mathrm{Re}\ d_k = -\cos 2\varphi_k \cosh\ r_k \sinh\ r_k \tag{3.4.18}$$

and

$$\langle |\Delta \hat{c}_{+k}|^2 \rangle + \langle |\Delta \hat{c}_{-k}|^2 \rangle = \cosh 2r_k \geq 1 \tag{3.4.19}$$

so that squeezing in the q -quadrature depends in general on the relative magnitude of the terms on the right hand side of Eq. (3.4.17). In the range of polariton modes examined in this paper, correlations contribute to the fluctuations in the quadrature $\hat{X}^q$ in CuCl and GaAs exciton-polariton respectively with (maximum) amounts of 0.6 and 0.66 for UBP modes, and slightly higher amounts, i.e 0.95 and 1.18, for LBP modes. An analogous discussion holds for the conjugate quadrature $\hat{X}^p$. Squeezing is achieved provided

$$ctgh 2r_k - \sec\ h\, 2r_k < \cos 2\varphi_k \tag{3.4.20}$$

This is satisfied for phases such that $|2\varphi_k| < \pi / 2$, since $r_k \geq 0$ in the present treatment (cf. Fig. 2.1). However, the main result of this section is indeed (3.4.18): it connects squeezing to the correlations in a polariton coherent state between $\hat{c}$'s with opposite wavevectors. Absence of correlations d_k =0, i.e. $r_k = 0$ from Eq. (3.4.18), implies the equal sign in (3.4.19) and $\langle |\Delta \hat{X}^q_k|^2 \rangle \rightarrow 1/4$, i.e. no squeezing. The converse is also true. In order to have correlations between $\hat{c}_{+k}$ and $\hat{c}_{-k}$ the requirement of squeezing is necessary and sufficient.

In our polariton system the exciton-polarization inside the dielectric produces the correlation between the $\hat{c}$'s. In addition to our exciton-polariton system, the viewpoint that correlations can give rise to squeezing has been shown to be true for multimode squeezed states of light [72], and for dipole fluctuations in multiatom squeezed states [73].

Another parameter one could analyse in the present context is the number correlation

$$D_{n_k} \equiv \langle \hat{n}_{+k}\hat{n}_{-k}\rangle - \langle \hat{n}_{+k}\rangle\langle \hat{n}_{-k}\rangle \qquad \hat{n}_{\pm k} \equiv \hat{c}^{\dagger}_{\pm k}\hat{c}_{\pm k} \tag{3.4.21}$$

This can be evaluated noting that $4D_{n_k} \equiv \langle |\Delta \hat{H}_o|^2\rangle - \langle |\hat{n}_{+k} - \hat{n}_{-k}|^2\rangle$. The number difference is a constant of motion with respect to $\hat{H}^{pol}$ and vanishes if we take the initial number of quasiparticles $\hat{c}$ to be equal in the two modes of opposite wavevector. The other term can be calculated, and in a polariton coherent state one has ($\mu_{\pm k}$ real)

$$D_{n_k} = \frac{\mu_{+k}^{\ 2} + \mu_{-k}^{\ 2}}{4}\{\cosh 2r_k - \frac{\sinh^2 2r_k}{\mu_{+k}^{\ 2} + \mu_{-k}^{\ 2}} + \frac{2\mu_{+k}\mu_{-k}\sinh 2r_k \cos 2\phi_k}{\mu_{+k}^{\ 2} + \mu_{-k}^{\ 2}}\} \tag{3.4.22}$$

D_{n_k} depends in a complicated way in general not only on the squeeze parameters, but also on the displacements $|\mu_{\pm k}|^2$, and it is not essentially related to squeezing as d is.

CHAPTER IV

Hopfield model polariton squeezing

In this chapter we establish squeezing within the Hopfield polariton model hamiltonian (see § 2.4). The Hopfield hamiltonian is discussed and derived in Appendix A5. Unlike the approach taken in chapter III, the demonstration of squeezing for this model will be achieved by exploiting the simple mathematical result that the linear Bogoliubov transformation [74] which diagonalizes the exciton-radiation hamiltonian to produce polaritons is a *squeeze transformation* [28,29,10]. Likewise, this procedure leads us to the understanding of the polariton as a squeezed particle, with squeezing occurring with respect to certain intermediate mixed bosons.

4.1 Hopfield hamiltonian: squeeze picture and magnitudes.

We shall recall $\hat{H}^{\circ}$ as given in Eq. (2.4.2). We infer squeezing from the states of $\hat{H}^{\circ}$ and we establish the amount of squeezing that one can attain in the framework of the Hopfield model compared to that of the generalized polariton model discussed in the previous chapter. We emphasize that only the local (non-spatially dispersive) Hopfield case will be treated here. In the second quantized form one has (cf. Eq. 2.4.2)

$$\hat{H}^{\circ} = \sum_{k}\{\hbar ck(\hat{a}_k^{\dagger}\hat{a}_k + \tfrac{1}{2}) + \hbar\omega_{\circ}(\hat{b}_k^{\dagger}\hat{b}_k + \tfrac{1}{2}) + B_k\,[\hat{a}_k^{\dagger}\hat{a}_k + \hat{a}_k\hat{a}_k^{\dagger} + \hat{a}_k^{\dagger}\hat{a}_{-k}^{\dagger} + \hat{a}_k\hat{a}_{-k}] + iA_k[-\hat{b}_k^{\dagger}\hat{a}_k - \hat{b}_k^{\dagger}\hat{a}_{-k}^{\dagger} + \hat{b}_k\hat{a}_{-k} + \hat{b}_k\hat{a}_k^{\dagger}]\}$$

$$\equiv \sum_{k>0}\{\hat{h}_k^\circ + \hat{h}_{-k}^\circ\} \tag{4.1.1}$$

$\hat{H}^\circ$ can be separated into the sum of hamiltonians for pairs of wavevector modes $+k$ and $-k$, so we begin by considering a polariton mode of given wavevector $+k$ in Eq. (4.1.1) and its relevant hamiltonian. Here ck and ω_o are the bare photon and exciton frequencies, respectively, $\hat{a}_k$ and $\hat{b}_k$ the associated annihilation operators,

$$A_k \equiv \frac{(\hbar\omega_o)^2(4\pi\beta_o)^{1/2}}{2(\hbar ck\,\hbar\omega_o)^{1/2}}, \quad B_k \equiv (\pi\beta_o)\frac{(\hbar\omega_o)^2}{\hbar ck} = \frac{A_k^2}{\hbar h\omega_o} \tag{4.1.2}$$

and β_o the photon-exciton oscillator coupling strength proportional to a dipole matrix element squared.

We temporarily replace

$$\hat{a}_{1,2} \to \hat{a}_{k,-k}; \quad \hat{b}_{1,2} \to \hat{b}_{k,-k}; \quad \hat{a}_{1,2}^\dagger \to \hat{a}_{k,-k}^\dagger; \quad \hat{b}_{1,2}^\dagger \to \hat{b}_{k,-k}^\dagger$$

$$\lambda \equiv \lambda_k \to \hbar ck; \qquad \mu \to \hbar\omega_o; \qquad \sigma \to 4\pi\beta_o \tag{4.1.3}$$

The hamiltonian (4.1.1), say for a fixed single mode, can then be represented by the generic bilinear form

$$\begin{aligned}\hat{h}_1(\lambda,\mu,\sigma) &= \lambda(\hat{a}_1^\dagger\hat{a}_1 + \tfrac{1}{2}) + \mu(\hat{b}_1^\dagger\hat{b}_1 + \tfrac{1}{2}) \\ &\quad + f[\hat{a}_1^\dagger\hat{b}_1 - \hat{a}_1\hat{b}_1^\dagger + \hat{a}_2\hat{b}_1 - \hat{a}_2^\dagger\hat{b}_1^\dagger] + g[\hat{a}_1^\dagger\hat{a}_1 + \hat{a}_1\hat{a}_1^\dagger + \hat{a}_1\hat{a}_2 + \hat{a}_1^\dagger\hat{a}_2^\dagger]\end{aligned} \tag{4.1.4}$$

with $f \equiv i\sqrt{\sigma}\mu^{3/2}/2\sqrt{\lambda}$, $g \equiv \sigma\mu^2/4\lambda$. Note here that with respect to the rotating wave approximation (RWA), usual in quantum optics, Eq. (4.1..4) contains additional terms ($\hat{a}_1^\dagger\hat{a}_2^\dagger, \hat{a}_2^\dagger\hat{b}_1^\dagger$ etc.). This particular notation enables one to make the connection with the results on multimode quantum states as given in the Appendix A6. It can be shown [74] that $\hat{h}_1$ can be diagonalized by using a Bogoliubov transformation in the particular form developed in Eq. (A6.21). The diagonalizing transformation is implemented with the values of $\{\alpha_1, \alpha_2, \beta_1, \beta_2, r, \varphi, \chi_1, \chi_2\}$ defined as

$$
\begin{aligned}
|\alpha_1|\cosh r &= \frac{(\lambda+\varepsilon)(\mu^2-\varepsilon^2)}{2\sqrt{\lambda\varepsilon}}\left\{(\mu^2-\varepsilon^2)^2+\sigma\mu^4\right\}^{-1/2} \\
e^{+i\chi_1}|\beta_1|\cosh r &= -i\sqrt{\frac{\sigma\mu^3}{\varepsilon}}(\mu+\varepsilon)\left\{(\mu^2-\varepsilon^2)^2+\sigma\mu^4\right\}^{-1/2} \\
e^{+i\varphi}|\alpha_2|\sinh r &= -\frac{(\lambda-\varepsilon)(\mu^2-\varepsilon^2)}{2\sqrt{\lambda\varepsilon}}\left\{(\mu^2-\varepsilon^2)^2+\sigma\mu^4\right\}^{-1/2} \\
e^{-i(\chi_2-\varphi)}|\beta_2|\sinh r &= -i\sqrt{\frac{\sigma\mu^3}{\varepsilon}}(\mu-\varepsilon)\left\{(\mu^2-\varepsilon^2)^2+\sigma\mu^4\right\}^{-1/2}
\end{aligned}
\tag{4.1.5}
$$

to obtain

$$
\hat{h}_1 = \varepsilon(\hat{\tilde{\Gamma}}_1^\dagger\hat{\tilde{\Gamma}}_1 + \tfrac{1}{2}) \tag{4.1.6}
$$

ε in Eqs. (4.1.5-6) is a parameter that satisfies a biquadratic equation

$$
\varepsilon^4 - F(\lambda, \mu, \sigma)\,\varepsilon^2 + G(\mu) = 0 \tag{4.1.7}
$$

with F, G certain functions of $\{\lambda, \mu, \sigma\}$.

Restoring the notation one finds

$$\hat{h}_k = \varepsilon\,[\hat{\tilde{\Gamma}}_k^{\dagger}\,\hat{\tilde{\Gamma}}_k + \tfrac{1}{2}] \tag{4.1.8}$$

where ε is a solution of (cf. Eqs. 4.1.3-7)

$$\varepsilon^4 - \varepsilon^2[(\hbar ck)^2 + (\hbar\omega_o)^2 + 4\pi\beta_o(\hbar\omega_o)^2] + (\hbar\omega_o\hbar ck)^2 = 0 \tag{4.1.9}$$

and

$$\hat{\tilde{\Gamma}}_k = |\alpha_k^+|c_{\eta_k}\,\hat{a}_k + e^{i\varphi_k}|\alpha_k^-|s_{\eta_k}\,\hat{a}_{-k}^{\dagger} + e^{i\chi_{+k}}|\beta_k^+|c_{\eta_k}\,\hat{b}_k + e^{i(\varphi_k-\chi_{-k})}|\beta_k^-|s_{\eta_k}\,\hat{b}_{-k}^{\dagger} \tag{4.1.10}$$

Here $c_{\eta_k} \equiv \cosh r_k$ and $s_{\eta_k} \equiv \sinh r_k$. Eq. (4.1.9) yields the correct energy dispersion for polaritons provided $\varepsilon \to \varepsilon_k$ is identified as the "physical" polariton energy for a given wavevector mode k. Solutions are such that $\varepsilon_k^L = \varepsilon_{-k}^L$ and $\varepsilon_k^U = \varepsilon_{-k}^U$, U and L denoting upper and lower branches of the energy dispersion curves. (cf. Fig. 1.8). Thus, owing to $\hat{h}_k = \hat{h}_k^o$, $\hat{\tilde{\Gamma}}_k$ is the annihilation operator for a polariton of mode $+k$.

More specifically, Eqs. (4.1.4-6) demonstrate that in the Hopfield hamiltonian the transformation from bare photon *plus* bare exciton, to a normal mode physical polariton is a two-mode particle squeeze transformation whose generator is of the form (1.17), i.e.

$$\hat{\tilde{\Gamma}}_k = S^{pol}\,\hat{\gamma}_k\,S^{pol\,\dagger} \qquad S^{pol} \equiv S^{pol}(r_k,\varphi_k) = e^{r_k[-\hat{\gamma}_k^{\dagger}\hat{\gamma}_{-k}^{\dagger}e^{2i\varphi_k} + \hat{\gamma}_{-k}\hat{\gamma}_k e^{-2i\varphi_k}]} \tag{4.1.11}$$

Hence states of the Hopfield polariton hamiltonian are equivalent to two-mode squeezed states of the mixed bosons [75]

$$\hat{\gamma}_{\pm k} = |\alpha_k^+| \hat{a}_{\pm k} + e^{i\chi_{\pm k}} |\beta_k^+| \hat{b}_{\pm k} \tag{4.1.12}$$

The *vacuum, number* and *coherent states* of $\hat{H}^\circ$ turn out to be squeezed with respect to the vacuum, number and coherent states of the mixed boson $\hat{\gamma}$. The latter is a photon-exciton mixed particle bearing the same structure of the $\hat{c}$-boson discussed in chapter III. In an analogous manner the $\hat{\gamma}$'s, intrinsic to the polariton structure, can be interpreted physically as the quanta of the propagating component of the polariton field. Again this kind of squeezing will be referred to as intrinsic because it occurs with respect to states of the intrinsic boson $\hat{\gamma}$. Recall, by contrast, that the more general hamiltonian of chapter III supports squeezing with respect to the intermediate boson $\hat{c}$.

The hamiltonian (4.1.8) depends in general on eight parameters $\{\alpha_k^\pm, \beta_k^\pm, \chi_{\pm k}, \varphi_k, r_k\}$. We will now give the explicit expressions for these parameters in terms of the starting coefficients in the hamiltonian of Eq. (4.1.1). This in particular will permit us to exhibit the squeeze factor, from which we obtain numerical values of the amount of squeezing for some specific materials. Eqs. (4.1.3) and (4.1.5) give [75,76]

$$\begin{aligned} |\alpha_k^+| \cosh r_k &= \frac{\hbar ck + \varepsilon_k}{2\sqrt{\varepsilon_k \hbar ck}} \frac{N_{2k}}{\sqrt{M_k}} \equiv C_{1k} \\ |\beta_k^+| \cosh r_k &= \frac{\sqrt{4\pi\beta_o}}{2\sqrt{M_k}} \left(1 + \frac{\varepsilon_k}{\hbar\omega_o}\right) \sqrt{\frac{\hbar\omega_o}{\varepsilon_k}} \equiv C_{2k} \end{aligned} \tag{4.1.13}$$

$$|\alpha_k^-|\sinh r_k = \frac{|\varepsilon_k - \hbar ck|}{2\sqrt{\varepsilon_k \hbar ck}} \frac{N_{2k}}{\sqrt{Mk}} \equiv C_{3,k}$$

$$|\beta_k^-|\sinh r_k = \frac{\sqrt{4\pi\beta_o}}{2\sqrt{M_k}} |1 - \frac{\varepsilon_k}{\hbar\omega_o}| \sqrt{\frac{\hbar\omega_o}{\varepsilon_k}} \equiv C_{4,k}$$

where $N_{2k} \equiv |1 - (\frac{\varepsilon_k}{\hbar\omega_o})^2|$, $M_k \equiv N_{2k}^2 + 4\pi\beta_o$. For the purposes we address in this paper we only need to consider absolute values in Eq. (4.1.5). Further, owing to the boson nature of the $\hat{\gamma}$s, the two parameters $|\beta_k^\pm|$ can be expressed in terms of $|\alpha_k^\pm|$ respectively as

$$|\beta_k^\pm|^2 = 1 - |\alpha_k^\pm|^2 \tag{4.1.14}$$

Thus the parameters left to determine are $|\alpha_k^+|, |\alpha_k^-|$ and r_k. We now give $|\alpha_k^\pm|$: from the first and second two Eqs. in (4.1.13) one obtains,

$$\left|\frac{\alpha_k^+}{\beta_k^+}\right| = \left|\frac{C_{1,k}}{C_{2,k}}\right| \quad \text{and} \quad \left|\frac{\alpha_k^-}{\beta_k^-}\right| = \left|\frac{C_{3,k}}{C_{4,k}}\right|. \tag{4.1.15}$$

Thus (4.1.15) and (4.1.16) yield

$$|\alpha_k^+|^{-1} = \sqrt{1 + \left|\frac{C_{2,k}}{C_{1,k}}\right|^2}\ ; \quad |\alpha_k^-|^{-1} = \sqrt{1 + \left|\frac{C_{2,k}}{C_{1,k}}\left[\frac{(1 - \frac{\varepsilon_k}{\hbar h\omega_o})(1 + \frac{\varepsilon_k}{\hbar ck})}{(1 + \frac{\varepsilon_k}{\hbar\omega_o})(1 - \frac{\varepsilon_k}{\hbar ck})}\right]\right|^2} \tag{4.1.16}$$

We finally evaluate r_k from the second and fourth Eqs. in (4.1.14) and the equalities (4.1.16). The other determination of r_k using the first and third Eqs. in (4.1.14) is equivalent owing to (4.1.16). We obtain

$$\tanh r_k^{U,L} = \left| \frac{\alpha_k^+}{\alpha_k^-} \left[\frac{(\hbar ck - \varepsilon_k^{U,L})}{(\hbar ck + \varepsilon_k^{U,L})} \right] \right|$$
$$= \sqrt{\frac{\xi_k}{1+\xi_k}} \qquad \xi_k \equiv |C_{3,k}|^2 + |C_{4,k}|^2 \tag{4.1.17}$$

From the second of these Eqs. $\tanh r_k < 1$ as it must, while the first one tells us that distinct squeeze factors correspond to upper and lower energy dispersion branches (cf. Fig. 1.8). Further by changing (tuning) the wavevector-energy along a given branch we explore all possible values of the squeeze factor relevant to that branch. With this we have connected $\alpha_k^{\pm}, \beta_k^{\pm}, r_k$, which parametrize the Hopfield polariton hamiltonian (4.1.8), to quantities subject to experimental control. Using $\varepsilon_k^{U,L}$ and $|\alpha_k^{\pm}|$ as obtained from Eq. (4.1.9) and (4.1.17), respectively, we evaluate the amount of squeezing for the upper and lower branches of exciton-polaritons in CuCl and GaAs for k ranging in the vicinity of the crossover wavevector k_o. These are plotted in Fig. 4.1.

It is instructive to solve Eq. (4.1.18) for the squeeze factor in terms of the ratio $n_k^{U,L} \equiv \hbar ck / \varepsilon_k^{U,L}$, that is,

$$r_k^{U,L} = \tfrac{1}{2} \ln \left[\frac{1 + \left| \frac{\alpha_k^+}{\alpha_k^-} \left(\frac{n_k^{U,L} - 1}{n_k^{U,L} + 1} \right) \right|}{1 - \left| \frac{\alpha_k^+}{\alpha_k^-} \left(\frac{n_k^{U,L} - 1}{n_k^{U,L} + 1} \right) \right|} \right] \tag{4.1.18}$$

$n_k^{U,L}$, obtained from solving Eq. (4.1.9),

$$[n_k^{U,L}]^2 = (\frac{ck}{\omega_k^{U,L}})^2 = 1 + \frac{4\pi\beta_o}{1-(\omega_k^{U,L}/\omega_o)^2} \qquad (4.1.19)$$

is just the square root of the exciton-polariton dielectric function. Two points are to be noted here. The squeeze factor is directly connected to:

1. *the index of refraction of the medium,*
2. *the weights of the exciton and photon components of the polariton*

This settles how squeezing in polaritons is related to intrinsic properties of the dielectric material [77]. A value of unity for the bulk (background) dielectric constant (ε_b) is assumed throughout this treatment: it derives from taking ck as photon frequency in Eq. (4.1.1). An $\varepsilon_b \neq 1$ is introduced by rescaling the speed of light in vacuum $c \rightarrow c/\sqrt{\varepsilon_b}$.

A special value of r_k which will become useful in the next sections is that evaluated at the wavevector crossover k_o of the uncoupled light and exciton energy dispersions (see Fig. 1.8); from (4.1.17) $|\alpha_{k_o}^+| = |\alpha_{k_o}^-|$, and then

$$r_o^{U,L} \equiv r_{k_o}^{U,L} = \tfrac{1}{2}\ln[n_{k_o}^{U,L}] \qquad (4.1.20)$$

From (4.1.18) one also has

$$r_o^U \equiv tgh^{-1}\left|\frac{\Delta_U + \hbar\omega_{LT}}{2\hbar\omega_o}\right| \qquad r_o^L \equiv tgh^{-1}\left|\frac{\Delta_L}{2\hbar\omega_o}\right| \tag{4.1.21}$$

Generally speaking r_o increases for small transverse exciton frequencies and large separations Δ.

CHAPTER V

Non classical photon statistics in polaritons

In this chapter we will continue investigating non-classical features associated with exciton-polaritons. The polariton as the actual normal mode of the photon-exciton interacting system that propagates inside the medium has *both* the characteristics of an e.m. wave and of a polarization wave. Here we develop a theory for studying the statistical properties associated with the radiative part of the polariton. The theory is qualitatively the same for both generalized and Hopfield model, yet it predicts quantitatively different results depending on which model is adopted. Non-classical features are again predicted, which will be illustrated in the case of the Hopfield model for definiteness. The change from a classical radiation field (*incident* coherent pump radiation) to a non-classical one (*propagating* radiation inside the crystal) upon interacting with the exciton polarization of the crystal is thoroughly discussed. Deviations from classical depend on the wavevector-frequency mode that is populated, giving rise to tunable non-classical photon statistics over the entire polariton dispersion spectrum.

In particular we investigate the reduction, below the vacuum value, of the fluctuations of the radiation field associated with a polariton wave as arising from squeezing. To do this we first separate out that portion of the total (polariton) field which is radiative from the rest. This kind of squeezing will be referred to as *optical squeezing* as opposed to the intrinsic one introduced in the previous two

chapters. It should be recalled here that non-poissonian photon statistics does not necessarily imply squeezing [51].

Finally we note that the theory presented here differs in one important qualitative fashion from usual treatments of electromagnetic squeezing because our theory is *linear*. It is commonly believed in fact that non-linearity is needed to produce squeezed light, e.g. parametric amplification, four-wave mixing etc. But our work shows that squeezing can occur owing to the particular polariton mixing in a linear dispersive medium. Non-linearities are not necessary, although non-linearity may be sufficient in other cases. A certain similarity in viewpoint to that of Abram [56], and Glauber and Lewenstein [57] is pointed out below, as well as differences.

5.1 Non-poissonian photon statistics.

The exciton-light polariton mixture alters the statistical properties of the vacuum radiation field. Specifically, the poissonian number distribution characteristics of vacuum (incident) photons in a coherent state turns into a non-poissonian one in an exciton-polariton quantum state. This will be discussed in this section, namely by studying the fluctuations of the number of *bare* photons in a polariton quantum state. As for quantum states of the polariton field one might consider either number states $|n_k^p\rangle$ [a mode k occupied by n_k^p polaritons, or coherent states. The former are a convenient basis when experiments with a fixed number of particles are involved, but they are not of direct significance however in a typical solid state optical experiment where the probe exciting the polariton is usually a light source with *no definite* numbers of photons such as a laser. This

more realistic situation can instead be properly described by using coherent states: in the following *polariton coherent states* will be considered as quantum states relevant to our problem. According to the treatment given in chapter IV the latter are the eigenstates $|\gamma_{\pm k}\rangle_z$ of the annihilation operator (4.1.11), or the two-mode states of Eq. (1.16). We first give the variance $\langle(\Delta N_k^{ph})^2\rangle$ of the bare photon number $N_k^{ph} \equiv \hat{a}_k^\dagger \hat{a}_k$ in a polariton coherent state. In Appendix A7 we show that [78]

$$\langle (\Delta N_k^{ph})^2 \rangle = e^{\pm 2r_k} \langle N_k^{ph} \rangle - |\alpha_k^+ \beta_k^+|\, A_{1,k} \tag{5.1.1}$$
$$+ \frac{1}{|\alpha_k^+|}[|\beta_k^+|\, A_{-1,k} e^{\pm 2r_k} - |\beta_k^+|^2 A_{-1,k}] + |\beta_k^+|^2 [\langle (\Delta N_k^{ph})^2 \rangle - A_{o,k}]$$
$$+ |\alpha_k^+|^{-2}[(1+\sinh 2r_k)\sinh^2 r_k + e^{\pm 2r_k}|\beta_k^+|^2 \langle N_k^{exc} \rangle - A_{-2,k}|\beta_k^+|^4]$$

where $A_{o,k}, A_{\pm 1,k}, A_{-1,k}, A_{-2,k}$ are complicated functions which, for clarity of exposition, are only given in the Appendix A7. In (5.1.1) the expectation values are all evaluated upon the states $|\gamma_{\pm k}\rangle_z$. If one denotes by $|\, vac\,\rangle$ the vacuum photon coherent state, the corresponding number distribution is such that $\langle vac|(\Delta N_k^{ph})^2|vac\rangle = \langle vac|N_k^{ph}|vac\rangle$; by comparison with (5.1.1) this thus shows that bare photons in a polariton coherent states do not have a poissonian (classical) distribution. Due to the complicated form of the general result (5.1.1), we will now note some special cases giving rise to simplifications.

i. High photon intensity

First of all, since $\langle N_k^{ph} \rangle$ is related to the intensity of the photon (cf. Appendix A8), one can always choose the intensity such that the first term on the right hand side of (5.1.1) dominates, with the squeeze amplitude $e^{\pm 2r_k}$ remaining unaltered. By

varying the intensity of the photon, the mode k of the polariton which is populated remains fixed and so does r_k. Thus under this circumstance (cf. also Eq.1.27):

$$\langle (\Delta N_k^{ph})^2 \rangle \equiv e^{\pm 2r_k} \langle N_k^{ph} \rangle \equiv s_k^2 \langle N_k^{ph} \rangle \tag{5.1.2}$$

In this case the distinction between poissonian and non-poissonian depends on the squeeze amplitude s_k only. The latter characterizes the noise-power reduction ratio in a semiconductor, which is nearly constant ($\equiv 0.99$) for GaAs, but slightly varying (0.91-0.99) for CuCl exciton-polariton modes in the vicinity of the crossing k_o. The above result readily shows that the change of the photon statistics when an exciton-polariton is created is related to intrinsic properties of the dielectric: it depends, through s_k, on the index of refraction.

ii. Selected polariton modes

Independent of the photon intensity, one may simplify the result (5.1.1) by using the fact that the magnitudes of $|\alpha_k^+|$ and $|\beta_k^+|$ vary by tuning the energy of the polariton mode. One can conveniently excite polariton modes such that for instance $|\beta_k^+|$ is appropriately smaller than $|\alpha_k^+|$ in which case neglecting terms quadratic and of higher order in $|\beta_k^+ / \alpha_k^+|$ (5.1.1) is approximated by

$$\langle (\Delta N_k^{ph})^2 \rangle = e^{\pm 2r_k} \langle N_k^{ph} \rangle + \frac{\sinh^2 r_k}{|\alpha_k^+|^2}(1 + \sinh 2r_k) + |\beta_k^+| [\frac{e^{\pm 2r_k}}{|\alpha_k^+|} A_{-1,k} - |\alpha_k^+| A_{1,k}] \tag{5.1.3}$$

More precisely the validity of the Eq. (5.1.3) not only depends on the relative magnitude of $|\alpha_k^+|$ and $|\beta_k^+|$ but also on their individual magnitudes, on the index of refraction, through r_k, and on the values of $A_{-1,k}$ and $A_{1,k}$. These are all mode-dependent quantities and the conditions under which the approximation (5.1.3) is valid must be accounted case by case.

We notice that Eqs. (5.1.1-3) may also be used to obtain specific results for the degree of second order coherence and the Mandel Q factor [79]. They provide an equivalent way to describe the photon statistics. For the former we have

$$g_k^{(2)}(0) \equiv \frac{\langle\, a_k^+ a_k a_k^+ a_k \,\rangle}{\langle\, a_k^+ a_k \,\rangle^2} \;; \qquad g_k^{(2)}(0) - 1 = \frac{Q_k}{\langle\, N_k^{ph} \,\rangle} \tag{5.1.4}$$

while the latter can be given as (cf. 5.1.1)

$$Q_k \equiv \frac{\langle\, (\Delta N_k^{ph})^2 \,\rangle - \langle\, N_k^{ph} \,\rangle}{\langle\, N_k^{ph} \,\rangle} \equiv e^{\pm 2r_k} - 1 + \Delta_k^{\pm} \tag{5.1.5}$$

where $\Delta_k^{\pm}$ is the rest.

In the case of high photon intensity or when the polariton mode can be singled out so that the approximation (5.1.3) holds, one has respectively

$$Q_k^{hi} = e^{\pm 2r_k} - 1 \tag{5.1.6}$$

and

$$Q_k^{s.m.} = (e^{\pm 2r_k} - 1)$$
$$+ \frac{1}{\langle N_k^{ph} \rangle} \{ \frac{\sinh^2 r_k}{|\alpha_k^+|^2} (1 + \sinh 2r_k) + |\beta_k^+| [\frac{e^{\pm 2r_k}}{|\alpha_k^+|} A_{-1,k} - |\alpha_k^+| A_{1,k}] \} \tag{5.1.7}$$

Recall that in the coherent case is $Q_k = 0$, while departures of the photon statistics from this case are measured by $Q_k \neq 0$. Sub-poissonian statistics carries a $Q_k < 0$ while the opposite holds in the super-poissonian case [79]. Let us also recall that the lower and upper signs correspond to $\phi_k = \varphi_k / 2$ and $\phi_k = (\varphi_k + \pi) / 2$, respectively. The phase ϕ_k of the complex eigenvalue γ_k is

$$\phi_k = tg^{-1} \left[\frac{|a_k| \sin \phi_k^a + |\frac{\beta_k^+}{\alpha_k^+} b_k| \sin(\phi_k^b + \chi_k)}{|a_k| \cos \phi_k^a + |\frac{\beta_k^+}{\alpha_k^+} b_k| \cos(\phi_k^b + \chi_k)} \right] \tag{5.1.8}$$

All parameters are defined in Appendix A6 (cf. Eqs. A6.2-6, A6.25). Owing to the rest $\Delta_k^{\pm}$ it is difficult to establish whether the two above choices for ϕ_k correspond to extremal values of the exact Mandel factor (5.1.5). They do so however, when the polariton modes can be tuned so that $|\alpha_k^+| >> |\beta_k^+|$, in which case

$$Q_{k,\max}^{s.m.} = (e^{+2r_k} - 1) + \delta_k^+ \qquad \text{for } \phi_k = (\varphi_k + \pi) / 2 \tag{5.1.9}$$

$$Q_{k,\min}^{s.m.} = (e^{-2r_k} - 1) + \delta_k^- \qquad \text{for } \phi_k = \varphi_k / 2 \tag{5.1.10}$$

$$\delta_k^{\pm} \equiv \frac{|\alpha_k^+|^2}{|a_k\alpha_k^+|^2+\sinh^2 r_k}\{\frac{\sinh^2 r_k}{|\alpha_k^+|^2}(1+\sinh 2r_k)+|\beta_k^+|[\frac{e^{\pm 2r_k}}{|\alpha_k^+|}A_{-1,k}^{\cdot}-|\alpha_k^+|A_{1,k}]\}$$

and clearly in the case of high photon intensity for which one has

$$Q_{k,\max}^{hi} = e^{+2r_k} - 1 \qquad \text{for } \phi_k = (\varphi_k + \pi)/2 \qquad (5.1.11)$$

$$Q_{k,\min}^{hi} = e^{-2r_k} - 1 \qquad \text{for } \phi_k = \varphi_k / 2 \qquad (5.1.12)$$

In both cases one simply has $\phi_k \equiv \phi_k^o$. The functional dependence of ϕ_k is otherwise quite complicated.

Typical values for Q in the wavevector region of interest to us are rather small and can be directly estimated from the results of fig.s 2,4,5. For exciton-polaritons in GaAs sub-poissonian statistics results in Q^{hi} varying in the range [-0.016,-0.020] and [-0.018,-0.021] for UBP and LBP modes, respectively. For exciton-polaritons in CuCl the deviations from poissonian are of the same order of magnitude, though slightly bigger: Q^{hi} ranges between [-0.079, -0.058] and [-0.095, -0.06] for UBP and LBP modes, respectively. In each semiconductor the same values, with positive sign, apply to the case of super-poissonian statistics, owing to the small r ($\sim 10^{-2}$) involved. On the other hand, when particular modes are selected ($|\alpha_k^+| >> |\beta_k^+|$) one has to include the additional δ to the relevant Q^{sm}, which however does not sensibly modify the previous estimations for Q. In the crossover region, taking e.g. $|a_k|^2 = 10$ (cf. Appendix A7-8), one has $\delta \approx 10^{-5}$ for GaAs and $\delta \approx 10^{-4}$ for CuCl.

5.2 Optical polariton squeezing.

Classically [36,37,39] an exciton-polariton wave has *both* the characteristics of an electromagnetic wave and of an exciton polarization wave. Quantum mechanically recall that $\hat{\tilde{\Gamma}}_{+k}$, the Fock space annihilation operator for a physical exciton-polariton mode k, can be separated to give the photon and exciton constituent particle operators [Eq. 4.1.10]. Its electromagnetic portion, described by a "dressed" photon of which we now analyse the quantum-optical properties, is for our purposes rewritten as

$$\hat{\tilde{\Gamma}}_{+k}^{ph} \equiv |\tilde{\alpha}_k^+| c_{r_k} \hat{a}_{+k} + e^{2i\varphi_k} |\tilde{\alpha}_k^-| s_{r_k} \hat{a}_{-k}^\dagger, \quad |\tilde{\alpha}_k^\pm| \equiv |\alpha_k^\pm| \, [|\alpha_k^\pm|^2 c_{r_k}^2 - |\alpha_k^\mp|^2 s_{r_k}^2]^{-1/2} \tag{5.2.1}$$

and an analogous expression for the mode $-k$. This equation emphasizes that the dressed photon field associated with the polariton inside the medium differs from the "bare" free space photon field. Examining Eq. (5.2.1) more closely, one notes that the photonic part of the polariton transformed operator has the form of a (two-mode) squeeze transformation from the bare photons $\hat{a}_{\pm k}$ to the dressed ones $\hat{\Gamma}_{+k}^{ph}$. We emphasize once more that we reserve the term *optical polariton squeezing* for just the process converting bare $(\hat{a}_{\pm k}) \rightarrow$ dressed $(\hat{\Gamma}_{+k}^{ph})$ photons according to Eq. (5.2.1). The transformation (5.2.1) is perfectly well defined for any value of k, however inspection of the expressions for $|\alpha_k^+|$ and $|\alpha_k^-|$ shows that only at the crossover wavevector k_o the squeeze transformation (5.2.1) takes on a particularly simple form ($|\alpha_{k_o}^+| = |\alpha_{k_o}^-|$). In Fig. 5.1 we report $|\alpha_k^+|$ and $|\alpha_k^-|$ for UBP states in the vicinity of k_o. Below we will illustrate optical polariton squeezing by referring for simplicity to the particular wavevector mode k_o.

Keeping in mind the restricted use of the term optical polariton squeezing, we then proceed to investigate the photon statistical properties connected with optical

squeezing in exciton-polariton coherent states $|\gamma_{\pm k}\rangle_z$. The results of § 5.1 will then be used: namely recall that in the case of high photon intensity one has a non-poissonian photocount statistics characterized by (cf. Eq. 5.1.2),

$$\langle (\Delta N_{k_o}^{ph})^2 \rangle \equiv e^{\pm 2r_o} \langle N_{k_o}^{ph} \rangle \qquad Q_{k_o}^{hi} \equiv e^{\pm 2r_o} - 1 \tag{5.2.2}$$

+ and - respectively refer to a photon phase $\phi_{k_o}^a \equiv (\varphi_{k_o} + \pi)/2$ or $\phi_{k_o}^a \equiv \varphi_{k_o}/2$. If restrictions on the photon intensity instead apply, one then should use the approximate result (5.1.3). This can be done when $|\beta_k^+|$ is appropriately smaller than $|\alpha_k^+|$, consistently with $|\alpha_k^+| \cong |\alpha_k^-|$. This possibility will be investigated in detail below and we begin by rewriting (4.1.15) as

$$\left|\frac{\alpha_k^+}{\beta_k^+}\right| = \kappa \left|\frac{(\varepsilon - \hbar\omega_o)(\varepsilon + \hbar ck)}{\sqrt{\hbar ck}}\right| \tag{5.2.3}$$

$\kappa \equiv [\hbar\omega_o \sqrt{4\pi\beta\hbar\omega_o}]^{-1}$ is a quantity characteristic of the dielectric material, while the rest of the ratio is mode-dependent. At $k \cong k_o$ (5.2.3) takes on the form (cf. Fig. 1.8)

$$\left|\frac{\alpha_{k_o}^+}{\beta_{k_o}^+}\right| = \frac{1}{\sqrt{4\pi\beta_o}} \left|\frac{(\hbar\omega_{LT} + \Delta_U)^2}{(\hbar\omega_o)^2} + \frac{2(\hbar\omega_{LT} + \Delta_U)}{(\hbar\omega_o)}\right| \quad (upper\ br.) \tag{5.2.4}$$

$$\left|\frac{\alpha_{k_o}^+}{\beta_{k_o}^+}\right| = \frac{1}{\sqrt{4\pi\beta_o}} \left|\frac{\Delta_L^2 - 2\hbar\omega_o\Delta_L}{(\hbar\omega_o)^2}\right| \quad (lower\ br.) \tag{5.2.5}$$

In principle small oscillator strengths and transverse exciton energies along with large separations Δ are required to have satisfactorily large ratios. In Fig. 5.2 we

report the ratio $|\alpha_k^+ / \beta_k^+|$ when we sweep the wavevector across k_o . Exactly at k_o, $|\alpha_k^+|$ and $|\beta_k^+|$ are practically equal, at least for the materials here examined; therefore approximating (5.1.1) with (5.1.3) may not be entirely justified by simply neglecting second and higher order of $|\beta_k^+ / \alpha_k^+|$, but in general the values of n_o (cf. Eq. 4.1.20) and of the values of the A 's must be also taken into account as discussed in § 5.1. Interestingly enough however, and especially in GaAs a slight detuning to the right of k_o shows a rather fast decrease of $|\beta_{k_o}^+ / \alpha_{k_o}^+|$, yet maintaining $|\alpha_k^+|$ and $|\alpha_k^-|$ satisfactorily close to one another. Thus non-poissonian statistics associated with *optical* squeezing in the vicinity of the crossover in the UBP can still be described using Eq. (5.1.3) . In the LBP the use of the same result (5.1.3) is even more legitimate because the$|\beta_{k_o}^+ / \alpha_{k_o}^+|$ is slightly bigger than the one for the UBP. This is directly estimated from Eqs. (5.2.4-5). In summary, for *arbitrary*photon intensities predictions about the non-classical behaviour of photons in a polariton coherent state due to optical squeezing are not in general as straightforward as for the high intensity case. The validity of the approximation (5.1.3) must be carefully examined case by case.

5.3 Remark on phonon-polaritons

Recalling Eq. (4.1.21) and considering that the present model can be applied to phonon-polaritons as well, a bigger order of magnitude for r_o can be expected in general because in this case the ratio $\Delta / \hbar\omega_o$ takes on values larger than in the exciton-polariton case. Typical values of r_o can be estimated using (4.1.21). For (TO) phonon-polaritons in ionic crystals such as e.g. GaP [49] typical values are nearly one order of magnitude bigger than in the exciton case.

CHAPTER VI

Detection techniques

Recently there has been much interest in producing squeezed states of light, by taking advantage of non-linear optical effects, and in measuring such non-classical effects [10]. At present, squeezed states have been generated via four-wave mixing or parameteric oscillations in an optically nonlinear medium. In general, squeezing is achieved in configurations which incorporate large nonlinearities and high pump intensities. On the other hand, squeezing is destroyed by losses. In general larger nonlinearities carry larger absorption losses, and so in a *nonlinear* material there is a delicate balance between loss and nonlinearities.

It has been shown above that *non-poissonian statistics* and *optical squeezing* can occur in *linear* resonant dispersive media via polariton creation. To date there has been no experimental reports of squeezed states generation is semiconductors. It will be thus important to subject our results to decisive experimental test.

In this chapter we propose and analyse theoretically methods which can be used to demonstrate the existence of optical squeezing and/or departures from classical photocount statistics in polaritons. Although our discussion emphasizes the exciton polariton the same theory carries over to the case of phonon polariton with suitable changes in numerical values, and that will be analysed also. The new idea here is to probe the evanescent radiation from the bulk polariton at the crystal surface in order to determine the quantum statistics of the radiation associated with the bulk polariton wave. The distinction between an evanescent polariton

wave, arising when the bulk wave is total internally reflected [80], and other surface waves such as e.g. surface polaritons [81] should be noted at this specific point. We assert here that the evanescent electromagnetic field carries the same quantum statistical properties as the one associated with the bulk polariton. A justification for this assertion will be given below. It is furthermore important to clarify that in the absence of total internal reflection then, outside the crystal, the transmitted optical field does not exhibit squeezing effects. A brief qualitative account of this is given here within the context of the *classical* Ewald-Oseen extinctiontheorem (see below). In classical optics the medium, following Lorentz and Plank, is represented by an assembly of dipoles: for a bounded medium, the array of dipoles terminates at some surface whereas for the unbounded case there is no termination. In the latter case the total propagating field emitted by the assembly of all dipoles (the sum of the fields emitted by all dipoles) is an optical (dipolar) plane wave which propagates in the medium at velocity c/n and wavevector $\vec{Q}$ where $|\vec{Q}|= n(\omega/c)$, and n is refractive index. For the bounded case an incident optical wave from vacuum entering the medium excites the dipolar array. The total emission from the assembly of dipoles now consists of two fields. One of these exactly cancels (extinguishes) the incident field at every point in the medium. The second constituent, in the medium, is the propagating refracted optical field with wavevector $\vec{Q}$. This is the extinctiontheorem. Since the extinctiontheorem is entirely in the framework of Maxwell's electrodynamics and the Lorentz-Plank picture of molecular optics, the overall description of the inside-outside fields according to this theorem is time-reversal. From this one can straightforwardly argue that the origin of the optical field external to the crystal is quite different from the dipolar field generated inside the crystal and, under certain

conditions, leaking off the surface of the crystal. As a peculiarity of this picture note that a surface is needed to distinguish inside and outside. But the surface plays an additional role via a surface integral (over fields) that regulates indeed the inner/outer fields. With this background one can firther discuss a *quantum-optical* generalisation of the extinction theorem [82].

6.1 Evanescent radiation field.

For our reference let us start by considering the electromagnetic field in vacuum. The electric field operator for a fixed polarization (positive-frequency part) is

$$\hat{E}_{\nu}^{(+)} \equiv \hat{E}_{\nu}^{(+)}(\vec{r},t) = \sum_{k} E_{k}^{o}\, u_{k}(\vec{r}) e^{-i\omega_{k}t}\, \hat{a}_{k} \qquad (6.1.1)$$

Harmonic time-dependence has been assumed, whereas $\{u_k\}$ is a complete orthonormal set of functions in terms of which the field operator can be expanded. $\hat{a}_k$ is the destruction operator for a photon of wavevector $\vec{k}$. Coherent states of the field are defined as the eigenstates of $\hat{E}_{\nu}^{(+)}$ [83,84],

$$\hat{E}_{\nu}^{(+)} |\alpha^{\nu}\rangle = \Im |\alpha^{\nu}\rangle \qquad \Im \equiv complex \qquad (6.1.2)$$

It then follows that

$$| \alpha^{\nu} \rangle = \prod_{k} | \alpha_{k}^{\nu} \rangle \qquad (6.1.3)$$

provided coherent states $| \alpha_k^{\nu} \rangle$ of the field single mode k be defined as

$$\hat{a}_k | \alpha_k^{\nu} \rangle = \alpha_k | \alpha_k^{\nu} \rangle \qquad \alpha_k = complex \tag{6.1.4}$$

Now consider the exciton-polariton. The e.m. part $\hat{\Gamma}^{ph}$ of the polariton operator is a certain linear combination of vacuum photon creation and annihilation operators. Adopting the Hopfield model as discussed in chapters IV-V one has for the mode k (cf. Eq. 5.2.1)

$$\hat{\Gamma}_k^{ph} = C_k \hat{a}_k + D_k \hat{a}_{-k}^{\dagger} \qquad C_k^2 - D_k^2 = 1 \tag{6.1.5}$$

where the coefficients depend on the mode, on the branch (UPB/LPB), and on the material. As shown in chapter V, the Eq. (6.1.5) implies squeezing in the photon portion of the polariton (*optical squeezing*) on both branches, and this is tunable. Non-poissonian photon statistics is also predicted.

The contribution to photons of given energy $\hbar\omega$ inside a medium where polaritons have been excited comes from the electromagnetic component of all those bulk polaritons carrying the same energy. At the vacuum-crystal interface the extension of a bulk polariton is an evanescent wave, if the bulk wave is total internally reflected [80]. The polarization (exciton or phonon) component of the polariton is restricted by the surface, hence the relevant field at the interface is not represented by $\hat{\Gamma}$ (cf. § 5.2) but rather by its radiative component $\hat{\Gamma}^{ph}$. The evanescent e.m. field carries the same quantum statistical properties as the one associated with the bulk polariton. The appropriate conceptual framework that permits one to understand this is a quantum optical version of the extinction

theorem [82,85,86] according to which the radiation field associated with the bulk polariton is nothing but the internal dipole field that does not extinguish the free-space incident field (pump) inside the medium. The evanescent radiation is thus arising from this internal field that at total internal reflection leaks away through the surface. The electric field operator associated with the evanescent wave portion of the bulk polariton (positive frequency part) is

$$\hat{E}_{ev.}^{(+)} \equiv \hat{E}_{ev.}^{(+)}(\vec{r},t) = \sum_{k} E_{ev.}^{o}\, u_k(\vec{r})\, e^{-i\omega t}\, \hat{\Gamma}_k^{ph} \tag{6.1.6}$$

The sum is over those wavevector modes obeying $\omega\sqrt{\varepsilon_d} = c|\vec{k}|$, ε_d being the polariton dielectric function at the given frequency ω (cf. Eq. 2.1.1). $E_{ev.}^{o}$ and $\hat{\Gamma}^{ph}$ represent respectively the electric field per evanescent photon and the photon annihilation operator for the leaky polariton radiation.

Next consider quantum states of the evanescent polariton radiation. One may take number states $|\, n_k^p \,\rangle$ in which the polariton mode k is occupied by n_k^p photons; these states form a convenient basis whenever experiments with a fixed number of particles are involved. They are not of direct significance however in a typical optical solid state experiment where the probe is usually a light source with no definite numbers of photons such as a laser [87]. This situation can instead be properly described by using coherent states. So we consider coherent states for the optical portion of the polariton of frequency ω leaking across the crystal surface. They are defined as

$$\hat{\Gamma}_k^{ph}\,|\alpha_k^{ev.}\rangle = \alpha_k^{ev.}\,|\alpha_k^{ev.}\rangle \qquad\qquad \alpha_k^{ev.} = complex \tag{6.1.7}$$

Within the framework of the Hopfield model it has been shown in § 5.2 that e.g. at $k = k_o$ one has,

$$|\alpha_{k_c}^{ev.}\rangle = S(r_{k_c})|\alpha_{k_c}^{ev.}\rangle \tag{6.1.8}$$

where S is a squeeze transformation in Eq. (4.1.11), and $r_{k_o} \equiv r_o$ is the squeeze factor evaluated at this particular wavevector mode. In this specific case, coherent states of the evanescent polariton radiation field are squeezed with respect to coherent states for the vacuum radiation field [88,10,28]. Estimates of the amount of squeezing given by r_o will be discussed later.

6.2 Detection schemes

In this section we illustrate methods which we propose can be used to detect optical squeezing in polaritons. Namely we adapt homodyne techniques already used to detect squeezing of cavity photons [10] to our case.

An *homodyne detector* [2,8-10] is a device with two input ports and two output ports: let $\hat{a}_{1in}$ and $\hat{a}_{2in}$ denote the annihilation operators for the particles entering the two input ports, and similarly $\hat{a}_{1out}$ and $\hat{a}_{2out}$ denote the annihilation operators leaving the two output ports. The scattering matrix for such a device has the form

$$\begin{pmatrix} \hat{a}_{1out} \\ \hat{a}_{2out} \end{pmatrix} = \begin{pmatrix} U_{11} & U_{12} \\ U_{21} & U_{22} \end{pmatrix} \begin{pmatrix} \hat{a}_{1in} \\ \hat{a}_{2in} \end{pmatrix} \tag{6.2.1}$$

where the matrix U is unitary for boson particles

Here we show how to realize the homodyne configuration making use of the crystal surface (matter-vacuum interface), which is the site of the evanescent leaky tail of the optical field of the bulk polariton, as an input port. We need the local oscillator, beam splitter, detectors, and we need to create the leaky polariton by methods which can be also employed in other polariton ATR configurations [89]. A polariton wave appropriately excited in the crystal undergoes total internal reflection at the vacuum interface: an inhomogeneous wave is generated on the surface and propagates parallel to it. In the direction normal to the surface this wave decays in a distance $s \equiv c(n^2 \sin^2\theta - 1)^{-1/2} / \omega$: ω and $n = n(\omega)$ are respectively the polariton frequency and the refractive index of the medium at the wavevector mode that is excited, θ the polariton angle of incidence, and c is the speed of light in vacuum. As previously mentioned the photon statistics of the bulk polariton is preserved in the leaky component. Thus, since the latter is confined within a quite narrow region (see Tab. 6.1) above the crystal surface, one can study the photon distribution of the evanescent radiation directly on the surface as a field whose statistical properties are to be determined. For simplicity, losses in the present analysis are not considered.

With minor modifications the schemes we will analyze are essentially suited to detecting either *non-poissonian photon statistics* or *optical squeezing* (see chapter V). To keep the treatment general the wavevector dependence is hereafter understood. Thus following the scheme of Fig. 6.1 we let for definiteness the input particle 1 be the photon from the polariton $\hat{a}_{1in} \rightarrow \hat{a}_p$, and the input particle 2 be the local oscillator photon $\hat{a}_{2in} \rightarrow \hat{a}_{L.O.}$.

6.3 Ordinary homodyne

As shown in Fig. 6.2 an incident laser beam from an external "local oscillator" (*L.O.*), in a coherent state, is superimposed on the leaky radiation at the detector *P*. It is assumed that a satisfactory mixing can be achieved by either optimizing the (space) mode-matching between the two signals or avoiding unwanted surface effects. The detected input annihilation operator is then

$$\hat{d} = T\,\hat{a}_p + R\,\hat{a}_{LO.} \tag{6.3.1}$$

$\hat{a}_p$ and $\hat{a}_{LO.}$ are the photon annihilation operators of the evanescent polariton and of the laser pump (*L.O.*), respectively. Wavevector phase-matching between the two can be achieved by varying the angle of incidence [90], while the frequency is the same. R and T are the complex amplitudes of the reflection and transmission coefficients at the beam splitter BS and at the leaky interface, respectively. They satisfy the conditions

$$|R|^2 + |T|^2 = 1 \qquad \text{and} \qquad RT^* + R^*T = 0 \tag{6.3.2}$$

which is the requirement for unitarity. The photons from the two fields fall onto the photocathode *P*, which is a layer of photoemissive material that emits electrons when illuminated. To prevent *P* from detecting stray light from beneath the surface, the portion of it hosting the photoemissive film can be isolated by a reflecting coating. Take the electric fields of the impinging radiation to be polarized perpendicular to the surface to optimize the photoemission efficiency. The emitted electrons, after crossing the multiplier *M* and being collected at the anode *A*, give

rise to a photocurrent which after a suitable processing provides the statistical distribution $P_n(T)$ of the number n of photocounts recorded during repeated time intervals of duration T .

This scheme will enable one to determine those quantum statistical properties of polariton light which are of interest to us. From Eq. (6.3.1) the number of photons measured at P is readily evaluated

$$\hat{N}_d \equiv \hat{d}^{\dagger}\hat{d} = |R|^2 \hat{a}^{\dagger}_{LO.}\hat{a}_{LO.} + |T|^2 \hat{a}^{\dagger}_{p}\hat{a}_{p} + |RT|\{e^{i(\varphi_R - \varphi_T)} \hat{a}^{\dagger}_{p}\hat{a}_{LO.} + h.c.\} \tag{6.3.3}$$

and so is the corresponding variance (fluctuations)

$$\begin{aligned}\langle(\Delta\hat{N}_d)^2\rangle = R\alpha_{LO.}|^2\{&|R|^2 + |T|^2[\langle(\hat{a}_p e^{-i\chi} + \hat{a}^{\dagger}_p e^{+i\chi})^2\rangle - \langle \hat{a}_p e^{-i\chi} + \hat{a}^{\dagger}_p e^{+i\chi}\rangle^2]\} \\ &+ |TR\alpha_{LO.}|\{[\langle \hat{a}_p\rangle e^{-i\chi} + \langle \hat{a}^{\dagger}_p\rangle e^{+i\chi}] \\ &+ 2|T|^2[e^{i\chi}\langle \hat{a}^{\dagger 2}_p \hat{a}_p\rangle - \langle \hat{a}^{\dagger}_p\hat{a}_p\rangle\langle \hat{a}^{\dagger}_p\rangle + h.c.]\} + |RT|^2\langle \hat{a}^{\dagger}_p\hat{a}_p\rangle\end{aligned} \tag{6.3.4}$$

The brackets here denote the input state at the detector (P), which is the (tensor) product of the $L.O.$ coherent state and the coherent state of Eq. (6.1.7) for the polariton radiation. One then adjusts the $L.O.$ light intensity so as to be sufficiently stronger than that of the evanescent radiation, and R and T so that [91]

$$|R||\alpha_{LO.}| >> |T||\alpha_p| \qquad\qquad |R| << |T| \tag{6.3.5}$$

$\alpha_{LO.}$ and α_p, the complex amplitudes of the $L.O.$ and of the leaky polariton light respectively, and the phase $\chi \equiv \varphi_{LO.} + \pi/2$ are all subject to experimental control and can be varied independently [92]. Under the conditions (6.3.5) the variance (6.3.4) is approximated by (second order in $|\alpha_{LO.}|$,

$$\langle(\Delta\hat{N}_d)^2\rangle = R\alpha_{LO}|^2\{|R|^2+|T|^2[\langle(\hat{a}_p e^{-iz}+\hat{a}_p^\dagger e^{+iz})^2\rangle-\langle\hat{a}_p e^{-iz}+\hat{a}_p^\dagger e^{+iz}\rangle^2]\} \qquad (6.3.6)$$

Measurements of this quantity enables one to decide, e.g. in the case of *optical squeezing*, whether or not the polariton evanescent light is squeezed i.e. by testing for a non-poissonian variance that is dependent on the *L.O.* phase. In fact when testing for *optical squeezing* one can evaluate the expectation values in the square bracket to obtain (cf, Eq. 6.1.8.)

$$\langle(\Delta\hat{N}_d)^2\rangle = |R\alpha_{LO}|^2\{|R|^2+|T|^2[e^{2r_o}\sin^2\varphi_{LO}+e^{-2r_o}\cos^2\varphi_{LO}]\} \qquad (6.3.7)$$

If the photon part of the polariton is in a coherent state ($r_o = 0$) then poissonian photocount statistics applies and $\langle(\Delta\hat{N}_d)^2\rangle = |R\alpha_{LO}|^2$ (shot-noise). On the other hand if optical squeezing occurs ($r_o \neq 0$), for some values of φ_{LO} the photocount variance becomes smaller than the shot-noise contribution alone.

In order to design an experiment we need numerical values of the *squeeze factor* r_o and of the expected *power of the evanescent radiation* component of the bulk polariton for particular materials. To this end recall the dielectric properties of the medium at the crossover mode k_o are represented by the dielectric constant

$$\varepsilon_c \equiv \varepsilon(\omega_c) = \varepsilon_b + \frac{4\pi\beta_o}{1-(\frac{\omega_c}{\omega_o})^2}$$

The essential material dependent parameters are: ε_b, the background dielectric constant, $4\pi\beta_o \equiv 2\varepsilon_b\Delta_{LT}/\omega_o$ the oscillator strength and ω_o the "bare" exciton or

phonon resonance frequency [48]. In Tab 6.1 we give values of these parameters for several materials such as GaAs, CdS, and KI. Since r_o is given as $r_o = 0.25 \ln \varepsilon_o$ (see chapter IV) it is clear that the larger Δ_{LT} and/or the closer ω_c to the resonance frequency ω_o , the bigger r_o. Exciton-polariton and phonon-polariton squeeze factors for these materials are reported in Tab. 6.1. These produce reductions of the noise ranging between 1% and 40% below the limit set by the vacuum fluctuations. Thus enhanced noise reductions are more likely to be achieved e.g. in phonon-polaritons or polaritons with relatively large LT splittings. The case of KI [93] is only "hypothetical" because the observed exciton-polariton dispersion in KI does not fit a single one-oscillator model $\varepsilon(\omega)$ within which we derive our theoretical predictions for r_c. It may be useful however to show that in materials analogous to KI exhibiting large LT splittings ($\Delta_{LT}^{KI} \approx 10^3 \Delta_{LT}^{GaAs}$), amounts of squeezing for exciton-polaritons can be made comparable to those for phonon-polaritons.

As for radiation power P_{evan} in the evanescent wave, an estimate can be given. Suppose that a laser, entering the dielectric normally through a plane surface, excites a polariton of the same frequency that propagates at an angle θ and whose electric field is p-polarized (Fig. 6.2). If $I_{inc.}$ is the laser intensity, a straightforward application of Fresnel's formulae gives an estimate for the evanescent intensity I_{evan}, which for the materials examined does not vary sensibly over the angular configurations of interest to us ($\theta_c \leq \theta < 90°$) and can be taken to be ~80% of the incident laser intensity [94]. Conversely the region in which the leaking radiation is confined in the direction perpendicular to the surface sensibly depends on θ: for phonon-polaritons the width of this region is in general bigger than for exciton-polaritons (see Tab. 6.1). Finally for the same angular range and an incident laser intensity $I_{inc.} = 20 \ W/cm^2$ we estimate the total power in the

evanescent polariton radiation. We find that power levels can be achieved which are comparable with those of output cavities, where squeezed light is usually generated via four-wave mixing or parametric amplification [10] (see Tab. 6.1).

It is important to observe that the second condition in Eq. (6.3.5) allows the noise from the *L.O.* to be in part suppressed but not completely, the overall noise being mainly determined by the fluctuations in the number of photons from the evanescent polariton. The two terms in the curly bracket come from the reflected *L.O.* uncertainty (fluctuations) and the uncertainty associated with the transmitted photons from the polariton leaking wave. In the next section we proceed to analyze a slightly more elaborate phase-sensitive device that enables one to display the non-classical effects of relevance to us, but eliminating the *L.O.* contribution to the noise completely.

6.4 Balanced homodyne

Consider the homodyne scheme of Fig. 6.3 operating above the leaky region. For this purpose we suppose that a part of the surface is shaped into a reflecting grating *G* that diverts the radiation into one of the detector inputs. Diffraction of an evanescent e.m. wave has been studied, and energy is carried away from the grating [95]. If photons from the evanescent wave are incident at angle θ_i relative to the surface normal of a reflecting groove ruled with spacing $2a$, the path difference for photons incident on any two adjacent grooves is $2a\sin(\theta_i + \delta)$ (see Fig. 6.4). When these photons are diffracted at some angle θ_d, the path difference is further increased by the amount $2a\sin(\delta - \theta_d)$. The phase condition requires that the path difference for photons incident on adjacent grooves be an integer p

multiple of λ. For a given wavelength the reflection from all the grooves will be in phase if

$$\sin(\delta - \theta_d) = p\frac{\lambda}{2a} - \sin(\delta + \theta_i) \tag{6.4.1}$$

namely only at certain angles defined by the order p. For the case $p = 0$ $\theta_i = \theta_d$ and the grating acts as a mirror. The number of diffracted maxima is however limited by $|\sin(\delta - \theta_d)| \leq 1$; in the *"echelette"* configuration as shown in Fig. 6.4 the order p therefore cannot exceed

$$|p| \leq \frac{4a}{\lambda} \tag{6.4.2}$$

Thus specifying a particular geometry of the strips of the grating can make the diffraction efficient in a practical order. For $a << \lambda$ the diffracted photons may be directed into the 0th-order, or few orders on the side, so as to maximize the energy to be diffracted. The diffracted evanescent wave is then focused into the homodyne detector input as shown in Fig. 6.4. The beam splitter *BS2*, with input arms (*I*) and (*II*), is fed by the light coming from both the evanescent wave and the local oscillator at the same frequency, whereas its output arms (*III*) and (*IV*) illuminate the two photodetectors D_3 and D_4. The beam splitter performs the important function of producing quantum-mechanical superposition of the input states

$$\hat{a}_3 = R_2\hat{a}_p + T_2\hat{a}_{LO.} \qquad \hat{a}_4 = T_2\hat{a}_p + R_2\hat{a}_{LO.} \tag{6.4.3}$$

R_2 and T_2 are the complex amplitude reflection and transmission coefficients of the beam splitter *BS2*, and satisfy conditions analogous to Eq. (6.3.2) provided the beam splitter is lossless and symmetric. Here we take $|R_2|=|T_2|=\sqrt{2}$. Since in this scheme the difference of the two photodetector readings D_3 and D_4 is considered, the detector input signal is now determined by the operator

$$\hat{d}_{12} \equiv \hat{d}_1^{\dagger}\hat{d}_1 - \hat{d}_2^{\dagger}\hat{d}_2 = i[\hat{a}_p^{\dagger}\hat{a}_{L.O.} - \hat{a}_{L.O.}^{\dagger}\hat{a}_p] \tag{6.4.4}$$

If one again testes for *optical squeezing* an analogous calculation to that carried out to obtain Eq. (6.3.6) gives for the fluctuations in the number difference of detected photons [96]

$$\langle(\Delta \hat{d}_{12})^2\rangle \equiv |\alpha_{L.O.}|^2\{e^{2r_o}\sin^2\varphi_{L.O.} + e^{-2r_o}\cos^2\varphi_{L.O.}]\} \tag{6.4.5}$$

Comparing to Eq. (6.3.7), this version with respect to the previous one has the remarkable advantage of removing the noise contributions from the intensity fluctuations of the *L.O.* light. Again the variance in Eq. (6.4.5), as the one in Eq. (6.3.7), characterizes the noise due to squeezing in the electromagnetic field associated with polaritons. Reductions of the noise level below the shot noise occur and in Tab. 6.1 we report the maximum reductions in exciton and phonon polaritons of some typical semiconductors.

If *optical squeezing* is to be detected, within this specific balanced scheme, one can in principle estimate the relevant amount of squeezing through r_o. It suffices for instance to measure the ratio of the maximum of (6.4.5) vs. $\varphi_{L.O.}$, suitably normalized, to obtain

$$r_c = \frac{1}{2}\ln\frac{|\max.\langle(\Delta \hat{d}_{12})^2\rangle_{in}|}{|\alpha_{L.O.}|^2} \qquad (6.4.6)$$

6.5 Detection of non-poissonian statistics

As previously mentioned optical squeezing is predicted at k_c (Hopfield model) while non-poissonian statistics is predicted throughout the spectrum in both branches (UPB & LPB). The magnitude of the departures from poissonian is k -dependent, i.e. is tunable as the laser frequency populating the exciton-polariton mode is changed. Non-poissonian features of the polariton radiation can be detected by measuring the associated photon-number mean and variance. This can be done for instance using the ordinary homodyne scheme in which the external *L.O.* be suppressed, directly by detecting the photocount mean and variance of the leaking polariton radiation at *P*. Different variances are relevant to different modes. Such a direct measurement is not phase-dependent, and is therefore not specifically sensitive to squeezing, but only to the associated bunching or antibunching (super or sub-poissonian) statistics, both of which can also occur for non-squeezed light [51].

Now we comment on certain effects of degradation. The main requirement in all the methods above is indeed the extraction of the bulk polariton values for the photon number mean and variance from measurements of photocount mean and variance of its leaking component across the surface. Namely, processing of the photocurrent at the counter (Fig. 6.2) or the S.A. (Fig. 6.3) provides a statistical distribution $P_n(T)$ of the number of photocounts recorded during repeated periods of time T . The latter provides a record of the actual photon distribution,

say $p_n(T)$, though distorted by *surface effects,* mostly dissipation connected with the propagation of an electromagnetic wave on the surface. The detection process will result in additional distortions due to the *non-unity quantum efficiency* of the photodetector. As discussed in [97] these two major sources of degradation can be included phenomenologically in the description by ascribing the loss (surface plus non-ideal detector) to the loss of light at a beam splitter which transmits only a fraction of the input amplitude. Generally speaking degradations result in a variance for the leaking polariton radiation, or equivalently the associated Mandel $\tilde{Q}$ factor [97,79],

$$\tilde{Q} = \gamma Q \qquad (0 < \gamma < 1) \tag{6.5.1}$$

that is distorted with respect to the actual one. Distortion effects can be characterized by an effective efficiency γ of the overall detection process. Contributions to γ, which physically represents the loss per unit photon, arise from γ_D, the photodetector efficiency, and γ_S, the efficiency for propagation on the surface limited by absorption, scattering, diffraction, etc. High detection quantum efficiency γ_D, typically $\gamma_D > 0.9$, are routinely obtained at present, whereas smaller values $\gamma_S \cong 0.8$ compete to surface propagation losses [98]. The useful noise reduction in polaritons are further limited by other deviations from ideal conditions that include *non ideal mode structures, thermal noise, amplifier noise* and other extraneous noise sources. All these extra non ideal factors have to be included into the effective optical efficiency so that $\gamma = \gamma_S \gamma_D \gamma_M \gamma_T \gamma_A \cong 0.45$, where we take $\gamma_A \cong 1$ as effective efficiency due to electronic amplifier noise, $\gamma_T \cong 1$ as efficiency limited by thermal noise, and $\gamma_M \cong 0.6$, the most crucial one,

as mode matching efficiency for the phase fronts of the evanescent wave and the local oscillator *L.O.*, [99]. As in cavity optical squeezing the non ideal efficiencies combine to limit the measured non-classical statistics associated with polariton radiation, even though polariton modes with substantial non-poissonian characteristics can be excited.

FIGURE CAPTIONS

Fig. 1.1

Light is represented as a combination of oscillating electric and magnetic fields. *Classically* coherent light (laser) can be represented by a thin line (a), because at any time the strengths of the electric and magnetic fields are known with certainty. *Quantum mechanically,* however the electromagnetic field strengths can be known only within an envelope of uncertainty (shaded region) and the measured fields (solid lines) can fluctuate anywhere within the envelope (b). The vertical width of the shaded region indicates the square root of the variance of the optical field amplitude.

Fig. 1.2

Even in complete darkness there must be some quantum uncertainty, and so the field strengths are not exactly zero; they too fluctuate within an envelope of uncertainty.

Fig. 1.3

In a squeezed state the envelope of uncertainty is pinched close together in some parts of the wave and made wider in other parts. For the *squeezed vacuum* (a) briefs periods in which random fluctuations are very small (narrow envelope of uncertainty) alternate with periods in which the fluctuations can be quite large. For *phase-squeezed light* the envelope of uncertainty is wide when the field strength passes through its maximum value, but narrow when the field strength passes

through zero (b). Hence the wave's amplitude is uncertain but its phase is relatively certain, because it is relatively certain when the wave will go through the start of its cycle. Conversely, for *amplitude-squeezed light* the amplitude is relatively certain but the phase fluctuates widely (c).

Fig. 1.4

Phase-space description of the mean values and uncertainties of the quadrature operators $\hat{X}$ and $\hat{Y}$ for a coherent state.

Fig. 1.5

Phase-space description of the mean values and uncertainties of the quadrature operators $\hat{X}$ and $\hat{Y}$ for a vacuum state.

Fig. 1.6

Phase-space description of the mean values and uncertainties of the quadrature operators $\hat{X}$ and $\hat{Y}$ for a squeezed state.

Fig. 1.7

Phase-space description of the mean values and uncertainties of the quadrature operators $\hat{X}$ and $\hat{Y}$ for a number state and a squeezed number state.

Fig. 1.8

Frequencies of the CuCl exciton-polariton coupled mode [48] as a function of the wavevector (solid line): two values, ω^U and ω^L, correspond to each given (real) k, one in the upper branch (UBP) and the other in the lower branch (LBP). One

wavevector only corresponds to a given energy (no spatial dispersion) on each branch. The broken lines show the dispersion relations of "uncoupled" photons and excitons. k_o is the wavevector crossover of the bare photon and bare exciton energy dispersion curves ($\hbar c k_o = \hbar \omega_o$). For an isotropic medium there is also a longitudinal exciton mode: $\hbar \omega_l$. $\omega_{LT} \equiv \omega_l - \omega_0$ is the transverse-longitudinal splitting frequency, ω_o is the transverse exciton energy, and $\Delta^{U,L}$ are the distances of the upper and lower polariton energy branches from the longitudinal and transverse exciton energies, respectively.

Fig. 3.1

Magnitude of the squeeze factor in CuCl and GaAs exciton-polaritons as a function of k calculated within the *generalized* polariton model for LBP (-.-.-.-.) and UBP (-..-..-..-..) modes in vicinity of the crossing wavevector k_o. All the numerical evaluations have been here obtained using material parameters as given in ref. [48]: $\hbar \omega_o^{CuCl} = 3.20 eV$, $\hbar \omega_o^{GaAsl} = 1.51 eV$, $\varepsilon_b^{CuCl} = 4.6$, $\varepsilon_b^{GaAsl} = 12.5$, $4\pi\beta_o^{CuCl} = 0.0158$, $4\pi\beta_o^{GaAsl} = 0.0013$.

Fig. 3.2

Normalized envelope of fluctuations ($\tilde{\Gamma}_k^p(t) \equiv \Gamma_k^p(t) / \Gamma_k^o$) of the propagating field of a polariton in a UBP CuCl exciton-polariton coherent state. We exhibit the time dependence over the polariton cycle while the wavevector sweeps through the crossover (k_o) region.

Fig. 3.3

Horizontal section of Fig. 3.2. Time and wavevector dependence of $\tilde{\Gamma}_{\underset{\sim}{k}}^{\ p}(t)$ in the squeezing region. In a polariton coherent state twice, half cycle distant one another, the fluctuations $\tilde{\Gamma}_{k}^{\ p}(t)$ reduce below the value 1/4 associated to the coherent-vacuum state. The squeezing arrives a maximum≈ 70%.

Fig. 3.4

Variation of the amount of squeezing in a UBP CuCl exciton-polariton during $\Delta T_{sq.}^{CuCl}$. "0" refers to the case of no squeezing i.e. $\Gamma_{k}^{p}(t) = \Gamma_{k}^{o}$; 40 (star) refers to the case in which $\Gamma_{k}^{p}(t) \leq 0.6\,\Gamma_{k}^{o}$, while 60 (triangle) refers to the case in which $\Gamma_{k}^{p}(t) \leq 0.4\,\Gamma_{k}^{o}$. Proceeding downwards the above explanation repeats itself. The vertical distance between e.g. two given triangles yields the time interval during which the width of the envelope of fluctuations falls below nearly 1/3 of the coherent-vacuum value, whereas twice the vertical distance between the solid lines gives $\Delta T_{sq.}^{CuCl}$. Here (-.-.) represents the quarterperiod: $t = T_{pol} / 4$.

Fig. 4.1

Magnitude of the squeeze factor in CuCl and GaAs exciton-polaritons as a function of k calculated within the *conventional* Hopfield model from the exact expressions (4.1.18) for LBP (-.-.-.-.) and UBP (-..-..-..-..) modes in vicinity of k_o. As for the generalized case (Fig. 3.1) the material parameters are taken from ref. [48].

Fig. 5.1

Photon partial weights $|\alpha_k^+|$ and $|\alpha_k^-|$ in the vicinity of k_o for CuCl (-.-.-.-.) and GaAs (-..-..-..-..) exciton-polariton UBP modes. Spanning the wavevector interval from left to right, $|\alpha_k^+|$ and $|\alpha_k^-|$ assume increasing and decreasing values respectively. A similar behaviour occurs for the exciton partial weights $|\beta_k^+|$ and $|\beta_k^-|$ going in the opposite direction.

Fig. 5.2

Ratio of $|\alpha_k^+|$ and $|\beta_k^+|$ in the vicinity of the crossover k_o for CuCl and GaAs.

Fig. 6.1

Homodyne detection scheme. The signal field $\hat{a}_{1in}$ and the local oscillator field $\hat{a}_{2in}$ are superimposed at the beam splitter. The combined fields $\hat{a}_{1out}$ and $\hat{a}_{2out}$ are incident on the two detectors D_1 and D_2 that measure the relevant numbers of photons N_1 and N_2 during a certain interval of time T. This produces a photocurrent that is measured out of one of the detectors (*ordinary* homodyne), or currents that are differenced (*balanced* homodyne) to form a photocurrent proportinal to $(N_1 - N_2)$ that is measured at the spectrum analizer S.A.

Fig. 6.2

Homodyne scheme for detecting squeezed fluctuations in the evanescent wave produced by total internal reflection at the matter-vacuum boundary of a bulk polariton excited by an external laser. The incident laser beam (lower left) splits at the beam splitter (*BS*): part enters the crystal and propagates as a polariton to the upper boundary, where it is totally internally reflected and produces the leaky evanescent wave. This is superimposed at P on the other portion (*L.O.*) of the

pump laser. Both fields are polarized perpendicular to the surface. A segment of the surface is coated with a film of photoemissive material (thickness~d) shielded from the crystal below. P(photocathode)-M(multiplier)-A(anode) form a photomultiplier generating a photocurrent that produces the statistical distribution $P_n(T)$ of the number n of photocounts recorded during repeated time intervals T. The local oscillator beam $L.O.$ is phase shifted ($\varphi_{L.o.}$) by a piezoelectrically controlled mirror $M_{\varphi_{L.o.}}$. A photocurrent variance that reduces below the shot-noise value for certain values of $\varphi_{L.o.}$ provides a signature of squeezing.

Fig. 6.3

Balanced homodyne detector. The difference photocount distribution from the detectors D_3 and D_4 is monitored by a spectrum analyzer ($S.A.$). The $L.O.$ contribution to the detected noise is here suppressed. The leaky radiation is brought into the port I via a reflecting grating G so designed as to direct all diffracted photons into a single order ($p = 0$). The grating G is described in Fig. 6.4.

Fig. 6.4

Echelette reflecting grating G. The crystal is cut so that the interface is bent at Q and blazed with right angle triangle grooves. N is the normal to the reflecting groove face and δ is the blaze angle. θ_i is the angle of incidence, θ_d is the angle of diffraction and $2a$ is the groove spacing. For $2a < \lambda / 2$ all photons are scattered into the 0-th order

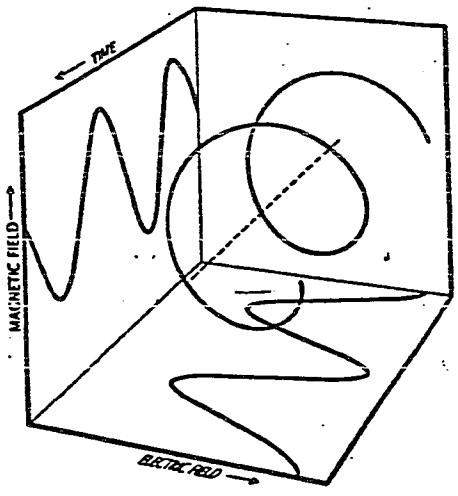

Fig 1.1a

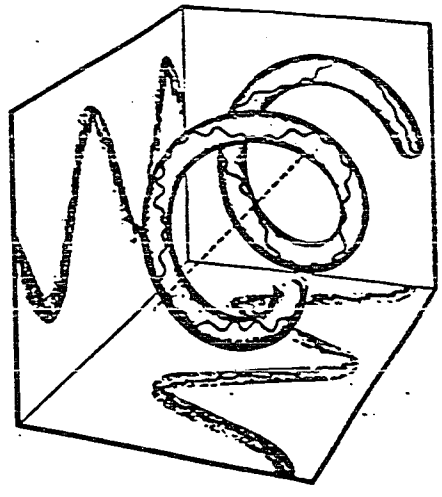

Fig. 1.1b

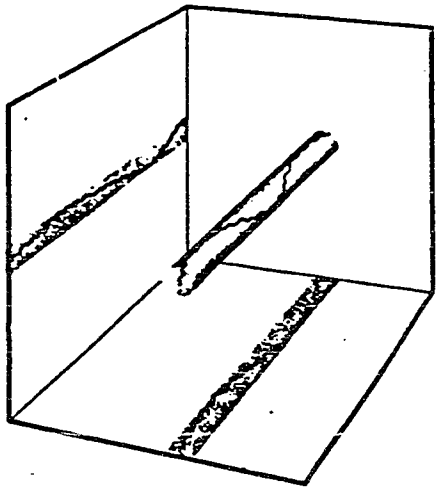

Fig. 1.2

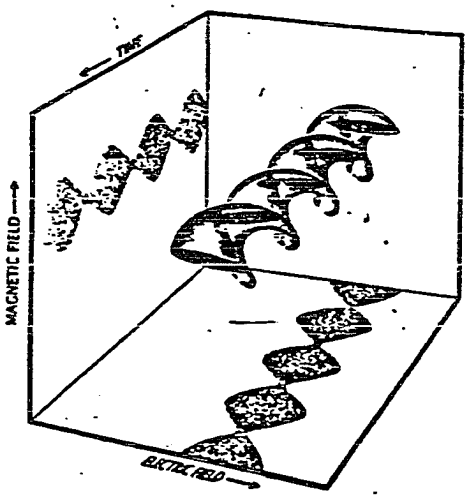

Fig 1.3a

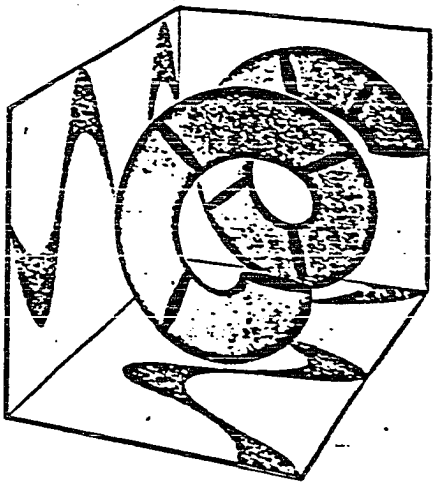

Fig. 1.3b

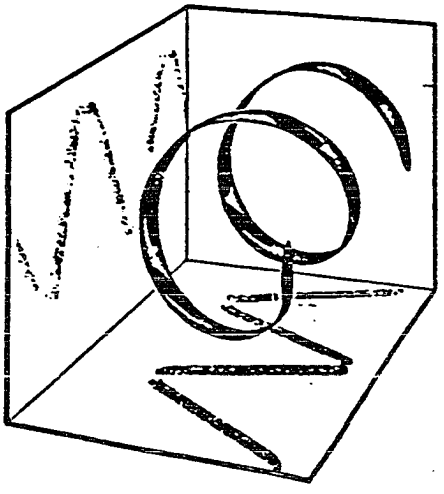

Fig. 1.3c

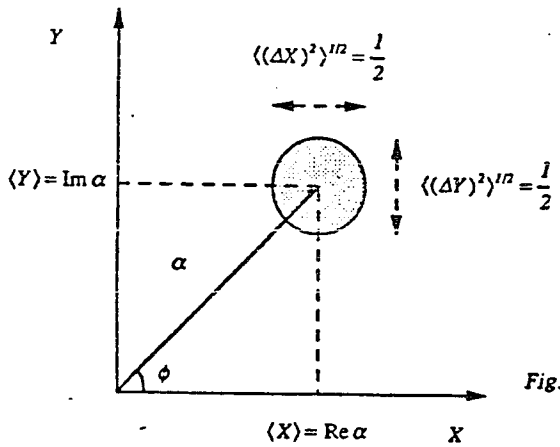

Fig. 1.4

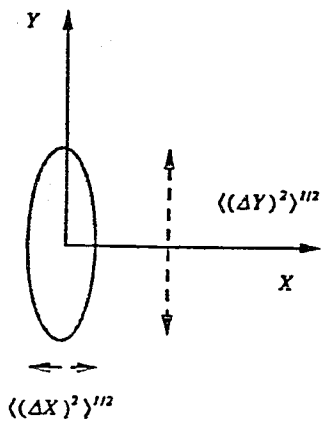

Fig. 1.5

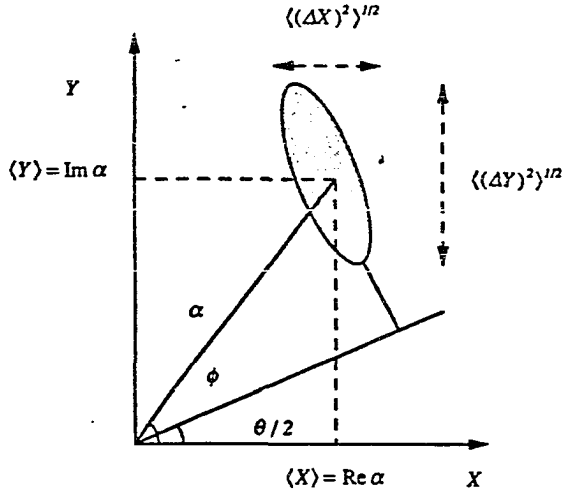

Fig. 1.6

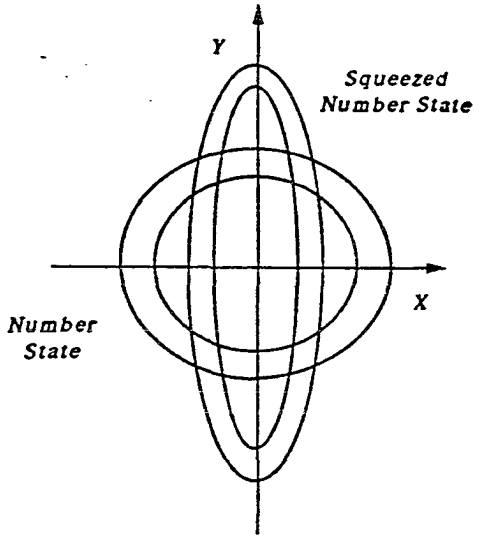

Fig. 1.7

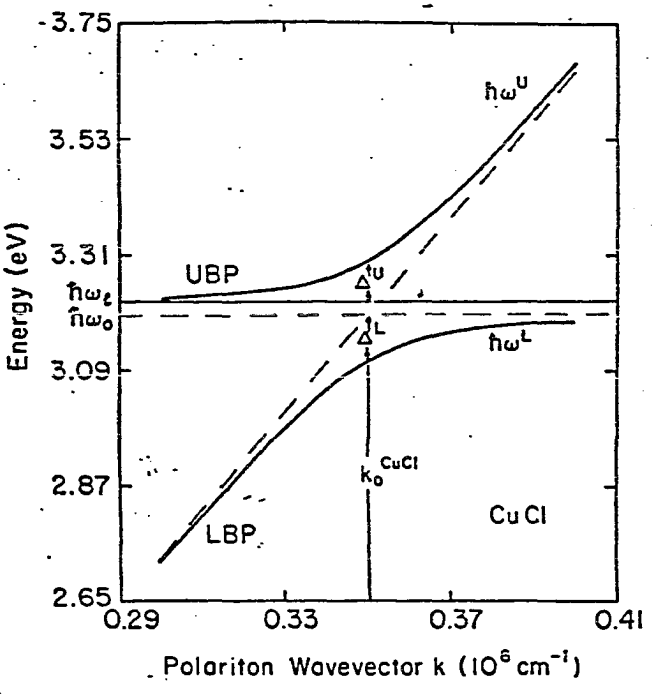

Fig. 1.S

Fig. 3.1

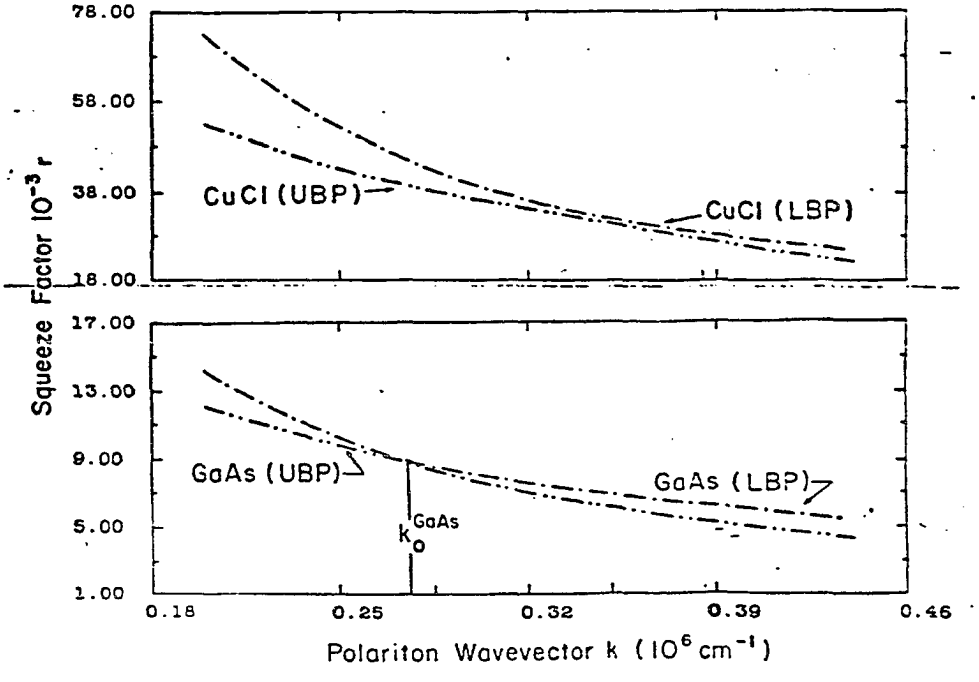

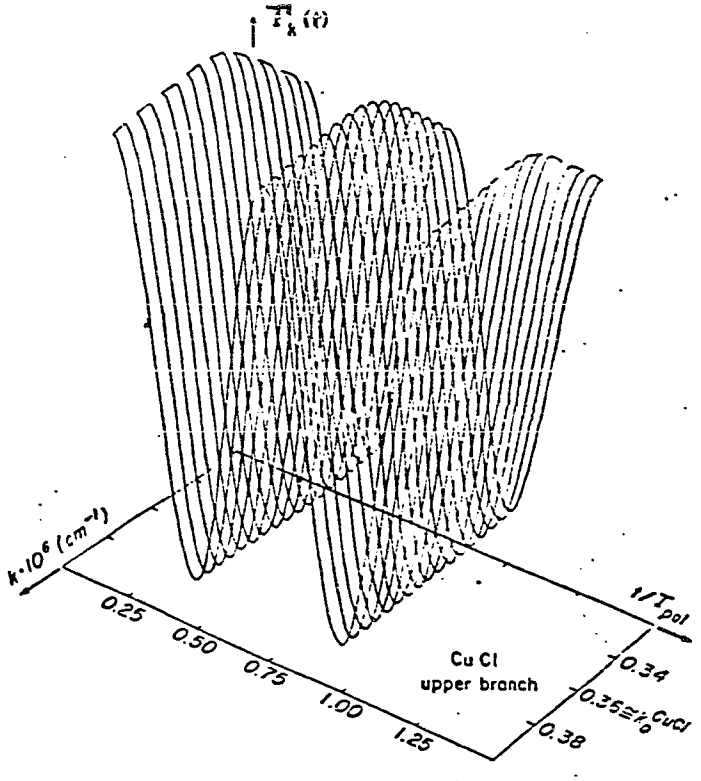

Fig. 3.2

Fig. 3.3

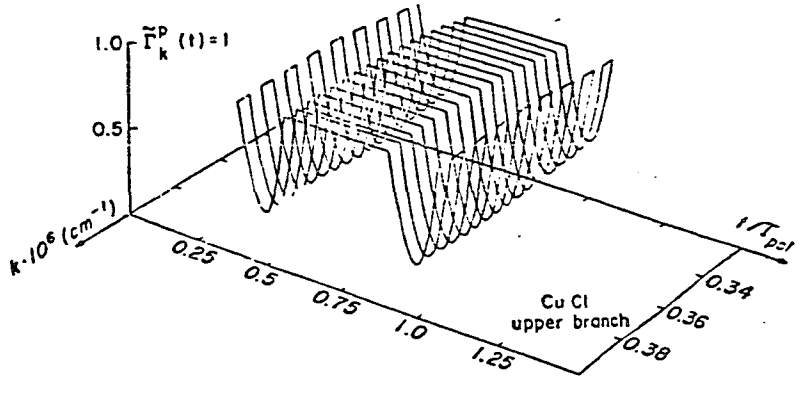

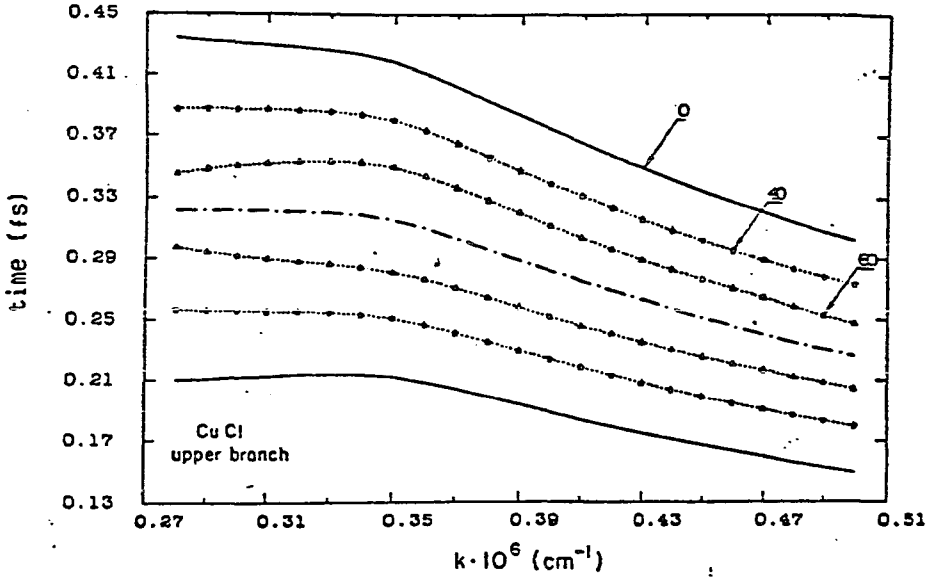

Fig. 3.4

Fig. 4.1

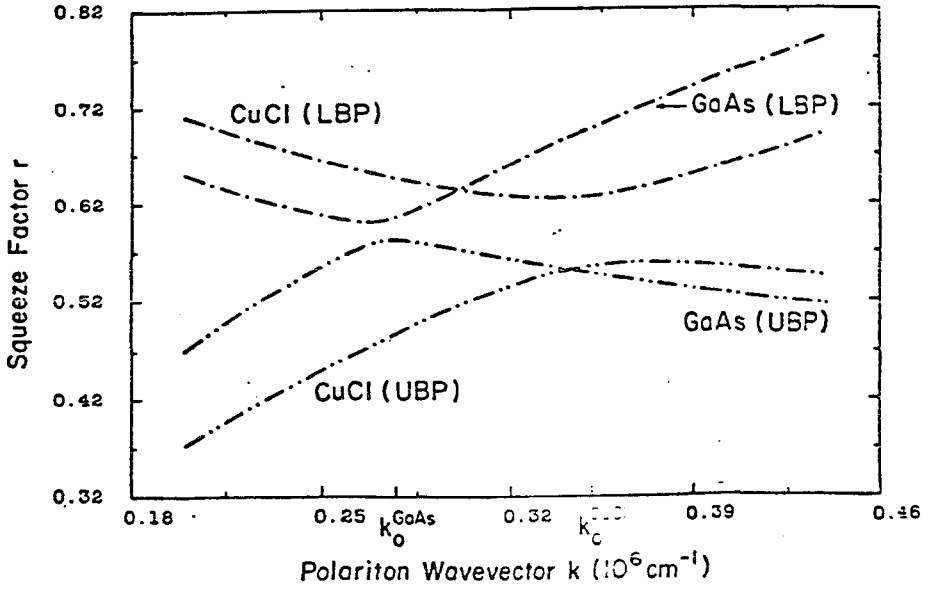

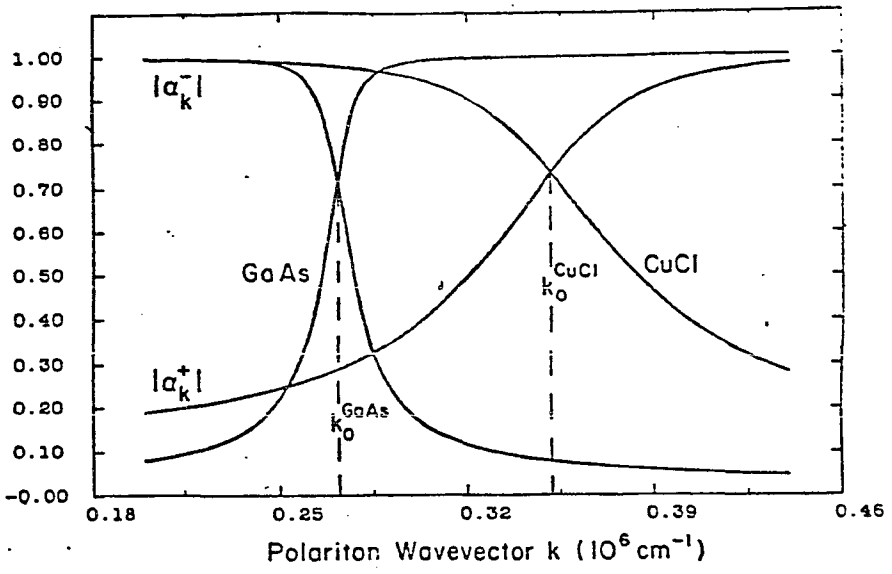

Fig. 5.1

Fig. 5.2

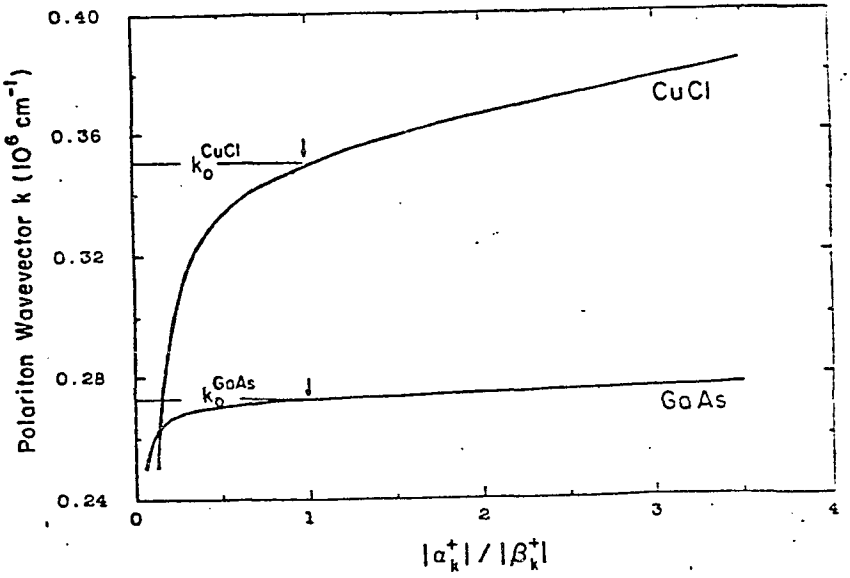

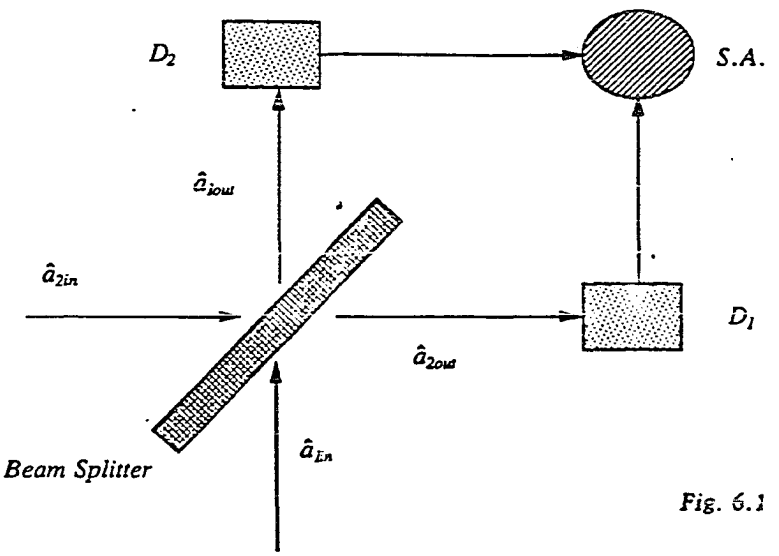

Fig. 6.1

Fig. 6.2

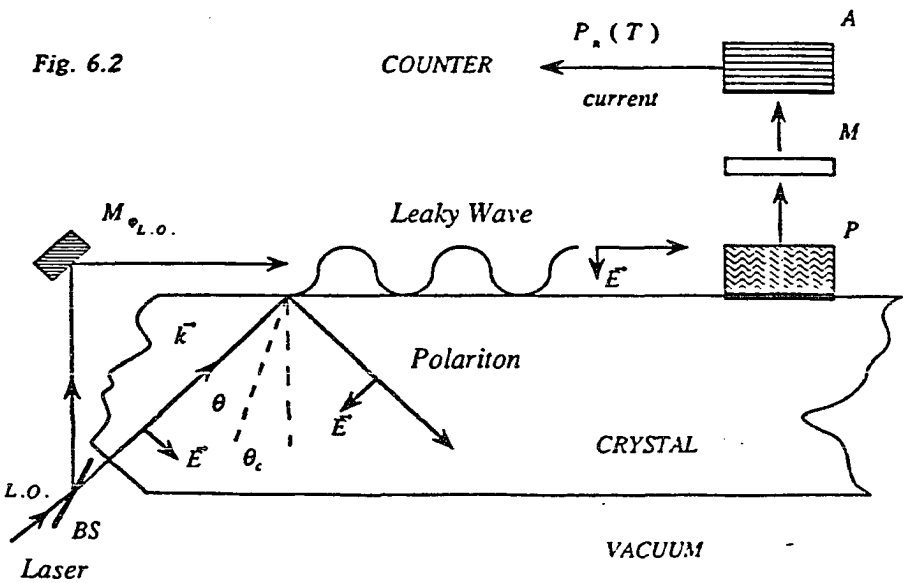

Fig. 6.3

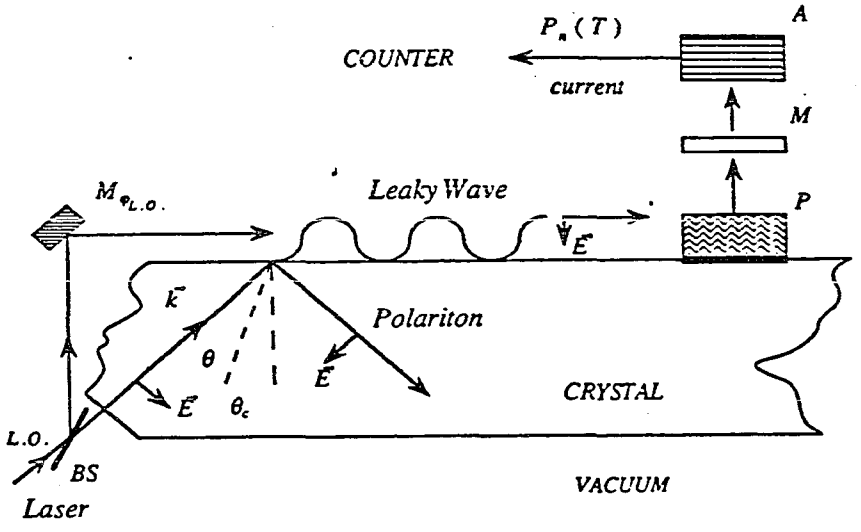

Fig. 6.4

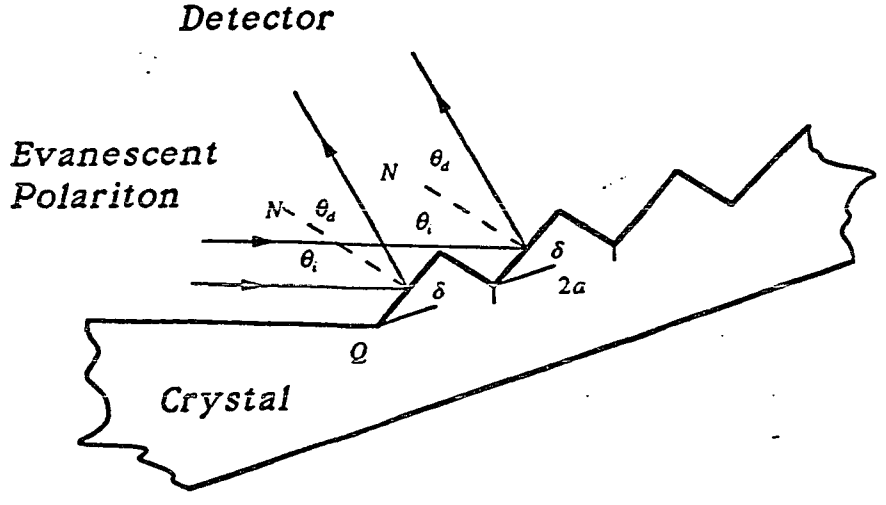

TABLE CAPTIONS

Tab. 6.1 [48,110]

ε_b: background dielectric constant; Δ_{LT} : longitudinal-transverse branch splitting at k =0; ω_o: resonace frequency. The frequencies (unit $\hbar$) are in eV. The crossover wavevector k_o (Fig. 1.8) is here the polariton mode which we consider for the present estimations. $r_o \equiv r_{k_o}$ gives the amount of optical squeezing in these semiconductors, as predicted after Ref. [97] within the Hopfield model, except for KI [93]. s (in μm) measures the extension of the evanescent polariton radiation across the surface into the vacuum. Extremal values are reported corresponding to incident angles $\theta_c \leq \theta < 90^o$ (total internal reflection). $\theta_c = \sin^{-1} n^{-1}$ (critical angle) with n the refractive index. P_{evan} (in mW) gives the useful total radiation power of the leaky polariton radiation for an incident laser intensity $I_{inc.} = 20W / cm^2$ and a transmission ratio $I_{evan.} / I_{inc.} \approx 0.8$. $R_{sq\,/\,vac}$ is the predicted maximum noise reduction ratio (%) due to optical squeezing. Reductions are with respect to the noise set by the vacuum fluctuations of the field.

Phonon/exciton polariton parameters and squeeze amplitudes

	CdS	*GaAs*	*KI*	*CdS*	*GaAs*
	Exciton			***Phonon***	
ε_b	9. 1	12. 5	1. 65	5. 6	10. 9
Δ_{LT}	0. 0019	0. 00008	0. 099	0. 0091	0. 0028
ω_o	2. 55	1. 51	5. 85	0. 031	0. 033
r_c	0. 028	0. 008	0. 061	0. 40	0. 32
s	2. 3 – 0. 25	5. 3 – 0. 85	0. 9 – 0. 07	170 – 7. 0	150 – 7. 1
P_{evan}	0. 8 – 0. 15	3. 2 – 0. 51	0. 5 – 0. 04	102 – 4. 2	90 – 4. 3
$R_{sq\,/\,vac}$	5. 4	1. 6	11. 5	55	47

CONCLUSION AND FUTURE WORK

There has been deep interest in non-classical aspects of the electromagnetic field. Squeezing of light has been demonstrated, following theoretical predictions . These new effects found in optics have a certain generality and it seems certain that many important ideas are likewise applicable to the phenomenology of condensed matter, and are yet to be discovered. In this thesis the effects of squeezing have been extended to the condensed matter system of a polariton. Among the interesting conclusions, one certainly concerns the intrinsic squeezed structure of the polariton. Precisely, exciton-polariton quantum states are found to be squeezed (*polariton intrinsic squeezing*) with respect to states of certain *intrinsic* photon-exciton mixed bosons, which are not polaritons. The polariton problem has been analysed within a hamiltonian formulation. Two different hamiltonians were investigated: one is the well known conventional Hopfield hamiltonian $\hat{H}^{Hopfield}$ whereas the other, $\hat{H}^{pol}$, is an enlarged version of the previous one, including the exciton-exciton interaction term. The amount of squeezing is measured by a squeeze factor " r " and depends on the model hamiltonian and, within each model, it depends on the frequency of the polariton that is excited.

Two interpretations are presented of the origin of squeezing in polariton states. One, within the framework of sudden transitions, the other relating to quantum correlations between *intrinsic* photon-exciton mixed bosons of opposite wavevectors. These approaches to polariton squeezing may also lead to further understanding of basic processes in the dynamics of radiation-matter mixing as in a polariton.

Non-classical optical effects in polaritons are studied using a representation through which a physical photon inside a dielectric is dressed, as a certain linear combination of vacuum annihilation and creation operators, and similarly for the

exciton. This gives us a straightforward mean to analyse the interaction of coherent electromagnetic radiation with a resonant polarization (exciton) and to study the influence of this resonant medium on the photon statistics of the radiation field. Squeezing in the electromagnetic component associated with a polariton is found (*polariton optical squeezing*). Moreover non-poissonian photon statistics is predicted, which also entails reduction of the fluctuations of the polariton electromagnetic field component below the limit set by the vacuum fluctuations of the field. Recently the problem of examining squeezing effects in a *homogeneous* dielectric medium has independently been studied by I. Abram [56] and R. Glauber and M. Lewenstein [57]. However to our acknowledge, non-classical optical effects in resonant dielectrics in interaction with the electromagnetic field is here studied for the first time.

The question of measurability of non-classical properties of the electromagneticf ield associated with polaritons as predicted here is of considerable importance. If verified, our predictions would demonstrate that the electromagnetic field may be driven into a non-classical state through the resonant coupling with another boson, i.e. the exciton. Detection of such non-classical effects will the main concern for future work, and the study of certain novel experiments to examine these effect are under way .

APPENDICES

A1: The polariton hamiltonian

The quantized form of $\hat{H}$ in Eq. (2.2.10) can be written as

$$\hat{H} = \sum_{k\geq 0} \{\hat{H}_k + \hat{H}_{-k}\} + h.c.$$

with

$$\begin{aligned}\hat{H}_k = {} & \hat{a}_k^{\dagger}\hat{a}_k[\varepsilon_k(v_k^2 - \frac{1}{2})(\frac{\alpha_{-k}^2 + \alpha_k^2}{2})] + \hat{b}_k^{\dagger}\hat{b}_k[\varepsilon_k(\upsilon_k^2 - \frac{1}{2})(\frac{\beta_{-k}^2 + \beta_k^2}{2})] \\ & + \hat{a}_k\hat{a}_{-k}[\varepsilon_k v_{-k}v_k\alpha_k^2] - \hat{b}_k\hat{b}_{-k}[\varepsilon_k \upsilon_{-k}\upsilon_k\beta_k^2] \\ & + i\hat{a}_{-k}\hat{b}_k[\varepsilon_k v_{-k}\upsilon_k(\alpha_k\beta_k + \alpha_{-k}\beta_{-k})] \\ & + i\hat{a}_k^{\dagger}\hat{b}_k[\varepsilon_k(v_k\upsilon_k - \frac{1}{2})(\alpha_k\beta_k + \alpha_{-k}\beta_{-k})] \\ & + \frac{\varepsilon_k}{4}[(\alpha_{-k}^2 + \alpha_k^2)v_k^2 + (\beta_{-k}^2 + \beta_k^2)\upsilon_k^2 - 1]\end{aligned} \tag{A1.1}$$

which we rewrite in compact form as

$$\hat{H}_k \equiv h_k^o + E_k^{ph.}\hat{a}_k^{\dagger}\hat{a}_k + E_k^{exc.}\hat{b}_k^{\dagger}\hat{b}_k + B_k'\hat{a}_k\hat{a}_{-k} - C_k'\hat{b}_k\hat{b}_{-k} + iA_{1k}\hat{a}_{-k}\hat{b}_k + iA_{2k}\hat{a}_k^{\dagger}\hat{b}_k \tag{A1.2}$$

The photon and exciton single particle energies $E_k^{ph.}$, $E_k^{exc.}$ are expressed in terms of the bare ones as

$$E_k^{ph.} \equiv \frac{\hbar ck}{2} + B_k \qquad\qquad E_k^{exc.} \equiv \frac{\hbar\omega_T}{2} - C_k \tag{A1.3}$$

and B_k, C_k define the respective deviations. The reparametrization (A1.1) $\rightarrow$ (A1.2), i.e. $\{\varepsilon_k, v_{\pm k}, \upsilon_{\pm k}, \alpha_{\pm k}, \beta_{\pm k}\} \rightarrow \{B_k, C_k, B_k^{'}, C_k^{'}, A_{1k}, A_{2k}, h\omega_{Tk}, hck\}$ follows the transformation

$$\begin{aligned}
&\varepsilon_k (v_k^2 - \frac{1}{2})(\frac{\alpha_k^2 + \alpha_{-k}^2}{2}) = \frac{\hbar ck}{2} + B_k \\
&\varepsilon_k (\upsilon_k^2 - \frac{1}{2})(\frac{\beta_{-k}^2 + \beta_k^2}{2}) = \frac{\hbar\omega_{Tk}}{2} - C_k \\
&\varepsilon_k \alpha_k^2 v_k v_{-k} = B_k^{'} \\
&\varepsilon_k \upsilon_k \upsilon_{-k} \beta_k^2 = C_k^{'} \\
&\varepsilon_k v_{-k} \upsilon_k (\alpha_k \beta_k + \alpha_{-k} \beta_{-k}) = A_{1k} \\
&\varepsilon_k (v_k \upsilon_k - \frac{1}{2})(\alpha_k \beta_k + \alpha_{-k} \beta_{-k}) = A_{2k} \\
&\frac{\varepsilon_k}{4}[(\alpha_{-k}^2 + \alpha_k^2) v_k^2 + (\beta_{-k}^2 + \beta_k^2) \upsilon_k^2 - 1] \equiv h_k^o = \frac{1}{4}[\hbar ck + 2B_k + \hbar\omega_T - 2C_k]
\end{aligned} \tag{A1.4a}$$

Here B_k relates to the contribution of the non-resonant part of the "photon-photon" coupling ($\hat{a}_k \hat{a}_k^{\dagger}$) to the single photon dressed energy, whereas $B_k^{'}$, distinct from B_k, relates to the resonant part ($\hat{a}_k \hat{a}_{-k}$) of the same interaction. These terms and h.c. physically originate from the interaction between the two wavevector modes of the electromagnetic field and bound electrons [52,100-103]. Similarly for C_k and $C_k^{'}$: they are associated to the non-resonant ($\hat{b}_k \hat{b}_k^{\dagger}$) and resonant ($\hat{b}_k \hat{b}_{-k}$) parts of the "exciton-exciton" interaction. These terms and h.c. arise from the exciton dispersion relation. For *Frankel* excitons [37,44], the transfer of excitation from site to site gives rise to such a term. For *Wannier* excitons [37,44], they are related to the effective mass of the exciton, although we do not account for such

type of excitons here. Aside from common physical origins, the distinction between $\bar{B}_k$ and $B_k^{'}$, so as between C_k and $C_k^{'}$ is intrinsic to our model that differs from the conventional one (chapter IV). The former involves a resonant mixing of *dressed* (physical) radiation and exciton-polarization fields, instead of *vacuum* fields to describe the quantum mechanics of the polariton and it naturally accounts for the "exciton-exciton" coupling term. The same explanation holds for the difference in the two coefficients A_{1k}, A_{2k}, which manifestly designate the resonant and non-resonant part of the interaction between photons and excitons in a polariton. Two cases of interest to us will be now analysed in detail.

Case A.

As an instance of the hamiltonian in Eq. (A1.2) we now consider the case in which

$$v_k = \upsilon_k \neq 1 \qquad \alpha_k = \alpha_{-k} \qquad \beta_k = \beta_{-k} \tag{A1.5}$$

$$\varepsilon_k (v_k^2 - \frac{1}{2})\alpha_k^2 = \frac{\hbar ck}{2} + \bar{B}_k \equiv \bar{E}_k^{ph} \qquad \varepsilon_k \alpha_k^2 v_k v_{-k} = \bar{B}_k^{'}$$

$$\varepsilon_k (v_k^2 - \frac{1}{2})\beta_k^2 = \frac{\hbar\omega_{Tk}}{2} - \bar{C}_k \equiv \bar{E}_k^{exc} \qquad \varepsilon_k \beta_k^2 v_k v_{-k} = \bar{C}_k^{'}$$

$$\varepsilon_k 2\alpha_k\beta_k v_k v_{-k} = \bar{A}_{1k} \qquad \varepsilon_k 2\alpha_k\beta_k (v_k^2 - \frac{1}{2}) = \bar{A}_{2k}$$

$$\varepsilon_k (2v_k^2 - 1) = \hbar ck + \hbar\omega_{Tk} + 2(\bar{B}_k - \bar{C}_k) \tag{A1.4b}$$

and the corresponding hamiltonian is

$$\hat{H}_k \rightarrow \hat{H}_k^{pol} = \hat{a}_k^{\dagger}\hat{a}_k[\varepsilon_k(v_k^2 - \frac{1}{2})\alpha_k^2] + \hat{b}_k^{\dagger}\hat{b}_k[\varepsilon_k(v_k^2 - \frac{1}{2})\beta_k^2]$$
$$+ \hat{a}_{-k}\hat{a}_k[\varepsilon_k v_{-k} v_k \alpha_k^2] - \hat{b}_{-k}\hat{b}_k[\varepsilon_k v_{-k} v_k \beta_k^2]$$
$$+ i\hat{a}_{-k}\hat{b}_k[\varepsilon_k v_{-k} v_k 2\alpha_k\beta_k] + i\hat{a}_k^{\dagger}\hat{b}_k[\varepsilon_k(v_k^2 - \frac{1}{2})2\alpha_k\beta_k]$$
$$+ \frac{\varepsilon_k}{4}[2v_k^2 - 1]$$
$$\equiv \overline{h}_k^o + \overline{E}_k^{ph.}\hat{a}_k^{\dagger}\hat{a}_k + \overline{E}_k^{exc.}\hat{b}_k^{\dagger}\hat{b}_k + \overline{B}_k\hat{a}_k\hat{a}_{-k} - \overline{C}_k\hat{b}_k\hat{b}_{-k}$$
$$+ i\overline{A}_{1k}\hat{a}_{-k}\hat{b}_k + i\overline{A}_{2k}\hat{a}_k^{\dagger}\hat{b}_k \qquad \text{(A1.6)}$$

Under the identifications

$$\Omega_k \equiv 2\varepsilon_k(v_k^2 - \frac{1}{2}) \qquad \zeta_k \equiv \varepsilon_k v_k v_{-k} \qquad \text{(A1.7)}$$

Eq. (A1.6) is rewritten as

$$\hat{H}_k^{pol} \equiv \frac{\Omega_k}{2}\alpha_k^2\hat{a}_k^{\dagger}\hat{a}_k + \frac{\Omega_k}{2}\beta_k^2\hat{b}_k^{\dagger}\hat{b}_k + \zeta_k\alpha_k^2\hat{a}_k\hat{a}_{-k} - \zeta_k\beta_k^2\hat{b}_k\hat{b}_{-k}$$
$$+ 2i\alpha_k\beta_k\zeta_k\hat{a}_{-k}\hat{b}_k + i\alpha_k\beta_k\Omega_k\hat{a}_k^{\dagger}\hat{b}_k + \frac{\Omega_k}{4} \qquad \text{(A1.8)}$$

This special instance of the hamiltonian in Eq. (A1.1-2), is exactly the generalized hamiltonian in Eq. (2.4.1/3.1.1). The first of the conditions (A1.5) implies "dressed" (physical) photons ($v_{-k} \neq 0$) and "dressed" (physical) excitons ($v_{-k} \neq 0$) as constituent components of the polariton. Also does it involve a common factor $s_k^{ph} = s_k^{exc}$ which we refer to as squeeze factor r_k in the chapter II.

Case B.

As a second example we derive the conventional Hopfield hamiltonian [42] from the expression (A1.2). It is readily seen from (A1.4a), which we may rewrite in the form

$$\varepsilon_k\ \alpha_k^2\ v_k v_{-k} = B_k^{'} \qquad \varepsilon_k\,\alpha_k^2\ v_k(v_k - \frac{1}{2}) = B_k$$

$$\hbar ck = \varepsilon_k[(\alpha_{-k}^2 - \alpha_k^2)\upsilon_k^2 + \alpha_k^2 v_k - \tfrac{1}{2}(\alpha_{-k}^2 + \alpha_k^2)]$$

$$\varepsilon_k\,\upsilon_k\,\upsilon_{-k}\beta_k^2 = C_k^{'} \qquad 2(\upsilon_k^2 - \frac{1}{2}) = 1 - \frac{2C_k}{\hbar\omega_T}$$

$$\hbar\omega_T = \varepsilon_k(\frac{\beta_{-k}^2 + \beta_k^2}{2})$$

$$\varepsilon_k\, v_{-k}\upsilon_k(\alpha_k\beta_k + \alpha_{-k}\beta_{-k}) = A_{1k} \qquad \varepsilon_k(v_k\upsilon_k - \frac{1}{2})(\alpha_k\beta_k + \alpha_{-k}\beta_{-k}) = A_{2k}$$

$$\frac{\varepsilon_k}{4}[(\alpha_{-k}^2 + \alpha_k^2)\, v_k^2 + (\beta_{-k}^2 + \beta_k^2)\,\upsilon_k^2 - 1] \equiv h_k^o = \frac{1}{4}[\hbar ck + 2B_k + \hbar\omega_T - 2C_k] \tag{A1.4c}$$

that the Hopfield result obtains when we take

$$\upsilon_{-k} = 0 \qquad (\upsilon_k = 1) \qquad\qquad v_{-k} = v_k - \frac{1}{2} \qquad (v_{-k} < v_k) \tag{A1.9}$$

Indeed here $C_k = C_k^{'} = 0$, $B_k = B_k^{'}$ and $A_{1k} = A_{2k}$, while the expression (A1.2) acquires the same structure as H^o in Eq. (2.4.2/4.1.1)

$$\hat{H}_k = (\frac{\hbar ck}{2} + B_k)\,\hat{a}_k^{\dagger}\hat{a}_k + \frac{\hbar\omega_T}{2}\hat{b}_k^{\dagger}\hat{b}_k$$
$$+ B_k\hat{a}_k\hat{a}_{-k} + iA_k(\hat{a}_{-k}\hat{b}_k + \hat{a}_k^{\dagger}\hat{b}_k) + (\hbar ck + \hbar\omega_T + 2B_k) \tag{A1.10}$$

A2: Polariton squeeze isomorphism

The polariton hamiltonian H^{pol} in Eq. (3.1.1) is characterized by the six parameters A_{1k}, A_{2k}, B_k, $B_k^{'}$, C_k, $C_k^{'}$, whereas H^{pol} in Eq. (3.1.4), a two-mode squeeze hamiltonian in form, is characterized by the six parameters Ω_k, ζ_k, α_k, $\beta_k, \psi_k^a, \psi_k^b$. The isomorphism between these two hamiltonians is effective provided the transformations in Eq. (3.1.7) are fulfilled. Consistency of Eq.s (3.1.7) results in a functional relation e.g. of the kind $B'_k = B'_k(B_k, C_k, C'_k)$ (first 4 Eq.s), and again allows A_{1k} and A_{2k} to be expressed in terms of B_k, B'_k, C_k, C'_k (last two Eq.s). At last only the three parameters B_k, C_k, C'_k are left free in the hamiltonian of Eq. (3.1.1). On the other hand by taking $\psi_k^a = 0$ and $\psi_k^b = \pi / 2$, $\alpha_k \equiv \cos\theta_k$ and $\beta_k \equiv \sin\theta_k$ only the parameters $\theta_k, \Omega_k, \zeta_k$ are left free in the hamiltonian of Eq. (3.1.4). The former and the latter sets of three parameters are connected by

$$\zeta_k = B_k^{'} + C_k^{'} \qquad \theta_k = \sin^{-1}\sqrt{\frac{C_k^{'}}{B_k^{'} + C_k^{'}}}$$
$$\Omega_k = (\hbar ck + 2B_k) + (\hbar\omega_o - 2C_k) = 2(E_k^{ph.} + E_k^{exc.}) \qquad \text{(A2.1)}$$

Now using these expressions for Ω_k and ζ_k, taking ε_k as the experimental polariton energy it is possible, with a three parameters fitting of the dispersion relation (3.1.13), to reproduce the energy dispersion branches (UBP & LBP) of a measured exciton-polariton spectrum. Next substituting back the numerical evaluations for B_k, C_k, C'_k in (A2.1), the energies for the intermediate quasiparticles c and the squeeze factor r_k given by Eq. (3.1.19) can be derived. It is

a sel-consistent procedure in which the fitting of experimental polariton energies for each branch is optimized through the use of Eq. (C.1) and (3.1.19) [104]. The existence of parameters that consistently satisfy the transformation (3.1.7) and reproduce the experimental polariton energies for dielectric materials such as e.g. CuCl and GaAs settles the isomorphism between the squeeze hamiltonian (3.1.4) and a hamiltonian that represents a "physical " polariton system.

A3: Polariton propagating field

Here we illustrate the physics underlying the mixed boson introduced in Eq. (3.1.1.2). In traversing a medium, a beam of photons exchanges energy with it. A photon in the crystal can transform directly into an exciton provided they both have the same energy and wavevector: if the exciton is not scattered by a phonon or some other defect in the crystal, the exciton transforms back into a photon indistinguishable from the original one, owing to energy and wavevector conservation. Energy thus oscillates back and forth between exciton and photon [105]. If absorption does not occur in the medium these physical processes can be described by the hamiltonian

$$\hat{H}^{pr.} = \sum_q [\overline{E}_q^{ph}\hat{a}_k^\dagger\hat{a}_k + \overline{E}_q^{exc}\hat{b}_k^\dagger\hat{b}_k + \frac{i}{2}\overline{A}_{2q}\hat{a}_k^\dagger\hat{b}_k - \frac{i}{2}\overline{A}_{2q}\hat{b}_k^\dagger\hat{a}_k] + h.c.. \qquad \text{(A3.1.1)}$$

The first two terms give the energies of free (uncorrelated) photons and excitons in the medium. The last two describe the destruction of a photon with the creation of an exciton and vice versa [36,66], they are therefore responsible for the back and forth switching of energy between photon and exciton. This photon-exciton energy exchange constitutes an intrinsic "phase" of the polariton and leads to a "propagating" coupled mode. The energy with which this coupled mode propagates inside the medium is found by diagonalizing (A3.1.1), and this can be shown to be possible using the transformation (3.1.1.2), i.e.

$$[\hat{c}_k, \hat{H}^{pr.}] = \Omega_k \hat{c}_k \qquad \hat{H}^{pr.} = \sum_q \frac{\Omega_q}{2}(\hat{c}_q^\dagger\hat{c}_q + \frac{1}{2}) + h.c. \qquad \text{(A3.2)}$$

Ω being the relevant energy. Since $\hat{H}_o = \hat{H}^{pr.}$, the propagating field of the polariton describes this "intrinsic phase" of the polariton, and the oscillations above can be ascribed to the oscillations of the mixed boson $\hat{c}$. The latter are estimated directly from Ω (cf. Eq. A2.1) and for an exciton-polariton in CdS at $k = k_o$, $\hbar^{-1}\Omega \sim 10^{15}$ sec^{-1}. This rate of energy exchange has been evaluated on other contexts and it is of the same order of magnitude [60].

Next consider momentum conserving interactions between bosons $\hat{c}$ with opposite wavevectors. The interaction hamiltonian for such new physical processes is [106]

$$\hat{H}_I = \sum_{q>0} \zeta_q \hat{c}_k \hat{c}_{-k} + h.c. \qquad \text{(A3.1.4)}$$

Counterpropagating modes in the medium arise due to the medium itself, whereas e.g. the creation of a photon or exciton is always accompanied by the creation of the conjugate particle but with opposite wavevector (cf. [56,57] and § 3.2). The polarization of the material instead turns on and mediates the couplings between opposite wavevector modes [56,57]. Including $\hat{H}_I$ one can find the energies of the new coupled mode by diagonalizing with a polariton transformation, i.e.

$$[\hat{\eta}_k, \hat{H}^{pr.} + \hat{H}_I] = \varepsilon_k \hat{\eta}_k \qquad \hat{H}^{pr.} + \hat{H}_I = \hat{H}^{pol.} \qquad \text{(A3.5)}$$

being ε_k the polariton energy.

In conclusion the physical processes in $\hat{H}_o$ are nothing other than those involved with resonant photon-exciton energy exchange in the absence of absorption. Thus the photon-exciton hybridized boson $\hat{c}$ (not a polariton) is the

"propagating" component along $\vec{k}$ of an undamped polariton wave. Owing to (A3.5), with respect to $\hat{H}_o$, $\hat{H}^{pol.}$ involves an extra interaction due to correlations of intrinsic bosons $\hat{c}$ with opposite wavevectors. This is discussed in detail in § 3.1.4. Accordingly one may interpret the process of polariton formation as arising from correlations of counterpropagating modes of the propagating component of the polariton field.

A4: Time-dependent squeezed fluctuations

What follows is relevant to the quadrature $\hat{X}_k^p$ [107]. First define the ratio

$$R_k(t) \equiv_t \langle \mu_{\pm k} || \Delta X_k^p |^2 | \mu_{\pm k} \rangle_t \; / \; \Gamma_k^o \qquad \text{(A4.1)}$$

and use Eq. (3.2.13) to obtain the squeeze time interval $\Delta T_{sq.}$ as solution of

$$R_k(t) \leq q \quad \text{for} \quad q = 1 \qquad \text{or} \qquad \cos 2\omega_k t < \sec h\, 2r_k - \coth 2r_k \qquad \text{(A4.2)}$$

For exciton-polaritons in CuCl we evaluate in fig. 3.a $\Delta T_{sq}^{Cu\,Cl}$ for a spectrum of wavevectors in the vicinity of k_o. Precisely, $\Delta T_{sq}^{Cu\,Cl}$ for a given k is twice the vertical distance between the two solid lines. This figure also shows how the amount of squeezing varies during $\Delta T_{sq}^{Cu\,Cl}$ (dotted lines); intermediate values of the squeezing with their respective durations are here explicitly reported.

The maximum squeezing $\Gamma_k^o e^{-2r_k}$ occurs twice during the period $T^{pol.}$ of the polariton. Its value depends on the mode that is excited: approaching k_o the squeezing becomes more pronounced.

According to Eq. (A4.2) the results of fig. 3.4 are mainly determined by the magnitude of r_k and the polariton frequency ω_k. Since r_k in the range of wavevectors considered here takes only slightly different values on the two materials examined (cf. Fig. 3.1) and their crossover frequencies are not significantly apart, we may expect that for exciton-polaritons ΔT_{sq}^{GaAsl} is quantitatively similar to that for CuCl. The same is true for the results presented in

fig.s 3.2 and 3.3.

A5: Microscopic Hopfield polariton model

The Hopfield exciton-polariton model hamiltonian discussed in chapter IV is here reviewed from a *microscopic* point of wiev. The problem consists in formulating the coupling between the quantized exciton and the quantized electromagnetic fields. We first regard the system in the absence of the electromagnetic field and consider N atoms arranged on the sites $\vec{r}_I$ of a Bravais lattice defined by the set of position vectors $\vec{r}_I = n_1\vec{a}_1 + n_2\vec{a}_2 + n_3\vec{a}_3$, where the n's are integers and the $\vec{a}_j$'s primitive vectors and impose Born-von Karman boundary conditions. The average distance between the atoms $|\vec{r}_I - \vec{r}_J|$ is much bigger than the average atomic radius $R_{atom} << |\vec{r}_I - \vec{r}_J|$. The complete hamiltonian of this electronic system is [52,100-103]

$$H_{exc} \equiv H_1 + H_2 + H_3 + H_4 + H_5 \qquad \text{(A5.1a)}$$

$$-\sum_{\vec{r}_I}\frac{h^2}{2M_I}\nabla^2_{\vec{r}_I} + \sum'_{\vec{r}_I,\vec{r}_J}\frac{e^2 Z_I Z_J}{|\vec{r}_I - \vec{r}_J|} - \sum_{\vec{x}_i}\frac{h^2}{2m_i}\nabla^2_{\vec{x}_i} - \sum_{\vec{r}_I}\sum_{\vec{x}_i}\frac{e^2 Z_I}{|\vec{r}_I - \vec{x}_i|} + \sum'_{i,j}\frac{e^2}{|\vec{x}_j - \vec{x}_i|} + H_s$$

where the various terms are, in the order: the kinetic energy of the nuclei, the potential energy of the nuclei interacting with each other, the kinetic energy of the electrons, the potential energy of the electrons interacting with the nuclei, the potential energy of the electrons interacting with each other, and the spin dependent electronic energy H_s. Here,

1) the adiabatic, harmonic, static approximation and, nuclei at rest,

2) the "one-electron" approximation,

are assumed. A "single" atom is associated to each lattice site and Z electrons to each atom. For simplicity, the atoms are further assumed to be "identical" and to have *s*-type ground state wavefunction ψ_o and *p*-type excited states wavefunction ψ_p . In the *Frenkel* model an exciton is a state in which one atom at $\vec{r}_I$ is excited and all the rest are in their ground states. Therefore if the ground state of the crystal (every atom in its ground state) is

$$\Psi_o = \prod_{\vec{r}_I} \psi_o(\vec{r}_I) \tag{A5.2a}$$

an exciton state of the crystal with given wavevector $\vec{k}$ (first Brillouin zone) and given atomic excited *p*-state is

$$\Psi_{k,p} = \sum_{\vec{r}_I} \phi_{k,p}(\vec{r}_I) \equiv \frac{1}{\sqrt{N}} \sum_{\vec{r}_I} e^{i\vec{k}\cdot\vec{r}_I} \psi_p(\vec{r}_I) \prod_{\vec{r}_{I'} \neq \vec{r}_I} \psi_o(\vec{r}_{I'}) \tag{A5.2b}$$

In the dipole approximation (A5.1a) reduces to

$$\begin{aligned} H_{exc.} \equiv & -\sum_{\vec{r}_I} \Big[\sum_{\vec{x}_i}^{Z_I} \frac{h^2}{2m_i} \nabla^2_{\vec{x}_{iI}} + \sum_{\vec{x}_i}^{Z_I} \frac{e^2 Z_I}{|\vec{r}_I - \vec{x}_i|} + \sum_{\substack{i,j \\ i<j}} \frac{e^2}{|\vec{x}_{jI} - \vec{x}_{iI}|} \Big] \\ & + \sum_{\vec{r}_I, \vec{r}_J}{}' \left\{ \frac{\vec{x}_I \cdot \vec{x}_J}{|\vec{r}_I - \vec{r}_J|^3} - \frac{3[\vec{x}_I \cdot (\vec{r}_I - \vec{r})][\vec{x}_J \cdot (\vec{r}_I - \vec{r})]}{|\vec{r}_I - \vec{r}_J|^5} \right\} \\ \equiv & \sum_{\vec{r}_I} H_I + \sum_{\vec{r}_I, \vec{r}_J}{}' H_{IJ} \end{aligned} \tag{A5.1b}$$

$\vec{x}_I \equiv e \sum_i \vec{x}_{iI} \equiv -e \sum_i (\vec{x}_i - \vec{r}_I)$ is the dipole moment of the atom I defined respect to the lattice site $\vec{r}_I$. A quantized form for (A5.1b) can be obtained, namely

$$\sum_{\vec{r}_I} H_I = \sum_{k,p} E_p (b_{kp}^+ b_{kp} + \tfrac{1}{2})$$
$$\sum_{\vec{r}_I, \vec{r}_J}{}' H_{IJ} = \sum_{kk'} \sum_{pp'} \{ h_{pkp'k'} b_{kp} b_{k'p'} + g_{pkp'k'} b_{kp}^+ b_{k'p'} \} + h.c. \qquad \text{(A5.1c)}$$

where

$$h_{pkp'k'} \equiv \sum_{\vec{r}_I, \vec{r}_J}{}' \{ e^{i\vec{k}\cdot\vec{r}_I + i\vec{k}'\cdot\vec{r}_J} \cdot \left[\frac{\langle \vec{x}_I \rangle^* \cdot \langle \vec{x}_J \rangle}{|\vec{r}_I - \vec{r}_J|^2} + \frac{3}{|\vec{r}_I - \vec{r}_J|^5} \langle \vec{x}_I \rangle \cdot (\vec{r}_I - \vec{r}_J) \langle \vec{x}_J \rangle^* \cdot (\vec{r}_I - \vec{r}_J) \right] \}$$
$$g_{pkp'k'} \equiv \sum_{\vec{r}_I, \vec{r}_J}{}' \{ e^{-i\vec{k}\cdot\vec{r}_I + i\vec{k}'\cdot\vec{r}_J} \cdot \left[\frac{\langle \vec{x}_I \rangle \cdot \langle \vec{x}_J \rangle^*}{|\vec{r}_I - \vec{r}_J|^2} + \frac{3}{|\vec{r}_I - \vec{r}_J|^5} \langle \vec{x}_I \rangle^* \cdot (\vec{r}_I - \vec{r}_J) \langle \vec{x}_J \rangle \cdot (\vec{r}_I - \vec{r}_J) \right] \} \qquad \text{(A5.3a)}$$

b_{kp} is the exciton annihilation operator of momentum $\vec{k}$ and atomic state p, E_p is the atomic excitation energy of the state p, and

$$\vec{x}_I \equiv \frac{1}{\sqrt{N}} \sum_{k,p} \langle \vec{x}_I \rangle b_{kp} e^{i\vec{k}\cdot\vec{r}_I} + h.c. \qquad \langle \vec{x}_I \rangle \equiv \langle 0 | \vec{x}_I | p \rangle \qquad \text{(A5.4)}$$

the dipole momentum operator. If ,

1) we neglect the second term in the square brackets of (A5.3a),
2) all dipole matrices are evaluated between the ground state $|0\rangle$ and the "same" excited state $|p\rangle$ at every lattice site $\vec{r}_I$ (p=p'),

3) they have a fixed magnitude and orientation independent of the site $\vec{r}_I$,

then

$$h_{pkp',k'} = \delta_{p,p'} |\langle \vec{x} \rangle|^2 \sum_{\vec{r}_I, \vec{r}_J}' \frac{e^{i\vec{k}\cdot\vec{r}_I + i\vec{k}'\cdot\vec{r}_J}}{|\vec{r}_I - \vec{r}_J|^3} \equiv \delta_{p,p'} |\langle \vec{x} \rangle|^2 S_{k,k'}$$

$$g_{pkp',k'} = \delta_{p,p'} |\langle \vec{x} \rangle|^2 \sum_{\vec{r}_I, \vec{r}_J}' \frac{e^{-i\vec{k}\cdot\vec{r}_I + i\vec{k}'\cdot\vec{r}_J}}{|\vec{r}_I - \vec{r}_J|^3} \equiv \delta_{p,p'} |\langle \vec{x} \rangle|^2 S_{-k,k'} \qquad \text{(A5.3b)}$$

In the Hopfield treatment the approximation (A5.3b) is adopted: $h_{pkp',k'}$ is taken to have the same magnitude as $g_{pkp',k'}$, with $|S_{k,k'}| = (2\pi N/3V)\,\delta_{k,k'} \equiv S_k\,\delta_{k,k'}$. When some of the above approximations are not met these two coefficients are certainly *different*.

Note that in deriving the Eq.s (A5.3) use has been made of the property

$$N\,\delta_{\vec{\xi},2\pi G} \equiv \sum_{\vec{r}} \exp(i\vec{\xi}\cdot\vec{r}) \qquad (\vec{G} = \textit{reciprocal lattice vector}) \qquad \text{(A5.5)}$$

Since the box where the radiation field is given boundary conditions is assumed to be of the same size of the crystal, the latter sum is zero unless $\vec{\xi} = 2\pi\,\vec{G}$. Here we take $\vec{G} = 0$, and $N\,\delta_{\vec{\xi},0} \equiv \sum_I \exp(i\vec{\xi}\cdot\vec{r}_I)$.

Along with the quantization of this simple model of dielectric in the absence of radiation, the quantization of the radiation field in the absence of dielectric (vacuum) can likewise be performed. It is a well known result [25] and it

is achieved with no need of approximations. For a given transverse polarization of the electromagnetic field the relevant quantized hamiltonian is

$$H_{rad} = \sum_k \hbar ck\,(a_k^{+} a_k + \tfrac{1}{2}) \tag{A5.6}$$

where ck is the frequency for a given mode of the field.

The interaction between the bare electromagnetic field (absence of dielectric) and the bare electronic polarization field (absence of radiation) is now considered. The interaction term reads as

$$H_{\text{int}} = -\frac{e}{mc} \sum_{\vec{r}_I} \vec{P}(\vec{r}_I) \cdot \vec{A}(\vec{r}_I) + \frac{e^2 Z}{2m\,c^2} \sum_{\vec{r}_I} \vec{A}^2(\vec{r}_I) \tag{A5.7}$$

e, m are charge and mass of the electron and Z the number of electrons in each (identical) atom. $\vec{P}(\vec{r}_I) = \sum_i \vec{p}_i(\vec{r}_I)$, the atom momentum operator (sum of all electron momenta of the atom at site $\vec{r}_I$), in the approximation in which $h = g$ takes the form

$$\vec{P}(\vec{r}_I) \equiv i\frac{h\,m}{e} \sum_{pk\eta} \frac{\omega_{po}}{N} \langle\, 0 |\, \vec{x}_I |\, p \,\rangle\, e^{i\vec{k}\cdot\vec{r}_I} b_{pk\eta} + h.\,c. \tag{A5.8}$$

ω_{po} is the single p -state atomic frequency, η is the polarization of the exciton and $\langle\, 0 |\, \vec{x}_I |\, p \,\rangle$ the single atomic state dipole transition. The first term in H_{int} can then be written as

$$\frac{i}{c}\sum_{pk}\omega_{po}\sqrt{\frac{2\pi\hbar c}{Vk}}\,\langle 0|\vec{x}|p\rangle\{-\hat{b}^{\dagger}_{kp}\hat{a}_{k}-\hat{b}^{\dagger}_{kp}\hat{a}^{\dagger}_{-k}+\hat{b}_{kp}\hat{a}_{-k}+\hat{b}_{kp}\hat{a}^{\dagger}_{k}\} \tag{A5.9}$$

Here all single state atomic dipole transitions are assumed real $|\langle 0|\vec{x}_l|p\rangle| \equiv |\langle 0|\vec{x}|p\rangle|$, with magnitude independent of the lattice site $\vec{r}_l$, with orientation fixed at every lattice site and parallel to the given transverse polarization of the radiation field. Also the property (A5.5) has been used here.

It is worthwhile mentioning that in general $h \neq g$ and under this circumstance not only the coefficients h and g in (A5.1c) are different from one another but also the coefficients of the exciton-photon bilinear operators in (A5.9) result to be distinct. Yet in the Hopfield treatment h is taken to be equal g, and (A5.9) holds. Since the excitons of interest in the optical properties of solids are those for which k is in the optical wavevector region they are coupled to photons having approximately the same energy, therefore unklapp processes ($\vec{G} \neq 0$) that couple excitons with wavevectors in the optical region with photons whose energy is thousand times the exciton energy are rather unfavorable and are neglected in (A5.9). On the contrary, unklapp is dominant when the exciton has the same energy as the photon whose wavelength is of the order than the lattice constant of the crystal.

Using the f-sum rule, the second term in (A5.7) reads as

$$\frac{2\pi}{V}\frac{}{ck}\sum_{pk}\omega_{po}\,|\langle 0|\vec{x}|p\rangle|^{2}\{a^{+}_{k}a_{k}+a_{k}a^{+}_{k}+a^{+}_{k}a^{+}_{-k}+a_{k}a_{-k}\} \tag{A5.11}$$

In conclusion the total hamiltonian that describes the Hopfield model of (bare) dielectric interacting with (bare) electromagnetic radiation is

$$\hat{H}_{pol} \equiv \hat{H}_{rad} + \hat{H}_{exc} + \hat{H}_{\text{int}} = \sum_{k} \hbar ck(\hat{a}_k^{\dagger}\hat{a}_k + \frac{1}{2}) + \sum_{k,p} E_p(\hat{b}_{kp}^{\dagger}\hat{b}_{kp} + \frac{1}{2})$$
$$+ \sum_{k,p} S_k |\langle 0|\vec{x}|p\rangle|^2 [\hat{b}_{kp}^{\dagger}\hat{b}_{kp} + \hat{b}_{kp}\hat{b}_{-kp} + h.c.]$$
$$- \frac{i}{c}\sum_{pk} \omega_{po}\sqrt{\frac{2\pi\hbar c}{Vk}} |\langle 0|\vec{x}|p\rangle|\{\hat{b}_{kp}^{\dagger}\hat{a}_k + \hat{b}_{kp}^{\dagger}\hat{a}_{-k}^{\dagger} - \hat{b}_{kp}\hat{a}_{-k} - \hat{b}_{kp}\hat{a}_k^{\dagger}\}$$
$$+ \frac{2\pi}{Vck}\sum_{pk} \omega_{po} |\langle 0|\vec{x}|p\rangle|^2 \{\hat{a}_k^{\dagger}\hat{a}_k + \hat{a}_k\hat{a}_k^{\dagger} + \hat{a}_k^{\dagger}\hat{a}_{-k}^{\dagger} + \hat{a}_k\hat{a}_{-k}\} \qquad \text{(A5.12)}$$

It is indeed an *approximate* hamiltonian. Even further, in order to stand by Hopfield's very well accepted hamiltonian [42], we will purposely "omit" the term H_{IJ} in (A5.1c) (exciton-exciton interaction), as done in his original paper [42]. For a single excited p -state with energy $E_p = h\omega_{op} \equiv h\omega_o$

$$\hat{H}_{pol}^{Hopfield} \equiv \sum_{\substack{k>0 \\ k<0}} \{\hbar ck(\hat{a}_k^{\dagger}\hat{a}_k + \tfrac{1}{2}) + \hbar\omega_o(\hat{b}_k^{\dagger}\hat{b}_k + \tfrac{1}{2}) + B(k)[\hat{a}_k^{\dagger}\hat{a}_k + \hat{a}_k\hat{a}_k^{\dagger}$$
$$+ \hat{a}_k^{\dagger}\hat{a}^{\dagger} + \hat{a}_k\hat{a}_{-k}] + iA(k)[-\hat{b}_k^{\dagger +}\hat{a}_k - \hat{b}_k^{\dagger}\hat{a}_{-k}^{\dagger} + \hat{b}_k\hat{a}_{-k} + \hat{b}_k\hat{a}_k^{\dagger}]\}$$
$$\equiv \sum_{\substack{k>0 \\ k<0}} \{\hat{H}_{pol}(k)\} = \sum_{k>0} \{\hat{H}_{pol}(k) + \hat{H}_{pol}(-k)\} \qquad \text{(A5.13)}$$

where

$$A(k) = \frac{(h\omega_o)^2(4\pi\beta_o)^{1/2}}{2(hck\,h\omega_o)^{1/2}}; \quad B(k) = (\pi\beta_o)\frac{(h\omega_o)^2}{hck} = \frac{A^2(k)}{h\omega_o}; \quad \beta_o \equiv \frac{2|\langle 0|\vec{x}|p\rangle|^2}{h\omega_o V}$$

A6: Multimode coherent and squeezed states

In this appendix we will establish notations, and we will review the definitions and some useful properties of number states, coherent states and squeezed states [1,28,29].

Let us denote by a and b two different bose particles while 1 and 2 denote two distinct modes for each particle; thus

$$[a_1,\ a_1^+] = [a_2,\ a_2^+] = [b_1,\ b_1^+] = [b_2,\ b_2^+] = 1$$

$$[a_1,\ a_1] = [a_1^+,\ a_1^+] = [a_2,\ a_2] = [a_2^+,\ a_2^+] = [a_1,\ a_2] = [a_2^+,\ a_2^+] = 0 \qquad \text{(A6.1)}$$

Recall that for the vacuum state $|\,0\,\rangle$ of each operator one has

$$a_1|\,0\,\rangle = a_2|\,0\,\rangle = b_1|\,0\,\rangle = b_2|\,0\,\rangle = 0$$

a. Number states

We denote a normalized number state for the mode 1 of particle a by $|\,n_1\,\rangle_a = [n_1!]^{-1/2}(a_1^+)^{n_1}|\,0\,\rangle$. Two-mode normalized number states for particle a are $|\,n_1 n_2\,\rangle_a = |\,n_1\rangle_a \otimes |\,n_2\rangle_a$ and likewise for particle b.

Let us introduce the mixed mode operator

$$\gamma_l \equiv \alpha_l a_l + \beta_l b_l \qquad (l = 1, 2) \qquad \text{(A6.2)}$$

as a bose particle destruction operator which is a linear combination of a_l and b_l with "weights" α_l and β_l. Then

$$[\gamma_l\ ,\ \gamma_l^+] = 1 \qquad \text{provided} \qquad |\ \alpha_l|^2 + |\ \beta_l|^2 = 1 \tag{A6.3}$$

A relative phase χ_l between two distinct bare particles may also be introduced by redefining (A6.2) as

$$\gamma_l = |\ \alpha_l|\ a_l + e^{i\ \chi_l}|\ \beta_l|\ b_l \tag{A6.4}$$

The number states of these operators can be defined in complete analogy with those for the a_l's and b_l's.

b. Coherent states

Following Glauber [82] coherent states of the bosons a_l, or b_l, or γ_l can be defined as eigenstates of the respective destruction operators, e.g.

$$a_l |\ a_l\ \rangle = a_l |\ a_l\ \rangle \tag{A6.5}$$

where a_l (no caret) is the complex (c-number) eigenvalue. Two-mode coherent states $|\ a_{12}\ \rangle$ are defined to be simultaneously eigenstates of both annihilation operators, e.g. for a_1 and a_2 one has

$$a_1 |\ a_{12}\ \rangle = a_1 |\ a_{12}\ \rangle \qquad a_2 |\ a_{12}\ \rangle = a_2 |\ a_{12}\ \rangle \tag{A6.6}$$

with continuous complex eigenvalues

$$a_1 \equiv |\, a_1| e^{i\phi_1^a} \qquad a_2 \equiv |\, a_2| e^{i\phi_2^a}$$

It is often useful to consider that the two-mode coherent states are generated by applying the two-mode displacement operator onto the vacuum $|\, 0\,\rangle$

$$|\, a_{12}\,\rangle = D(a_{12})|\, 0\,\rangle \equiv \exp\left[-\tfrac{1}{2}(|\, a_1|^2 + |\, a_2|^2)\right] e^{a_1 a_1^+} e^{a_2 a_2^+} |\, 0\,\rangle \qquad \text{(A6.7)}$$

Here $|\, a_{1,2}|^2$ is the average number of bosons a in the mode 1 or 2. In the configuration space, these states represent minimum uncertainty (M.U.) Gaussian wavepackets whose width is fixed in time. In a time-dependent picture of the e.m. field this property is referred to as time-stationarity of the noise of the light field in a coherent state [20]. We can proceed similarly to introduce single-mode and two-mode coherent states for the b_l 's and γ_l 's.

c. Squeezed states

Here our particular interest is in squeezed ("low noise") states, and especially in two-mode squeezed states. They have been discussed in the literature [10-22]. One useful definition of a two-mode squeeze state is that it is obtained by displacing the squeezed vacuum, e.g. one has

$$|\, a_{12}\,\rangle_z = D(a_{12}) S_{12}^a(z)\,|\, 0\,\rangle \qquad \text{(A6.8)}$$

$$S_{12}^{a}(z) \equiv S_{12}^{a}(r,\ \varphi) = \exp(r[a_1 a_2 e^{-2i\varphi} - a_1^{+} a_2^{+} e^{2i\varphi}]) \qquad \text{(A6.9)}$$

is the two-mode squeeze operator, r is the squeeze factor and φ is a phase. $z \equiv \{r, \varphi\}$ is used as short notation. Of course identical formulae hold for the b_l 's and γ_l 's bosons.

There is an alternate useful way to obtain the state $| a_{12} \rangle_z$ i.e. by transforming the two annihilation operators a_1 and a_2 into squeeze annihilation operators. For example we may transform a_1 as

$$S_{12}^{a}(z) a_1 (S_{12}^{a})^{+} = a_1 \cosh r + a_2^{+} e^{i\varphi} \sinh r \equiv A_1 \qquad \text{(A6.10)}$$

and likewise for a_2 to obtain A_2. In analogy with the coherent states, they can be defined alternatively as eigenstates of the two-mode operators (A6.10)

$$A_1 | a_{12} \rangle_z = A_1(z) | a_{12} \rangle_z \qquad A_2 | a_{12} \rangle_z = A_2(z) | a_{12} \rangle_z \qquad \text{(A6.11)}$$

where $A_1(z)$ and $A_2(z)$ are complex eigenvalues. If there is no possible confusion, we may write

$$A_{1,2} | a_{12} \rangle_z = A_{1,2}(z) | a_{12} \rangle_z \qquad \text{(A6.12)}$$

In the configuration space these states represent Gaussian wavepackets. For a suitable hamiltonian the width of these gaussians vary periodically in time becoming smaller and bigger than that of the vacuum state: they are not therefore

minimum uncertainty states for all times as the state evolves, but only for certain specific times during the entire oscillation cycle [1,71]. For the cavity photon this property reflects the non-stationarity of the noise of the e.m. field in a squeezed state [1,29].

For the mixed boson γ_l one proceeds identically, defining single-mode (l=1,2) squeezed states $| \gamma_l \rangle_z$

$$\Gamma_l | \gamma_l \rangle_z = \Gamma_l(z) | \gamma_l \rangle_z \qquad (l = 1, 2) \tag{A6.13}$$

as eigenstates of the squeeze annihilation operator

$$\Gamma_l \equiv S_l^{\gamma}(z) \gamma_l S_l^{\gamma^+}(z) = \gamma_l \cosh r + \gamma_l^+ e^{i\varphi} \sinh r \tag{A6.14}$$

$$\text{with } S_l^{\gamma}(z) = \exp(\tfrac{r}{2}[\gamma_l \gamma_l e^{-i\varphi} - \gamma_l^+ \gamma_l^+ e^{i\varphi}]) \qquad (l = 1, 2) \tag{A6.15}$$

The corresponding two-mode squeezed states $| \gamma_{1,2} \rangle_z$ for the mixed bosons γ_1 and γ_2 are defined as eigenstates of

$$\tilde{\Gamma}_1 | \gamma_{12} \rangle_z = \tilde{\Gamma}_1(z) | \gamma_{12} \rangle_z \qquad \tilde{\Gamma}_2 | \gamma_{12} \rangle_z = \tilde{\Gamma}_2(z) | \gamma_{12} \rangle_z \tag{A6.16}$$

Here

$$\tilde{\Gamma}_1 \equiv S_{12}^{\gamma}(z) \gamma_1 S_{12}^{\gamma^+}(z) = \gamma_1 \cosh r + \gamma_2^+ e^{i2\varphi} \sinh r \tag{A6.17}$$

$$\tilde{\Gamma}_2 \equiv S_{12}^{\gamma}(z) \gamma_2 S_{12}^{\gamma^+}(z) = \gamma_2 \cosh r + \gamma_1^+ e^{i2\varphi} \sinh r \tag{A6.18}$$

and

$$S_{12}^{\gamma}(z) = \exp(r[-\gamma_1^{+}\gamma_2^{+}e^{2i\varphi} + \gamma_1\gamma_2 e^{-2i\varphi}]) \tag{A6.19}$$

Again the squeezed state $|\gamma_{12}\rangle_z$ can be generated by first applying (A6.19) on the vacuum followed by a displacement (cf. A6.7)

$$|\gamma_{12}\rangle_z = D(\gamma_{12})S_{12}^{\gamma}(z)|0\rangle \tag{A6.20}$$

In the two-mode case the meaning we assign to α, β, r, φ is the same as for the single-mode, except for the squeeze factor. In the former case r mediates the coupling between two *distinct* modes 1 and 2, while in the latter r mediates the coupling between the *same* mode. Compare e.g. S in (A6.19) with S in (A6.15). This point may be made even clearer if one lets $r \to 0$ in the explicit expression for the annihilation operator $\tilde{\Gamma}_1$ (or $\tilde{\Gamma}_2$)

$$\begin{aligned}\tilde{\Gamma}_1 = {} & a_1|\alpha_1|\cosh r + a_2^{+}e^{i\varphi}|\alpha_2|\sinh r \\ & + b_1 e^{i\chi_1}|\beta_1|\cosh r + b_2^{+}e^{i(\varphi-\chi_2)}|\beta_2|\sinh r\end{aligned} \tag{A6.21}$$

In this limit $\tilde{\Gamma}_1$ only couples a_1 to b_1. In the states $|\gamma_{12}\rangle_z$ instead the two distinct modes become so tightly correlated that they no longer fluctuate independently by even the small amount allowed in a coherent state [2,108]. States like $|\gamma_{12}\rangle_z$ turn out to be a good physical representation for a polariton quantum state where the two distinct bosons are: excitons and photons coupling inside the crystal with *pairs*

of opposite wavevector modes to form a new excitation of the combined radiation-dielectric material [42].

d. Non-poissonian statistics and squeezing

One useful figure of merit for a squeezed state is the departure from poissonian statistics for the number of bosons in the state [2,10]. Consider the distribution (P) of the number of bosons γ_l in the state $| \gamma_{12} \rangle_z$. Results which will be used in the following sections are now derived. The width of P can be characterized by the square root of

$$\langle (\Delta N_l)^2 \rangle \equiv_z \langle \gamma_{12} | (\gamma_l^+ \gamma_l)^2 | \gamma_{12} \rangle_z - \{_z \langle \gamma_{12} | \gamma_l^+ \gamma_l | \gamma_{12} \rangle_z \}^2 \qquad (l = 1, 2),$$

namely the variance of the fluctuations of the number of bosons γ_l in the squeezed state $| \gamma_{12} \rangle_z$. In order to evaluate say $\langle (\Delta N_1)^2 \rangle$, we first give

$$_z\langle \gamma_{12} | \gamma_1 | \gamma_{12} \rangle_z = \gamma_1 \qquad \text{(A6.22)}$$

Then

$$\langle N_1 \rangle \equiv_z \langle \gamma_{12} | \gamma_1^+ \gamma_1 | \gamma_{12} \rangle_z = | \gamma_1 |^2 + \sinh^2 r \qquad \text{(A6.23)}$$

where

$$| \gamma_1 |^2 = | a_1 |^2 | \alpha_1 |^2 + | b_1 |^2 | \beta_1 |^2 + | \alpha_1 \beta_1 | (a_1 b_1^* e^{-i \chi_1} + c.c.) \qquad \text{(A6.24)}$$

is obtained from (A6.2). It is clearly seen from (A6.23-24) that in the state $| \gamma_{12} \rangle_z$ the mean number has two contributions: one arising from the coherent excitation of the mixed boson γ_1 i.e. $| \gamma_1|^2$, and the other from the squeezing. Thus P strongly depends on the relative weight of these two contributions. Furthermore as shown by (A6.24), several elements influence the coherent contribution. A straightforward calculation yields:

$$\langle (\Delta N_1)^2 \rangle \equiv | \gamma_1|^2 \{ e^{-2r} \cos^2 [\tfrac{1}{2}(\varphi - 2\phi_1)] + e^{2r} \sin^2 [\tfrac{1}{2}(\varphi - 2\phi_1)] \} + \tfrac{1}{2} \sinh^2 2r \quad \text{(A6.25)}$$

where we set $\gamma_1 \equiv | \gamma_1 | e^{i\phi_1}$. For a given r, extremal values for (A6.25) obtain when $2\phi_1 = \varphi$ and $2\phi_1 = \varphi + \pi$, that is

$$\langle (\Delta N_1)^2 \rangle \equiv e^{\pm 2r} \langle N_1 \rangle + \sinh^2 r \, [1 + \sinh 2r] \quad \text{(A6.26)}$$

The upper sign corresponds to π and the lower to 0.

For clarity of exposition in the remainder of this paper we will treat only these two limits rather than intermediate cases. Furthermore, we consider the limit $| \gamma_1|^2 >> e^{2r}$ which will turn out to be of some importance to us. Under this circumstance the coherent contribution to the mean number (first term in A6.23) greatly exceeds the squeeze contribution (second term), and $\langle N_1 \rangle \approx | \gamma_1|^2$. Also, the first term on the right hand side of (A6.26) exceeds the second one [109] and the variance can be approximated as

$$\langle (\Delta N_1)^2 \rangle = \langle N_1 \rangle e^{\pm 2r} \equiv s^{\pm 2} \langle N_1 \rangle \qquad \langle N_1 \rangle \cong | \gamma_1|^2 \quad \text{(A6.27)}$$

This result should be compared with the equivalent result for a coherent state(Poisson distribution), for which $\langle (\Delta N_1)^2 \rangle = \langle N_1 \rangle$. Thus the state $| \gamma_{12} \rangle_z$ carries a non-poissonian counting statistics whose deviations are measured by the squeeze amplitude $s \equiv e^r$. In particular depending on whether $\varphi - 2\phi_1$ is 0 or π, $P(N_1)$ represents a distribution broader or narrower than a poissonian: $s^2 \rightarrow$ super-poissonian or $s^{-2} \rightarrow$ sub-poissonian. When $|\gamma_1|^2$ is not sufficiently dominant in $\langle N_1 \rangle$ it is not straightforward to understand the connection between $\langle (\Delta N_1)^2 \rangle$ and $\langle N_1 \rangle$.

A completely analogous discussion can be given for the other mode.

A7: Photon fluctuations (variance)

We start from the result (A6.26). We rewrite variance and mean for $N_1 \rightarrow \gamma_{+k}^{+}\gamma_{+k}$ in terms of the bare operators a_{+k} and b_{+k} (cf. Eq. A6.4)

$$\langle N_1 \rangle \rightarrow \langle \gamma_{+k}^{+}\gamma_{+k} \rangle = |\alpha_k^{+}|^2 \langle a_{+k}^{+} a_{+k} \rangle \qquad \text{(A7.1)}$$
$$+ |\alpha_k^{+}\beta_k^{+}|[e^{-i\chi_{+k}} \langle b_{+k}^{+} a_{+k} \rangle + e^{+i\chi_{+k}} \langle a_{+k}^{+} b_{+k} \rangle] + |\beta_k^{+}|^2 \langle b_{+k}^{+} b_{+k} \rangle$$

and $\langle (\Delta N_1)^2 \rangle \rightarrow \langle (\Delta \gamma_{+k}^{+}\gamma_{+k})^2 \rangle \equiv \langle \gamma_{+k}^{+}\gamma_{+k}\gamma_{+k}^{+}\gamma_{+k} \rangle - \langle \gamma_{+k}^{+}\gamma_{+k} \rangle^2$

and $\langle (\Delta N_1)^2 \rangle \rightarrow \langle (\Delta \gamma_{+k}^{+}\gamma_{+k})^2 \rangle \equiv \langle \gamma_{+k}^{+}\gamma_{+k}\gamma_{+k}^{+}\gamma_{+k} \rangle - \langle \gamma_{+k}^{+}\gamma_{+k} \rangle^2$

The expectation values < > are all evaluated on the states $|\gamma_{\pm k}\rangle_z$. Thus [78]

$$\langle \gamma_k^{+}\gamma_k\gamma_k^{+}\gamma_k \rangle = |\alpha_k^{+}|^4 \langle a_k^{+}a_k a_k^{+}a_k \rangle + |\beta_{k\,k}^{+}|^4 \langle b_k^{+}b_k b_k^{+}b_k \rangle$$
$$+ |\alpha_k^{+}|^3|\beta_k^{+}|\{[\langle a_k b_k^{+} \rangle + 2\langle a_k^{+}a_k a_k b_k^{+} \rangle] e^{-i\chi_k} + c.c.\}$$
$$+ |\alpha_k^{+}||\beta_k^{+}|^3 \{[\langle a_k b_k^{+} \rangle + 2\langle b_k^{+}b_k^{+}b_k a_k \rangle] e^{-i\chi_k} + c.c.\}$$
$$+ |\alpha_k^{+}|^2|\beta_k^{+}|^2 \{[2\langle a_k^{+}a_k b_k^{+}b_k \rangle + e^{-i2\chi_k}\langle a_k a_k b_k^{+}b_k^{+} \rangle] + c.c.\}$$

and from (A7.1)

$$\langle \gamma_k^{+}\gamma_k \rangle^2 = |\alpha_k^{+}|^4 \langle a_k^{+}a_k \rangle^2 + |\beta_k^{+}|^4 \langle b_k^{+}b_k \rangle^2$$
$$+ 2|\alpha_k^{+}|^3|\beta_k^{+}|\{\langle a_k^{+}a_k \rangle \langle a_k b_k^{+} \rangle e^{-i\chi_k} + c.c.\}$$
$$+ 2|\alpha_k^{+}||\beta_k^{+}|^3 \{\langle b_k^{+}b_k \rangle \langle a_k b_k^{+} \rangle e^{-i\chi_k} + c.c.\}$$
$$+ |\alpha_k^{+}|^2|\beta_k^{+}|^2 \{\langle a_k^{+}a_k \rangle \langle b_k^{+}b_k \rangle + \langle a_k b_k^{+} \rangle \langle b_k a_k^{+} \rangle + \langle a_k b_k^{+} \rangle^2 e^{-i2\chi_k} + c.c.\}$$

Therefore:

$$\langle(\Delta\,\gamma_k^{+}\gamma_k)^2\rangle = |\alpha_k^{+}|^4\langle(\Delta\,a_k^{+}a_k)^2\rangle$$
$$+|\alpha_k^{+}|^3|\beta_k^{+}|\{[\langle d_k\rangle + 2C(N_k^{ph}, d_k)]e^{-i\chi_k} + c.c\}$$
$$+|\alpha_k^{+}|^2|\beta_k^{+}|^2\{e^{-i2\chi_k}\langle(\Delta\,d_k)^2\rangle + C(N_k^{ph}, N_k^{exc}) + C(d_k, d_k^{+}) - \langle N_k^{exc}\rangle + c.c.\}$$
$$+|\alpha_k^{+}||\beta_k^{+}|^3\{[-\langle d_k\rangle + 2C(N_k^{exc}, d_k)]e^{-i\chi_k} + c.c.\}$$
$$+|\beta_k^{+}|^4\langle(\Delta\;N_k^{exc})^2\rangle \qquad \text{(A7.2)}$$

where we have set

$$N_k^{ph} \equiv a_k^{+}a_k\,; \qquad N_k^{exc} \equiv b_k^{+}b_k\,; \qquad d_k \equiv a_k\,b_k^{+};$$

and (A7.3)

$$C(X\;,\;Y) \equiv \langle X\;Y\;\rangle - \langle X\;\rangle\langle Y\;\rangle; \qquad \langle(\Delta X)^2\rangle \equiv \langle X^2\rangle - \langle X\;\rangle^2$$

Substituting Eq.s (A7.1) and (A7.2) in (A6.26) and using Eq. (A6.3) the exact expression follows

$$\langle(\Delta N_k^{ph})^2\rangle = e^{\pm 2r_k}\langle N_k^{ph}\rangle - |\,\alpha_k^{+}\beta_k^{+}|\,A_{1,\,k}$$
$$+|\,\beta_k^{+}|^2[\,\langle(\Delta N_k^{ph})^2\rangle - A_{o,\,k}] + \frac{1}{|\,\alpha_k^{+}|}\{e^{\pm 2r_k}A'_{-1,\,k}|\,\beta_k^{+}| - A_{-1,\,k}|\,\beta_k^{+}|^3\}$$
$$+\frac{1}{|\,\alpha_k^{+}|^2}\{+\sinh^2 r_k\,[1+\sinh 2r_k] + e^{\pm 2r_k}|\,\beta_k^{+}|^2\langle N_k^{exc}\rangle - A_{-2,\,k}|\,\beta_k^{+}|^4\} \qquad \text{(A7.4)}$$

Here we defined:

$$A_{-2,\,k} \equiv \langle(\Delta\,N_k^{exc})^2\rangle$$
$$A_{-1,\,k} \equiv [-\langle d_k\rangle + 2C(N_k^{exc},\,d_k)]e^{-i\chi_k} + c.c.$$
$$A'_{-1,\,k} \equiv \langle d_k\rangle e^{-i\chi_k} + \langle d_k^{+}\rangle e^{+i\chi_k} \qquad \text{(A7.5)}$$

$$A_{o,k} \equiv e^{-i2\chi_k} \langle (\Delta d_k)^2 \rangle + C(N_k^{ph}, N_k^{exc}) + C(d_k, d_k^{+}) - \langle N_k^{exc} \rangle + c.c.$$

$$A_{1,k} \equiv [\langle d_k \rangle + 2C(N_k^{ph}, d_k)] e^{-i\chi_k} + c.c.$$

A8: Photo number (mean value)

We evaluate the expectation value of the number of photons in a polariton coherent state. We start from Eq. (A6.23) where we substitute the expression (A7.1) on the left hand side and the expression (A6.24) on the right hand side [78]:

$$\langle N_1 \rangle \rightarrow \langle \gamma_k^+ \gamma_k \rangle = \sinh^2 r_k + | \gamma_k |^2 \tag{A8.1}$$

or

$$| \alpha_k^+ |^2 \langle a_k^+ a_k \rangle + | \alpha_k^+ \beta_k^+ | [\langle d_k \rangle e^{-i\chi_k} + c.c.] + | \beta_k^+ |^2 \langle b_k^+ b_k \rangle = \sinh^2 r_k$$
$$+ | a_k |^2 | \alpha_k^+ |^2 + | b_k |^2 | \beta_k^+ |^2 + a_k b_k^* | \alpha_k^+ \beta_k^+ | e^{-i\chi_k} + b_k a_k^* | \alpha_k^+ \beta_k^+ | e^{+i\chi_k}$$

All expectation values are evaluated on the states $| \gamma_\pm \rangle$. Dividing by $| \alpha_k^+ |^2$ and ordering in the powers of $| \beta_k^+ |^2$ one gets:

$$\langle N_k^{ph} \rangle \equiv \langle a_k^+ a_k \rangle = | a_k |^2 + \frac{\sinh^2 r_k}{| \alpha_k^+ |^2} \tag{A8.2}$$
$$+ | \beta_k^+ | \{ \frac{e^{-i\chi_k}}{| \alpha_k^+ |} (a_k b_k^* - \langle d_k \rangle) + c.c. \} + | \beta_k^+ |^2 [| b_k |^2 - \langle b_k^+ b_k \rangle]$$

$| a_k |^2$ is the average value of the number of bare photons (cf. Eq. A6.6). Within the context of the detection experiment of section II c this is interpreted as the coherent photon flux multiplied by the integration time period T .

REFERENCES

[1] R. Loudon, "The Quantum Theory of Light", Oxford Press (1973);

[2] R. Loudon et al. J. of Mod. Opt., **34**, 709, (1987);

[3] M. Sargent, M.O. Scully, and W.L. Lamb in "Laser Physics" by Addison - Wesley 1(974);

[4] D. Bohm, Quantum Theory, Prentice-Hall, Englewood Cliffs, N.J. (1951);

[5] J.J.Sakuray, "Modern Quantum Mechanics", Benjamin/Cummings, Publ. Co. Inc.(1985);

[6] C. Caves, Phys. Rev. D, **23**, 1693, (1981). See also ref. [19];

[7] "Squeezed and non-classical light", Ed.s P. Tombesi and R.P. Pike, (NATO ASI series B, Vol. **190**, Plenum Press1989);

[8] J. of Mod. Opt., **34**, 709, (1987) special issue on squeezed states;

[9] J. of Opt. Soc. Am. B, **4**, 1453, (1987) special issue on squeezed states;

[10] D.F. Walls, Nature **306**, 141, (1993); J.H. Shapiro, IEEE Quantum Electron. QE-**21**, 237, (1985); C. Caves in "Coherence, Cooperation and Fluctuations", Ed.s F. Haake, L.M. Narducci and D.F. Walls Cambridhe University Press 1985; R. Slusher and B. Yurke, Sci. Am. **258**, (no 5), 50 , (1988); R. Henry and S. Glotzer Am. J. of Physics **56**, 318, (1988); M.C. Teich and B.E.A. Saleh in "Progress in Optics" **26**, 1, Ed. E. Wolf, North-Holland (1988); P. Meystre & M. Sargent III, "Element of Quantum Optics", Springer Verlag 1990;

[11] R. Loudon, Rep. Prog. Phys. **43**, 913, (1980);

[12] H. Takahasi, Adv. Commun. Syst. **1**, 227, (1965);

[13] D. Robinson, Commun. Math. Phys. **1**, 159, (1965);

[14] D. Stoler, Phys. Rev., D, **1**, 3217, (1970);

[15] D. Stoler, Phys. Rev.,D, **4**, 1925, (1971);

[16] Y.E. Lu, Lett. Nuovo Cimento, 2, 1241, (1971);

[17] Y.E. Lu, Lett. Nuovo Cimento, 3, 585, (1972);

[18] H.P. Yuen, Phys. Rev. A, **13**, 2226, (1976);

[19] J. Hollenhorst, Phys. Rev. D, 19, 1669 (1979);

[20] R.E. Slusher et al., Phys. Rev. Lett. **55**, 2409, (1985);

[21] R. Shelby et al., Phys. Rev. Lett. **57**, 691, (1986);

[22] L. Wu et al. Phys. Rev. Lett. **57**, 2520, (1986);

[23] E. Power in "Introductory quantum electrodynamics", Longmans, London (1964) chapter III;

[24] L.D. Landau & E.M. Lifshitz in "Electrodynamics of continuos media", Pergamon Press, (1960);

[25] L.I. Schiff, in "Quantum Mechanics" (McGraw-Hill, third edition);

[26] See, for instance, M. C. Teich & B.E.A. Saleh, Quantum Opt. , **5**, 153, (1990);

[27] R. Loudon, Opt. Commun., **70**, 109, (1989);

[28] C. Caves and B.L. Schumaker, I & II, Phys. Rev. A, **31**, 3068 & 3099, (1985);

[29] B.L. Shumaker, Phys. Rep. **135**, 317, (1985);

[30] C. Caves, Phys. Rev. D, **26**, 1817, (1982);

[31] W. G. Unruh in "Quantum Optics, Experimental Gravitation and Measurement Theory" P. Meystre and M. O. Scully Eds, Plenum N.Y. 1983;

[32] A.O. Barut et al., Commun. Math. Phys. **21**, 41, (1971);

[33] A.M. Perelomov, Sov. Phys. Usp. **20**, 703, (1977);

[34] G.J. Milburn, J. of Phys. A, **17**, 737, (1984);

[35] S.M. Barnett & P.L. Knight, J. of Mod. Opt., **34**, 841, (1987);

[36] C. Kittel, "Introduction to Solid State Physics" (J. Wiley & Sons, New York 1964); C. Kittel, "Quantum Theory of Solids" (J. Wiley & Sons, 1964);

[37] "Polaritons" [Proceedings of the first Taormina Research Conference on the Structure of Matter], Ed.s E. Burstein & F. De Martini, (Pergamon Press 1972). It is of interest to note that the term polariton was originally coined by Hopfield to designate the "uncoupled polarization field particles" of the medium, i.e. the excitons, optical phonons, etc. The term was however, misconstrued by Russian investigators as designating the coupled polarization exciton-photo modes, and through extensive use in the Russian literature polariton has become the generic name for the coupled modes. Further we should mention that the term "polariton" is usually employed in a much narrower sense than we do here. In much of the mentioned literature, in fact an e.m. wave propagating in a material is referred to as a polariton only when its frequency lies close to one (or more) resonance of the medium. However, even if the frequency of the wave is *far* from a discrete resonance, a fraction of the energy of the wave will still be stored in the polarization induced in the medium so long as the dielectric constant differs from unity by an appreciable amount. This consideration leads us to use the term polariton in a sense much broader than the standard one.

[38] K.B. Tolpygo, Zh. E.T.F., **20**, 947, (1950) (in russian);

[39] M. Born and K. Huang, "Dynamical Theory of Crystal Lattices", (Oxford Press 1985);

[40] S.I. Pekar, Sov. Phys. JETP 6, 785, (1958); **11**, 1286, (1960); S.I. Pekar, "Crystal optics and additional light waves" (Benjamin-Cummings 1983);

[41] V.M. Agranovich, Sov. Phys. JETP **10**, 307, (1960);

[42] J.J. Hopfield, Phys. Rev., **112**, 1555, (1958); J. of Phys. Soc. of Japan, 21 (Suppl.); J.J. Hopfield, Phys. Rev., 182, 945, (1969);

[43] Agronovich & V.L. Ginzburg, "Crystal optics with spatial dispersion and excitons" (Springer Verlag, 2nd ed. 1984);

[44] J.L. Birman in "Excitons", Ed.s M.D. Sturge & E.I. Rashba, (North Holland 1982) p.27;

[45] U. Fano, Phys. Rev. 103, 1202, (1956);

[46] R. Loudon in "Non-linear optics with polaritons" [Proc. S.I.F., LXIV], Ed. N. Bloembergen, (North Holland1977);

[47] W. Brenig, R, Zeyher, J.L. Birman, Phys. Rev. B6, 4617, (1972);

[48] E.S. Koteles, "Investigation of Exciton-Polariton Dispersion Using Laser Techniques", in "Excitons" M. Sturge & E. Rashba Ed.s, North Holland (1982); Polaritons" [Proceedings of the first Taormina Research Conference on the Structure of Matter], Ed.s E. Burstein & F. De Martini, (Pergamon Press 1972);

[49] See, for instance, D.L. Mills & E. Burstein, Rep. Prog. Phys. 1974, **37**, 817;

[50] H. P. Yuen , Phys. Rev. A **13**, 2226, (1976); H.P. Yuen, J.H. Shapiro, IEEE Trans. Inf. Theory, **26**, 78, 1980. H.P. Yuen, J.H. Shapiro IEEE Trans. Inf. Theory **24**, 657, (1978); idem, **25**, 179, (1979); H.P. Yuen, in "Quantum

Optics, Experimental Gravitation and Measurement Theory" P. Meystre and M. O. Scully Eds, Plenum N.Y. 1983 (p. 249);

[51] X. Zou and L. Mandel, Phys. Rev. A, **41**, 475, (1990);

[52] R. Knox, "Theory of excitons", (Academic Press 1963);

[53] The Eq.s for the field variables in Eq. (2.2.8), that is Eq.s (2.2.4) and (2.2.6), is unchanged if we add the total derivative $d_t[(4\pi c^2)^{-1}\varepsilon_d \vec{A}_{exc.}\cdot d_t \vec{A}_{e.m.}]$ because this vanishes once the action is varied. Further using Eq. (2.2.4) L can be rewritten as in Eq. (2.2.9) except for a term that reduces to a vanishing surface contribution when integration over V is carried out (divergence theorem). Notice that in L the photon-exciton coupling *does not* appear: it already is *implicit* in the dressing of the vacuum particle components constituting the polariton.

[54] For a given polarization the full Fourier transform is $\vec{A}_{e.m.}(\vec{r},t) = \int d\omega \int d\vec{k}\, \vec{A}_{e.m.}(\vec{r},t)_{\vec{k},\omega}$; for a single frequency $\vec{A}_{e.m.}(\vec{r},t) = \int d\vec{k}\, \vec{A}_{e.m.}(\vec{r},t)_{\vec{k},\omega} \rightarrow \sum_{\vec{k}} \vec{A}_{e.m.}(\vec{r},t)_{\vec{k},\omega}$. In the expression for $\vec{A}_{e.m.}$ we omit the ω-suffix and the vector notation in $\vec{k}$, assumed for simplicity parallel to z.

[55] Owing to the transformation A1.4, the parametrizations of H in terms of $\{ A_{1k}, A_{2k}, B_k, B'_k, C_k, C'_k \}$ or $\{ \varepsilon_k, \nu_{\pm k}, \upsilon_{\pm k}, \alpha_{\pm k}, \beta_{\pm k} \}$ are equivalent and we will use them indistinctly: we will refer to them as "new" and "old" parametrizations, respectively.

[56] I.Abram, Phys. Rev. A 33, 11, 4661, (1987);

[57] R. Glauber and M. Lewenstein, in "Squeezed and non-classical light" edited by P. Tombesi and R.P. Pike, NATO ASI series B, Vol. 190, (1988);

[58] Beside vacuum particles, the presence of the conjugate particles of opposite wavevector in Eq. (2.3.2) is essential, the lack of it would destroy the polariton structure as a linear combination of two distinct boson particles with their opposite wavevector conjugate particles;

[59] A discussion on the group structure of other polariton hamiltonians may be found e.g. in S. Kim and J. Birman [Phys. Rev. B, 38, 6, 4291 (1988)];

[60] The propagating field component of the polariton is discussed e.g. by T. Skettrup, Phys. Rev. B 24, 884, (1981). A photon in the crystal can transform directly into an exciton provided they both have the same energy and wavevector. If the exciton is not scattered by a phonon or some other defects, energy "oscillates" back and forth between exciton and photon owing to energy-wavevector conservation as discussed e.g. in ref. [42]. The propagating field of the polariton describes this "intrinsic phase" of the polariton, and the oscillations above can be ascribed to the oscillations of the mixed boson c . The latter are estimated directly from Ω and for an exciton-polariton in CdS at $k = k_o, h^{-1}\Omega \sim 10^{15}$ sec^{-1}. This rate of energy exchange has been evaluated on other contexts and it is of the same order of magnitude [W.C. Tait & R.L. Weheir Phys. Rev. 166, 769, (1968) and "Dynamical Processes in Solid State Optics" (part I) Ed. R. Kubo (W.A. Benjamin N.Y. 1967)];

[61] R. Graham in J. of Mod. Opt., 34, 709, (1987);

[62] J. Janszky, Optics Comm. 59, (1986) 151;

[63] J.A. Wheeler Lett. Math. Phys. 10,201, (1985);

[64] The eigenvectors are taken to be even functions of the wavevector consistently with the squeeze parameters and the energies;

[65] The μ 's and η 's represent the same operator: we introduced two different symbols purely for clarity;

[66] S.A. in "Solid State Physics", M.I.R. Moscow, (1976);

[67] R. Loudon, J. Phys. A vol. 3, 233, (1970);

[68] Especially e.g. in the second case where for a paramplifier ζ contains the appropriate pump field, which has no counterparts in the present physical system.

[69] Before $\hat{H}_{int}$ is turned on the photon and exciton bare fields and the propagating $\hat{c}$-field of the polariton share the *same* vacuum state; if $|0\rangle \equiv |0_{ph}\rangle |0_{exc}\rangle$, then $a_{\pm k}|0\rangle = b_{\pm k}|0\rangle = 0$ and from Eq. (3.1.2) $c_{\pm k}|0\rangle = 0$.

[70] Here t=0 is a reference time. Without loss of generality we will also consider in this subsection a fixed phase φ_k =0.

[71] M.Nieto, in "Frontiers in Non Equilibrium Statistical Mechanics", Ed. G. Moore and M.O. Scully (Plenum Press 1986);

[72] S.M. Barnett & M.A. Dupertuis, J. Opt. Soc. Am. B4, 505, (1987);

[73] G.J. Milburn, J. Phys. A, 17, 737;

[74] N.N. Bogolubov, J.Phys. (Moscow) 11, 23 (1047);

[75] We restore the notation accordingly: $\gamma_1 \rightarrow \gamma_{+k}$; $\gamma_2 \rightarrow \gamma_{-k}$; $\alpha_1 \rightarrow \alpha_k^+$; $\alpha_2 \rightarrow \alpha_k^-$; $\beta_1 \rightarrow \beta_k^+$; $\beta_2 \rightarrow \beta_k^-$;

[76] For different wavevector magnitudes we include the k - dependence on the squeeze factor and angle r and φ ;

[77] Although in different contexts, results that relate the squeezing to the dielectric properties of a medium have independently been obtained by R. Glauber & M. Lewenstein ref. [57] and by I. Abram ref. [56]. However, unlike these works, here we analyse non-classical properties in a *resonant* material, essential to create a polariton;

[78] To simplify the notation we suppress the sign "+" in the $+ k$ subindexes where it does not create confusion;

[79] L. Mandel, Opt. Lett. 4, 205, (1979);

[80] The evanescent part of a bulk polariton is obtained by total internal reflection at the vacuum-dielectric interface and it is distinct from a *surface polariton*. Total internal reflection of a bulk polariton, e.g. within the context of the Goos Hanchen effect, is discussed in J.L. Birman, D. N. Pattanayak, A.Puri, Phys. Rev. Lett. **50**, 1664, (1983), and A.Puri, D. N. Pattanayak, J.L. Birman, Phys. Rev. **B28**, 5877, (1983) and ref.s therein. For a description of the G. H. effect see e.g. H. K. Lotsch J. Opt. Soc. Am., **58**, 4, 551, (1968) and the original paper by F. Goos, H. Hanchen [Ann. Physik, (6) **1**, 333 (1947)]. Various electrodynamical investigations of this effect have been given based on using a wave "bundle" analysis within the framework of Maxwell theory.

[81] A surface polariton propagates along the surface where it is excited and to which it is coupled. Its amplitude decays exponentially with increasing distance from the surface *both* into the dielectric *and* into the vacuum in contact with it. Surface polaritons are longitudinally polarized while the bulk and evanescent waves are transverse (in the absence of spatial dispersion). The surface and leaky modes not only

have different origins, but also different properties such as e.g. their dispersion equations [e.g. V.M. Agranovich & D.L. Mills, in "Surface Polaritons" (North Holland Publ. Co. 1982)];

[82] An incident coherent light beam enters the medium from outside. As a result of the field-matter (dipolar) interaction the dipolar matter emits the secondary radiation which, as before, when summed, consists of two parts. One is a coherent part which, in the medium extinguishes the external coherent beam. The second, refracted wave, is squeezed and pro pagates in the medium as the coupled photon-exciton (or phonon) polariton. This scenario can now be *time-reversal*. A squeezed polariton wave, incident inside the medium travels toward the boundary. If the incident angle is less than critical, part of the wave is internally reflected, part transmitted. The latter, external to the medium travels at velocity c and is not squeezed. The reflected light retains the squeezed properties. If however the incident squeezed polariton wave is at the critical angle for total internal reflection, there is no transmitted beam, but an evanescent lateral wave is formed which decays in the vacuum exponentially away from the surface. This wave plus the internal incident and the totally internal reflected form one mode and constituients of which retain the squeezed properties. A partially complete proof of this is given by J.L. Birman (in preparation) which is valid for dilute media. But for our purpose we can, on the physical ground just discussed, examine the consequences of assuming that the evanescent wave has the full statistical properties (squeezing) of the internal constituents (incident and totally reflected polaritons) to which it is attached.

[83] R.J. Glauber, Phys. Rev. **131**, 2766, (1963);

[84] R. Glauber & P. Sudarshan, "Coherent States", World Scientific

[85] See P.P. Ewald [Ann. d. Physik, **49**, 1, (1916)] for the corresponding classical version of the exctinction theorem;
Publishers (1986);

[86] It is important to stress that the e.m. field leaking off the surface is not the free transmitted field propagating in vacuum. It is described by the radiative component of a polariton mixed wave excited inside the crystal. See e.g. A.D. Boardman, "Electromagnetic Surface Modes" (J. Wiley & Sons, New York 1982). The appropriate conceptual framework that permits one to understand this distinction is the extinction theorem [84] extended to quantum optics regime: accordingly the evanescent field is in our case the portion (dipole field) of the inside field that does not extinguish the vacuum incident field. This is discussed in detail in ref. [82];

[87] In this context recent developments in the production of number states should be mentioned. It is in fact possible to generate extremely sub-poissonian light fields by feed-back stabilized laser [Y. Yamamoto & H.A. Haus, Rev. Mod. Phys. **58**, 1001, (1986)] and even one-photon wavepackets using an optical shutter technique based on coincidence counting of the the output of a paramplifier [J. Rarity, in "Photon and quantum fluctuations", ed.s E.R. Pike and H. Walther, Adam Hilger Bristol (1988), p. 122];

[88] Precisely $|\alpha_k^{ev.}\rangle$ is a two-mode squeezed coherent state, two distinct wavevector modes being involved. Other kinds of states such as

polariton number states, and the polariton vacuum state itself, all exhibit the same feature. They all derive from the result (6.1.8) that is a typical squeeze transformation;

[89] Polariton radiation falling upon a prism base at an angle bigger than critical leaks off. This can either couple to an already existing e.m. mode on a surface spaced few mm from the prism base or can excite an e.m. mode therein. See e.g. A.D. Boardman, in "Electromagnetic Surface Modes" (J. Wiley & Sons, New York 1982);

[90] Varying θ modulates the wavevector of the evanescent radiation propagating parallel to the L.O. beam (phase-matching), leaving unaltered the frequency-wavevector mode of the excited bulk polariton. The wavevector dependence is hereafter understood;

[91] This condition implies that almost all of the evanescent light reaches the photocathode, but even the small fraction of the *L.O.* light reaching the detector still dominates the input contribution;

[92] The *L.O.* intensity can be regulated by the beam splitter *BS*, while the intensity of the leaky radiation depends on the beam splitter *BS* and on the dielectric properties of the crystal. $\varphi_{L.\,o.}$ is instead varied through the piezoelectric mirror $M_{\varphi_{L.\,o.}}$;

[93] The hypothetical KI parameters used are based on results given by D. Frohlich et al. (to be published in Physica Status Sol. b);

[94] J. Jackson, "Classical Electrodynamics" (J. Wiley & Sons,1962). A rigorous calculation of the evanescent intensity I_{evan} should take into account a *"bundle"* of wavevectors k as in a realistic case, instead of a *single* k as assumed in the present estimation;

[95] L. Ronchi, Optica Acta 8, 281, (1961) and references therein;

[96] The *L.O.* is still assumed to be stronger than the evanescent wave, i.e. $|\alpha_{L.O.}|^2 << |\alpha|^2$, although this requirement is less stringent than in the ordinary case (cf. Eq. 3.4);

[97] M. Artoni & J.L. Birman, Phys. Rev. B, 43, 4221, (1991);

[98] The value 0.9 is usally taken for reduction of the efficiency due to ransmission losses in optical cavities, where most of the factors causing the reduction (absorption, reflection and scattering) are the same of relevance to us;

[99] $\gamma_M = 0.8$ for conventional homodyne detectors. Here however the beam geometry is slyghtly more complicated by the fact that the evanescent and the *L.O.* waves have different mode profiles that may further spoil mode matching. Thermal light noise is typically not a problem in the visible and in the near infrared where $\hbar\omega >> kT$;

[100] D.L. Dexter and W.R. Heller, Phys. Rev. **91**, 273 (1953); W.R. Heller, A. Marcus, Phys. Rev. **84**, 809, (1951);

[101] R. Peierls, Ann. Physik **13**, 905 (1932)];

[102] L. Apker and Taft. Phys. Rev. ,**79**, 964, (1950); **87**, 814 (1951);

[103] F. Seitz, in "The Modern Theory of Solids" (McGraw-Hill, Inc. N.Y.1940);

[104] Actually we use trial functions so as to express the three free c-functions in terms of one of them, say e.g. $B_k(C_k)$ and $C_k'(C_k)$, and we then construct C_k by inverting Eq. (3.1.13) - now function of C_k only - taking ε_k as the experimental energy. This fitting procedure by which we give the parametrization of $H^{pol.}$ in Eq. (3.1.1) is not unique;

[105] If inelastic scattering instead occurs, the energy is stored in those crystal states which, through their coupling with the excitons, cause finite lifetimes (absorption) [36,37,42,43];

[106] Notice that the physical processes involved in the simultaneous creation (annihilation) of two bosons $\hat{c}_k$ and $\hat{c}_{-k}$ appearing in $\hat{H}_I$ are in violation with the conservation of energy and they represent *virtual processes*. The physical origin of these virtual terms is clarified e.g. in the extreme tight-binding exciton plus photon model as discussed, e.g. in Peierls' early work [101] on the absorption of light in solids, and also in ref.s [100,102,103]. The tight-binding model with the relevant virtual terms has been also considered by J.J. Hopfield (cf. § IV of his original paper [42] where a microscopic exciton-polariton hamiltonian is constructed). Incidentally, one should note that in discussing the photon-exciton interaction for this microscopic polariton hamitonian, among the interaction terms the exciton-exciton interaction term here appears. In spite of this the commonly used Hopfield model is the one of § III of the same paper [42], with no exciton-exciton term!

[107] An analogous tretment holds for the conjugate quadrature $\hat{X}_k^q$;

[108] S.M. Barnett & P.L. Knight, J. Opt. Soc. Am. B3, 467, (1985);

[109] This is certainly true for any value of r_k, when we take the upper sign; for the lower sign this is true for $0 < r_k < 0.8$. Since the values of r_k relevant to us fall on this range, eq (A6.27) is valid;

[110] We have used material parameters as found in T.S. Moss "Handbook on semiconductors" Vol. 1 (ch. 5), and in ref. [48];